Some aspects of the surface and bulk chemistry of cellulose nitrates as studied by ESCA and other spectroscopic techniques

Andrew H. K. Fowler

A thesis entitled

SOME ASPECTS OF THE SURFACE AND BULK CHEMISTRY OF CELLULOSE NITRATES AS STUDIED BY ESCA AND OTHER SPECTROSCOPIC TECHNIQUES

by

ANDREW H. K. FOWLER, B.Sc.(Hons.), GRSC.

A Candidate for the Degree of Doctor of Philosophy

Hatfield College,
University of Durham

September 1984

To my wife

Jane

ACKNOWLEDGEMENTS

First, and foremost, my sincere gratitude and thanks must be placed upon my two supervisors, Professor David T. Clark and Dr. Hugh S. Munro, during my term at Durham. Without whose help and enthusiasm this thesis would not have been possible.

I am also indebted to Drs. Tom Lewis and Frank Baker of the Ministry of Defence, Waltham Abbey, for advice and criticism. For their help with the N.M.R. studies I would like to thank Dr. Ian Sadler of the University of Edinburgh and Professor Jim Peeling of the University of Petroleum and Minerals, Dhahran, Saudi Arabia for running the excellent spectra used in this thesis. I have also drawn on the expertise and skill of Mr. Ron Hardy for the X-ray diffraction measurements.

Many thanks to all at Kratos (UK) Ltd., Manchester for allowing me to use their latest SIMS equipment.

Thanks are also due to Pete Stephenson for early advice and members of the "NC annual seminar" who grow too numerous to mention.

For friendship, advice and criticism, many thanks are due to the members of the ESCA lab. who are the best of pals. These people are Hugh, Dick, Bill, Steve, Jeff, Clare, Mohammad, Umar and last, but not least, our friendly and helpful technician Rob.

Finally, I would like to thank Elizabeth Thompson for excellent photographic work, and Mrs. Marion Wilson for her skill and expertise in the typing of this thesis.

ABSTRACT

X-ray photoelectron spectroscopy (E.S.C.A.) has been used to investigate the surface chemistry of cellulose nitrates.

The heterogeneous nitration and denitration of cellulose nitrates has been studied as a function of time and temperature and important conclusions have been drawn on the complex equilibria established at the surface. ^{13}C solution state n.m.r. has been employed also in these reactions to monitor the bulk chemistry; partial degrees of substitution established at individual sites of a β-D-anhydropyranose ring. Correlations are drawn between these partial DOS's and the mean d(110) interchain spacings in cellulose nitrates, and show evidence for possible morphological changes.

The nature of the nitrating species in a technical acid mix has been alluded to by the use of laser Raman spectroscopy. Evidence exists for the species being the nitronium ion, NO_2^+.

The X-ray induced and thermal degradation of cellulose nitrates, both surface and bulk has been addressed by the use of ESCA, FAB/SIMS and ^{13}C n.m.r. New information on the build up of degradation products at the surface is postulated by the formation of an oxime structure, with concomitant increases in carbonyl and ester functionalities. Conclusions are given which suggest that electromagnetically induced degradation is a surface phenomenon, whereas thermal degradation is predominantly bulk orientated.

The use of trifluoroacetic anhydride as a hydroxyl tagging agent has been investigated on cellulosic materials. Incomplete esterification of the hydroxyl groups occurs.

MEMORANDUM

The work outlined in this thesis is wholly original except where referenced, and this thesis contains material which forms part or whole of the following publications:

1. Clark, D.T., Fowler, A.H.K. and Peeling, J., Polymer Communications, 1983, 24, 117-119.
2. Clark, D.T. and Fowler, A.H.K., Polymer Communications, 1983, 24, 140-141.
3. Clark, D.T., Fowler, A.H.K. and Stephenson, P.J., Macromolecular Science - Reviews in Macromolecular Chemistry and Physics, C23(2), 217-246 (1983).
4. Clark, D.T., Fowler, A.H.K. and Munro, H.S., Polym.Degd. and Stab., in press, 1984.
5. *Clark, D.T., Fowler, A.H.K. and Munro, H.S. (Proceedings of Cellucon '84", Eds.
6. *Clark, D.T., Fowler, A.H.K. and Munro, H.S. "Proceedings of Cellucon '84", Eds., J.F. Kennedy, D.J. Wedlock, G.O. Phillips and P.A. Williams. Ellis-Horwood Publ. (1984).
7. Fowler, A.H.K. and Munro, H.S., Polym.Degd. and Stab., submitted (1984).
8. Clark, D.T., Fowler, A.H.K. and Munro, H.S., Polymer, submitted, 1984.

* papers presented by the author.

CONTENTS

Page No.

Page No.

CHAPTER ONE

APPLICATION OF MODERN ANALYTICAL TECHNIQUES TO THE INVESTIGATION OF CELLULOSE NITRATES - A REVIEW

1.1 Introduction

Cellulose remains one of the world's most important textile materials, despite contemporary inroads made into the textile market by synthetic fibres. The most important factor as to why this is so is its ready availability and continuing supply of this naturally occurring fibre, coupled with its "wearability". In fact, Hon[1] has estimated that vegetation produces about 100 billion tons of cellulose a year. It is, therefore, of no great surprise that cellulose has maintained its competitive price and position in world markets.

Cellulose, being a natural fibre, has of course a myriad of desirable properties, and by methods of derivatisation a multitude of uses. For example, cellulose acetates are a valuable textile material in their own right, and oxidised cellulose and the carboxy-methyl derivative have found many useful applications in chromatography.[2] Perhaps the earliest derivatisation of cellulose came in 1819 in the laboratory of H. Bracconot[3], who observed the effect of fuming nitric acid on cotton. The resulting cellulose nitrate (see Figure 1.1) was found to be an extremely unstable and explosive material which quickly found military applications in propellant formulations.

In fact, cellulose nitrate was for many years used in such diverse applications as billiard balls and shirt collars.

Indeed, the history of western civilisation was materially changed by the production of cellulose nitrates, both in terms of military applications and the large impact which the

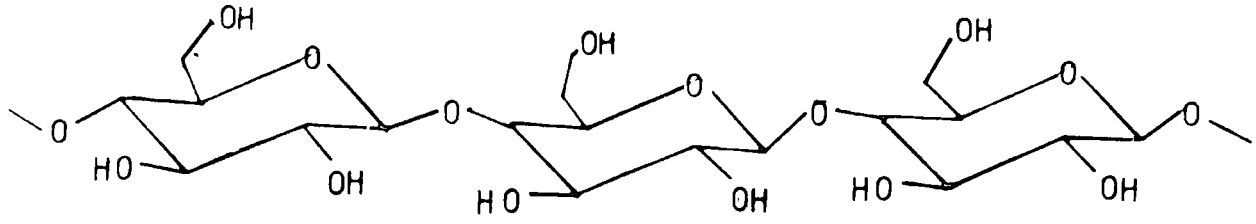

CELLULOSE

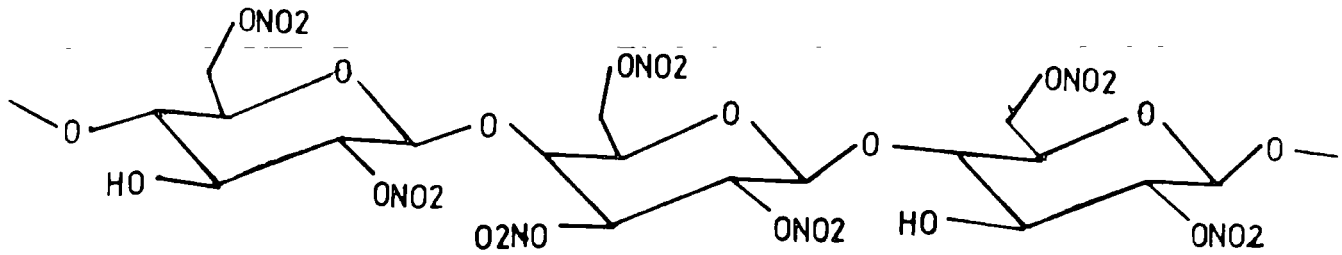

A CELLULOSE NITRATE

Figure 1.1 The chemical structure of cellulose and a possible structure of a cellulose nitrate

photographic and cinematographic industries invoked. In addition to propellant formulations, extensive use is still made today of nitrocelluloses in such diverse fields as the automotive, packaging and magnetic tape industries.

From a cellulose chemist's point of view, the nitrate ester of cellulose is of great interest for a number of reasons, some of which are listed below:

(1) cellulose nitrate is produced in a heterogeneous reaction, whereas most other derivatives are regenerated from solution;

(ii) the nitration reaction is believed to be an equilibrium reaction and hence the extent of nitration may be varied by the acid composition. In most other reactions of cellulose, the derivative is obtained by quenching a rate-controlled process[4];

(iii) cellulose nitrate exhibits a range of birefringent properties depending on the degree of substitution (DOS).* The low DOS materials are always positively birefringent whereas the higher derivatives show strong negative birefringence; the neutral point occurring around a DOS = 2.2 Many other cellulose derivatives are also positively birefringent, like cellulose itself, but chitin, a cellulose-like material shows a negative birefringence;

(iv) x-ray studies of the d(110) interchain spacings have revealed that materials of the same DOS prepared by nitration of cotton linters and denitration of a high DOS cellulose nitrate, have quite different structures and properties.

In addition, despite the voluminous literature available on the chemistry and structure of cellulose and its nitrates, there are still a number of questions that remain unanswered which are of great interest in the industrial manufacture and storage of these materials.

For a complete overview of the problems to be considered these, too, are listed below.

Footnote

* DOS - degree of substitution, i.e. the average number of ester groups per β-D-anhydroglucopyranose ring.

(a) The nitration reaction never achieves the theoretical maximum esterification level of three nitrate groups per β-D-anhydroglucose ring. This is particularly noticeable in mixed acid preparations.

(b) The distribution of nitrate groups along a chain and around a residue is of great interest with respect to the broader macromolecular structure of cellulose itself.

(c) The mode of degradation of these materials is of great interest, especially to the munitions industry, as modification of burn rates and accidental detonation would have grave consequences.

These aspects will be further discussed in a later section, but it is the purpose of the remainder of this chapter to present a brief review of the relevant literature pertaining to the chemistry and structure of cellulose nitrates.

1.2 Cellulose Nitrate

1.2.1 A Brief History of Cellulose Nitrate Production

The nitration of cellulose has had a long and chequered history since the discovery in 1819 by Bracconot[3,5] that the reaction of fuming nitric acid and cotton produced a highly unstable, explosive material which changed the course of modern warfare. In 1846, a patent was granted to Schönbein[6] specifying the production of nitrocellulose and it was not until the first unscheduled explosion in 1847, that work on the technical production of cellulose nitrates became a little restrained.

However, this explosion did cause the recognition of the possibility for the use of cellulose nitrates in propulsion if the burn rate could be modified. By 1867, the basis of the production of smokeless propellants for guns, rifles and shells was established. In 1862, Parkes'[7] use of camphor as a plasticiser for cellulose nitrate in the celluloid production undoubtedly aceelerated photography as we know it.

However, despite the many applications of cellulose nitrate it is the military establishments where most interest lies. It is therefore pertinent to mention the production methods used today.

1.2.2 Production Methods

Cotton linters or woodpulp[4] is by far the greatest raw material used in the manufacture of cellulose nitrates. The cotton linters receive a preliminary treatment called 'kiering'. This kiering treatment reduces the viscosity of the cotton and is achieved by heating under pressure with dilute sodium hydroxide. However, kiering is found to be more effective in lowering the total viscosity after the nitration process. There are two basic nitration procedures used which will be considered in turn.

(1) Mechanical Nitration[4,8]

The vessels used in the nitration are upright oval cylinders made of stainless steel, in each of which operates two paddles on vertical shafts, and a centrifuge is situated below the vessels. The acid is pumped into the vessels with

a charge of cotton linters, and the nitration reaction is allowed to proceed with agitation. During this time the temperature of the mix does not rise by more than $2^{o}C$. Once the reaction has proceeded for a fixed period of time, the contents are emptied into the centrifuge, where the waste acid is spun off and recycled.

The spun cellulose nitrate has its own weight of spent mixed acid adhering to it, and this is eliminated *via* a jet of cold water. This is done rapidly to alleviate denitration effects. The resulting nitrocellulose is then washed in several changes of hot water before stabilisation.

(2) The Displacement Process[4,8]

The nitration vessels are usually shallow square vessels with a central bottom outlet. A perforated false bottom is included into the vessel. About 800 lbs. of fresh acid is run into the pan and ∿24-27 lbs. of cotton is dipped into the acids with stainless steel forks. Heavy tiles are laid over the cotton to exclude air for periods up to one hour, when the acid is displaced with a regulated flow of water, while the spent acid is slowly run out of the bottom outlet. The water-wet, but acid-free, nitrocellulose is removed from the vessel and is ready for stabilisation.

There is evidence that the cellulose nitrate prepared *via* this process is more likely to suffer denitration; a fact that has recently been alluded to by Lewis[9] from birefringence measurements.

1.2.3 Laboratory Preparation

The esterification reaction of cellulose to form cellulose nitrate can be accomplished using various nitrating mixes. The various acid mixes used shall now be considered.

(i) Nitric Acid: Water Mixes

According to Miles[4], products produced in this mix dissolve in an acid concentration >80%, and are therefore considered unsatisfactory. The nitration is also believed to be uneven, although there is little evidence for this. However, it is known that cellulose nitrate prepared in this mix has a very low viscosity and gelatinisation of the fibre may also occur. The gelatinisation problem can be overcome by the use of sodium and potassium nitrates[12] in the acids, although no explanation has been given of this phenomenon. However such acid mixes have been used in the work of Trommel[10] and Stephenson[11] to denitrate high DOS materials.

(ii) Phosphoric Acid: Nitric Acid Mixes

This acid mix is considered the best in the laboratory as high DOS material can be achieved which is particularly easy to stabilise. However, the attack of the reagent on steel and glass, and the difficulty in recycling the spent acids, precludes its use on a large scale production.

(iii) Nitric Acid with Organic Liquids

The use of organic liquids in the nitrating mix have led to very high DOS materials being achieved, although little is known about the kinetics of the reaction. High

percentage nitrogen material can be obtained using acetic anhydride,[13] chloroform,[14] propionic acid,[15] acetic acid[16] and butyric acid[17] with fuming nitric acid.

(iv) Sulphuric Acid: Nitric Acid Mixes

It is in this acid mix that most nitration processes take place in this thesis and in the technical production of cellulose nitrate. In fact, almost every possible ratio of nitric acid and sulphuric acid has been investigated, and this has led to a three-way nitration diagram[4] being drawn up. Hence, the expected degree of substitution can be read off for a particular acid mix, (see Figure 1.2). Although experience has shown that the diagram is not particularly accurate (it is argued that the diagram takes no account of the effect of starting material on the final degree of substitution), it can be used to give an approximate value. The diagram is split by areas of swelling and solution. These areas must be avoided if a product of even nitration and high viscosity is desired. Nitration may also be accompanied by changes in the physical condition of the fibre, especially in acid mixes where the nitric acid content is greater than 25%. This point shall be returned to in Chapters Three and Four of this thesis.

It is still not established what the nitrating agent is, although the nitronium ion, NO_2^+,[18] has been postulated in mixes where the water content is low, according to the equation

$$NO_2OH + 2H_2SO_3 \longrightarrow NO_2^+ + 2HSO_4^- + H_3O^+$$

The nitronium ion is not observed spectroscopically in acid mixes containing less than 80% sulphuric acid; a range far outside those encountered normally.

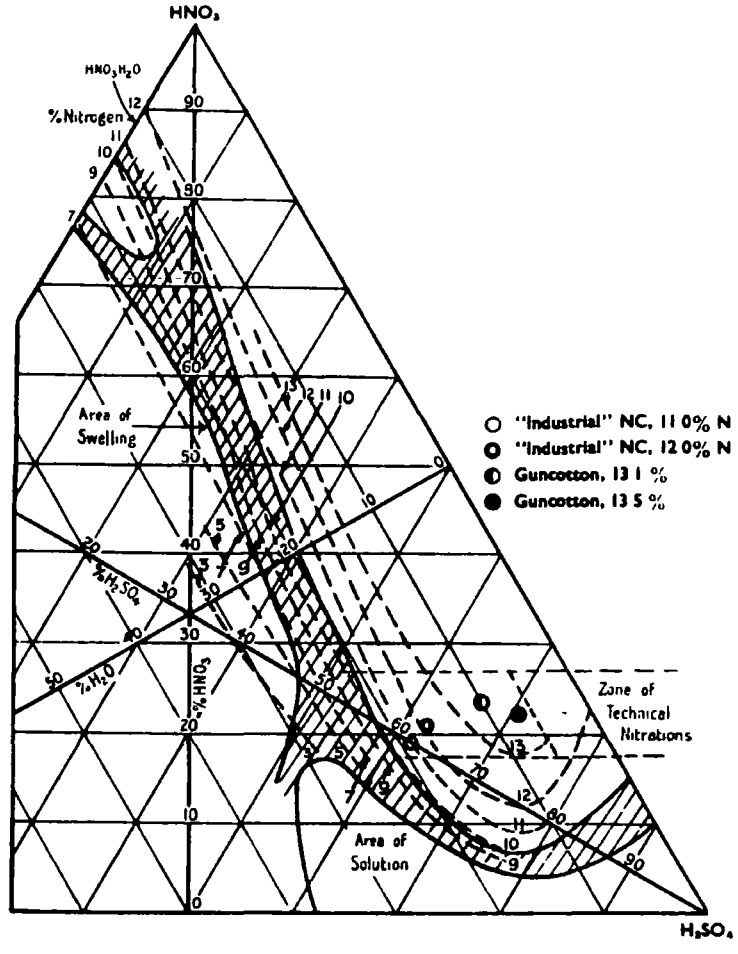

Mixed acid chart Lines of constant nitrogen and areas of swelling and solution

Figure 1.2 Three-way composition diagram for nitration of cellulose[4]

1.2.4 Stabilisation

Stabilisation of cellulose nitrate is achieved by boiling or steaming with many changes of water, and this renders the material quite safe to handle in a dry state. For blasting explosive nitrocellulose, a stabilisation period of several days is used, although several hours is probably sufficient in the laboratory. The stability is generally measured by the Abel Heat Test[19] or the Bergmann-Junk Test.[20]

It has been suggested that the nitrate group oxidises the cellulose residue liberating nitrogen oxides which autocatalyse the degradation.[21] The instability could be due to small amounts of the mineral acids being present, and hence be more marked for high DOS materials and less in those nitrocelluloses prepared without the use of sulphuric acid.[22]

The formation of sulphate esters during nitration in mixed acid is well substantiated,[4] and boiling removes such esters although some authors[23] believe that free acid is trapped in the fibrillar structure and is difficult to remove. Gagnon and co-workers[24] have examined the relationship between sulphate and nitrogen content of unstabilised cellulose nitrates and found that the sulphate ester content decreased steadily with increasing nitrogen content.

However, it is not possible to explain the instability of cellulose nitrate purely to sulphuric acid or sulphate esters since cellulose nitrate prepared by other acid mixes are also known to be unstable unless washed thoroughly and boiled. Hence it was suggested[25] that an oxidation product of cellulose was formed in nitration which could

initiate degradation, and which could be removed by boiling in water. These points shall be returned to in Chapter Five of this thesis.

1.3 The Nitration Equilibrium of Cellulose

Cellulose nitrate is an ester of cellulose and hence one would expect that the composition of the acid mix would determine the degree of esterification. Similarly, if a high DOS cellulose nitrate is placed in an acid mix which normally would nitrate to a low DOS, then denitration or saponification would occur. The first workers to check this experimentally were Berl and Klaye[26] who found that cellulose nitrate would denitrate under these conditions, but also that the degree of substitution attained was higher than expected. Later Fabel,[27] Demougin[28] and Bonnet[29] reached the same conclusion; that is, the equilibrium had not been reached. These experiments were reviewed by Miles[4] and repeated and expanded by Trommel[10]. It is largely as a result of this work that many workers prefer to explain the observations *via* an accessibility theory, although it is now accepted that the nitration of cellulosic materials is an equilibrium reaction. The remainder of this chapter hopes to reach come conclusions about these conflicting ideas by reviewing the very recent literature.

1.4 Structural Studies

In general, cellulose chemists have been quick to apply new analytical techniques to the study of the structural and

synthetic problems encountered in the wide field of cellulose chemistry. Cellulose, for example, may be counted amongst the first materials to be studied under the polarising microscope; soon after the discovery of the diffraction of x-rays by crystalline materials by Bragg,[136] Mathieu[42] recorded the powder pattern of a series of celluloses.

In more recent years, high technology has provided the cellulose chemist with such tools as infra-red spectroscopy, high resolution nuclear magnetic resonance spectroscopy for analysis both in solution and in the solid state, and Electron Spectroscopy for Chemical Applications (ESCA, X-ray Photoelectron Spectroscopy), for studying the surfaces of cellulose fibrils. However, it is something of a surprise to learn that despite this ever increasing number of analytical tools, the number of reports of the applications to cellulose nitrate chemistry is extremely limited. It is true that much of the literature is lost in the secrecy that surrounds the military establishments.

It is the aim of this section to review the uses of some of these analytical techniques in cellulose nitrate chemistry.

1.4.1 Infra-Red Spectroscopy

Infra-red spectroscopy is a very useful tool when dealing in those fields of chemistry where a number of compounds of similar chemical and physical properties require analysis and identification. The technique has been widely applied in carbohydrate chemistry. Cellulose and its derivatives have undergone several investigations by infra-red spectroscopy.[30,31] For instance, the technique has proved

especially useful in the oxidation of cellulose by monitoring the increase in carboxyl and carbonyl groups.[30]

The many absorption bands of cellulose have been assigned by Rowan,[32] and many workers have concentrated on the nature of the hydroxyl bonds in the 3 micron region[33]. Marrian and Mann[34] have attributed specific absorptions to various types of hydrogen bonds by using deuteration techniques. Barker[35] *et al* have studied cellulose and discussed the nature of the bonds at 112 microns.

The various polymorphic forms of cellulose, especially the important transition between the crystal forms of cellulose I and II, has received much attention.[36] Kuhn[37] has attempted to assess the nitrate ester groups in cellulose nitrates using infra-red spectroscopy, whilst Higgins[38] has reviewed the application of the technique to cellulosic materials.

1.4.2 X-Ray Diffraction

The change in the macromolecular structure of cellulose nitrate as the hydroxyl groups of the cellulose chains are progressively replaced by nitrate ester groups has been well studied, and it is now well established that the conversion coincides with a substantial change in the unit cell.[39] Changes in the spiral angle and nature of the helix have also been recorded and it is proposed that the anti-parallel arrangement of chain molecules that persist in the cellulose I structure is maintained in the cellulose nitrates, except for those nitrated in or near the swelling or solution areas of the Miles diagram.[6] However, it is likely that

some intermediate chain arrangement is adopted similar to that in mercerised cellulose.[40] This form of cellulose is produced *via* a heterogeneous reaction, and has recently been investigated using solid state n.m.r.[41] (see Section 1.4.4).

Much of the initial X-ray work was carried out by French workers,[42] who claimed to distinguish three distinct diffraction patterns for the trinitrate, dinitrate and cellulose structures; the trinitrate diagram being extremely sharp and clear. An assignment of a pure dinitrate structure is untenable from recent ^{13}C n.m.r. data.[43] (see Section 1.4.3).

Much of the early work is reviewed by Miles.[6] Perhaps, the first to observe a linear relationship between d(110) interchain spacing and the nitrogen content of cellulose nitrates was Mathieu.[42] Trommel[10] has also investigated this problem over a range of D.O.S. and his results can be summarised in Figure 1.3.

It is clear from Figure 1.3 that the d(110) spacing is very sensitive to DOS, and that the lattice spacing of denitrated materials is maintained, despite substantial loss of nitrate ester groups. It would appear that once the cellulose trinitrate structure is attained it is extremely stable, perhaps because of the hydrogen bonding, which makes it resistant to hydrolysis.

An accessibility rationale was put forward by Trommel[10] to explain this data. Briefly, large portions of trinitrate structure are expected to be crystalline, and hence resistant to attack by acids. Several lengths of such material would possibly hold the chains apart and hence the

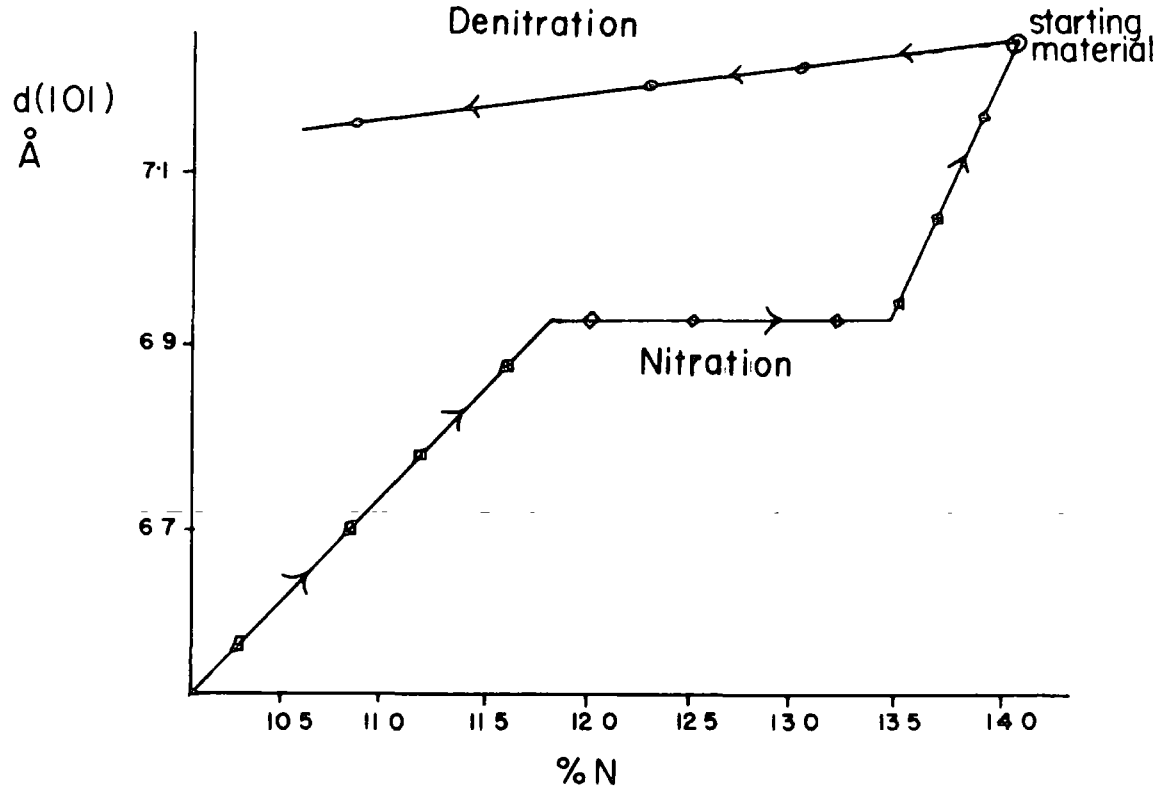

Figure 1.3 Graph of mean X-ray d(110) spacings against DOS for nitration and denitration[10]

d(110) interchain spacings would remain similar. A similar argument was adopted, again by Trommel,[10] to explain anomalous solubilities of nitrocelluloses prepared by nitration or denitration; in general, denitrated materials are less soluble in mixtures of alcohol and ether (2:1).

Even in a recent study by Atkins,[44] the unit cell of cellulose and its polymorphs has not been clearly adduced. What has been established though, is that the spiral angle in cellulose II and possibly cellulose I is 180° coinciding with an axial advance of 0.519nm. Crystallographically, the flat

ribbon helix is defined as 2_1.

In the case of the cellulose trinitrate structure the helix is 5_2, *i.e.* five monomers in two turns resulting in an axial advance of 0.508nm. The rotation between monomers is now 144° and therefore there is a relaxation within the cellulose structure of 36° per monomer. It is likely that in this arrangement both left and right-hand macro chiralities are equally probable and hence an accumulation of twist would not occur.

1.4.3 Solution state n.m.r.

The resolution of many of the problems discussed earlier requires an understanding of the bulk chemistry of these materials. Recent investigations of the bulk composition of cellulose nitrates have been carried out using high resolution solution state nuclear magnetic resonance spectroscopy, and have led to a greater understanding of the reaction mechanisms involved.[45] In 1980, Wu[46] published ^{13}C n.m.r. spectra of nitrated celluloses and made initial assignments of the peaks in the anomeric region of the C_1 carbon in variously substituted glucose residues. This has unambiguously demonstrated that the equilibrium partial DOS is of the order $C_6 > C_2 > C_3$ (see Figure 1.1). However, an analysis based solely on the anomeric C_1 carbon has certain inherent weaknesses which can largely be eliminated by using the remainder of the ^{13}C n.m.r. data from C_2-C_6 once appropriate assignments have been made.[47] Such assignments allow a considerable amount of information to be extracted from spectra.

Further use of this technique has been employed in this thesis in Chapters Three and Four; hence it is there that further consideration of the analysis will be encountered. The remainder of this section will discuss the relevant literature pertaining to the use of ^{13}C solution n.m.r. in cellulose nitrate chemistry.

With respect to the problem of anomalous lattice spacings addressed in Section 1.4.2, it is of great interest to examine the available data for information pertaining to sequence distribution. A typical low DOS cellulose nitrate yields an n.m.r. analysis of:[45]

DOS 2.31	Partial DOS			Trisub.	2,6 sub	3,6 sub	6 mono
	C_6	C_2	C_3				
	1.0	0.71	0.6	47%	24%	13%	17%.

Since Wu[46] has shown that substitution at the C_6 position largely leaves the C_1 position unaffected, sequence distribution will be manifest from the effect of substitution at the C_3 position in adjacent rings. Hence, by knowing partitioning of the nitrate groups and the assignments of the peaks in the anomeric region, it is possible to come to some conclusions on sequence distribution in a given sample.[47] From these studies, it is certain that substitution is non-random and that substitution at a given site is influenced by substitution patterns in adjacent rings. It is also clear from the work of Clark and Stephenson[47] that differences in substitution patterns occur for samples of the same DOS prepared by different means.

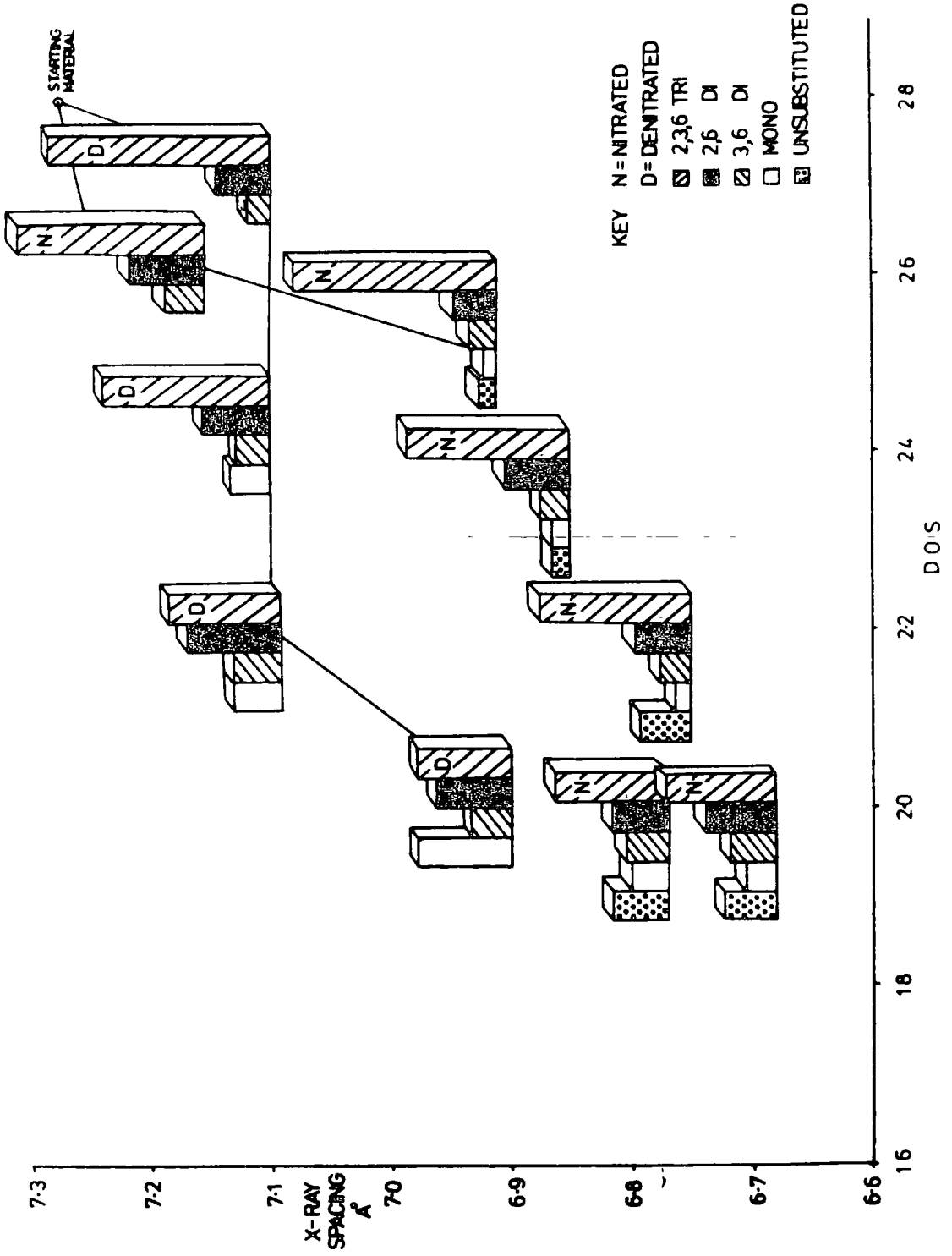

Figure 1.4 Block histogram of nitrate ester distributions for given degrees of substitution *versus* the mean interchain d(110) spacings as measured by X-ray diffraction[47]

Detailed investigations of the relationship between d(110) lattice spacings and substitution patterns have shown that those materials having unsubstituted primary hydroxyls prepared by nitration in general have lower d(110) spacings than those prepared by denitration which do not have unsubstituted hydroxyls at C_6. Figure 1.4[47] summarizes these data in the form of a block histogram set on an X-ray spacing *versus* DOS graph. It is also interesting to note from this graph that in the cases where denitrated and nitrated materials have similar interchain spacings, the general distribution of nitrate groups around the residue are similar.

1.4.4 Solid-State n.m.r.

It has become apparent in recent years that ^{13}C n.m.r. spectra of solid polymeric materials can be obtained with a resolution comparable or approaching that of solution studies.[48-51] How well such experiments work depends upon the physical nature of the polymer and the use of several techniques known as high power decoupling, cross-polarisation and magic angle spinning. Several excellent articles are available on such topics, and hence will not be explained further here.[52-54]

The application of these new techniques to cellulosic materials has recently been reviewed,[52] and as such will not be developed on here. It is sufficient to mention that the various polymorphs of cellulose have been investigated, and also the transformation of cellulose I to cellulose II has partly been explained by a study of the oligomers of cellulose.[53]

The advantage of solid state ^{13}C n.m.r. to the investigation of cellulose nitrates is that now the heterogeneous nitration or denitration can be studied. Not only is this complimentary to similar ESCA studies at the surface (see Section 1.5.1), but it provides an interesting foresight into the diffusion of the nitrating media into the bulk of the fibrils. For example, Figure 1.5[54] records the spectra obtained of the nitration of cellulose I in increasing concentrations of nitric acid. The typical cellulose I spectrum is maintained over the range of 51% to 59% nitric acid, although at 67% there are signs of splitting in the C_1 regions. It is interesting to note that this concentration of acid produces considerable swelling of the fibres which increases until dissolution occurs at ∿70% nitric acid. Within a 2% range, Stephenson[54] observed a total change in the spectra, resulting in the broad characteristic nitrate peaks. This rapid conversion is somewhat unexpected but compliments limited X-ray data[6] which suggests large changes in the dimensions of the unit cell at these concentrations.

The method is clearly of great importance in cellulose nitrate chemistry, and may be used to follow time dependent studies in a variety of nitrating media, yielding complimentary information to ESCA studies of the surface.

1.4.5 Optical Microscopy

As was alluded to in Section 1.4.2, the chain arrangement of cellulose nitrate is of particular importance in birefringence studies. This subject was originally addressed by Kohlbeck[55] and more recently re-examined by Lewis.[56]

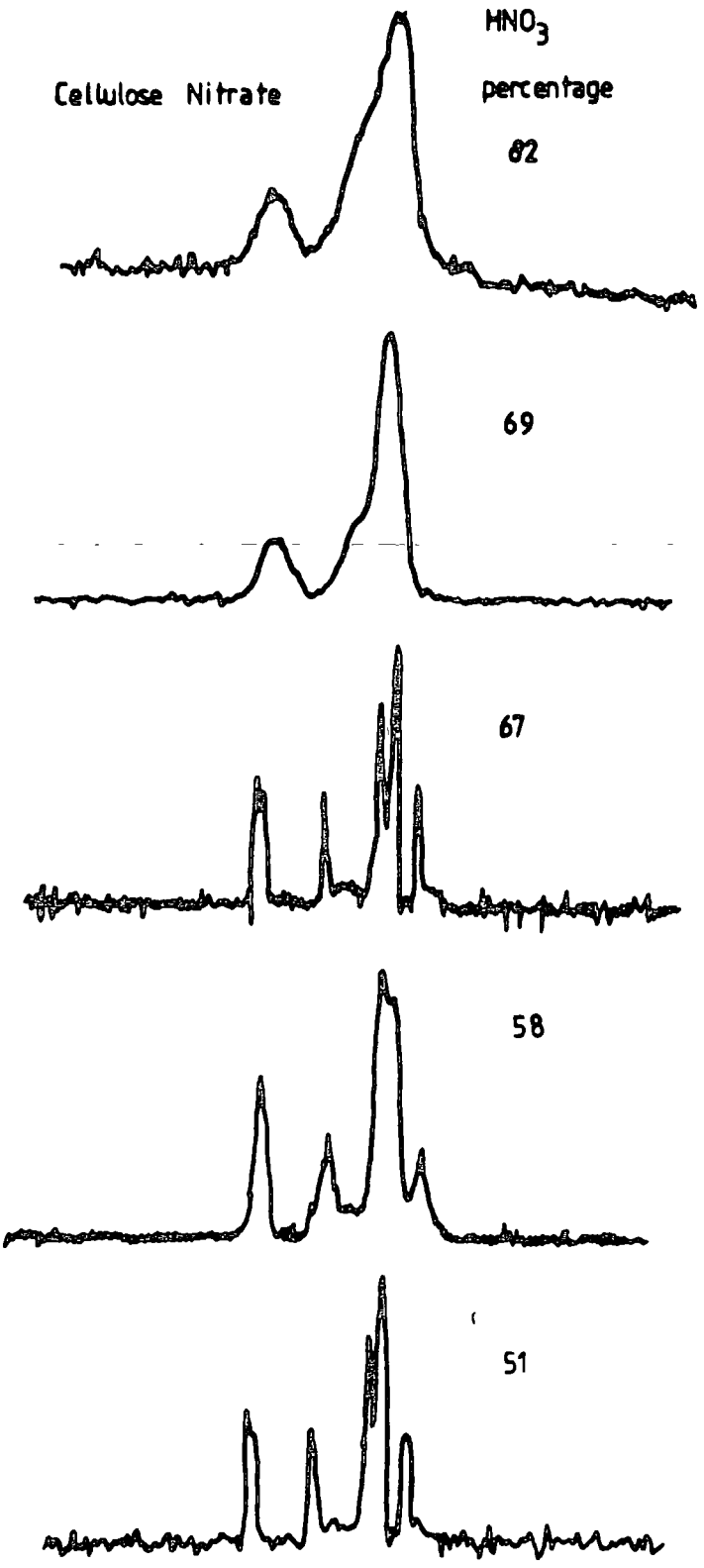

Figure 1.5 ^{13}C CP/MAS solid state NMR spectra of cellulose linters nitrated in increasing concentrations of nitric acid

It is possible to estimate the DOS of cellulose nitrates from birefringence data, whereas the only method previously available was the Kjeldahl nitrogen determination.[57] Although X-ray diffraction has now established the spiral angle to be 144° in certain cellulose nitrates and the helix to be 5_2,[44] the conformation of the C_6 nitrate group was still in doubt. This is presumably due to the disorder at this position because of the possible arrangements of the group *e.g.* the tg, gt and gg forms.

Recent studies by Lewis[56] have suggested that birefringence measurements on individual fibres (taking into account a statistical distribution of fibre thickness) can be linked to calculations of the theoretical birefringence of mono-, di- and tri-substituted cellulose nitrates from the polarizability, orientation, and substitution pattern of a relevant cellulose nitrate of the relevant DOS. These calculations were carried out for C_6 nitrate groups in all three possible orientations and compared to experimental data. The conclusion made was that the gg conformation was essentially forbidden and that only the tg and gt forms are possible in cellulose nitrates. The three conformations available are shown in Figure 1.6.

CELLULOSE TRINITRATE

tg

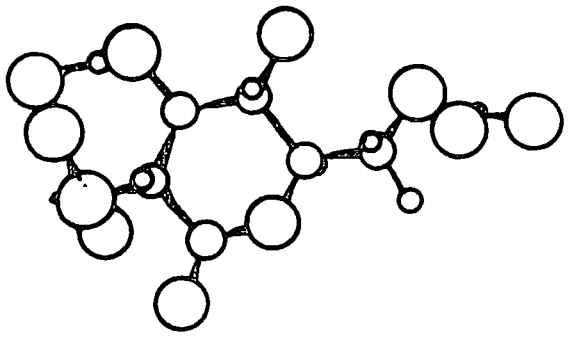

gt

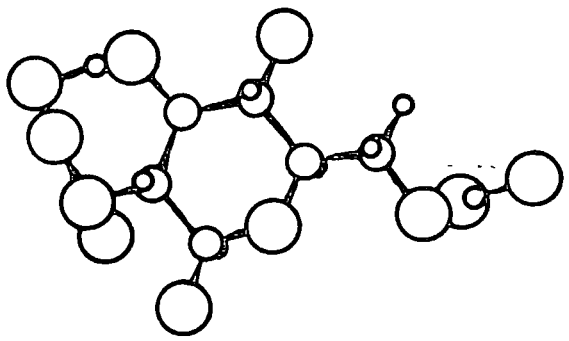

gg

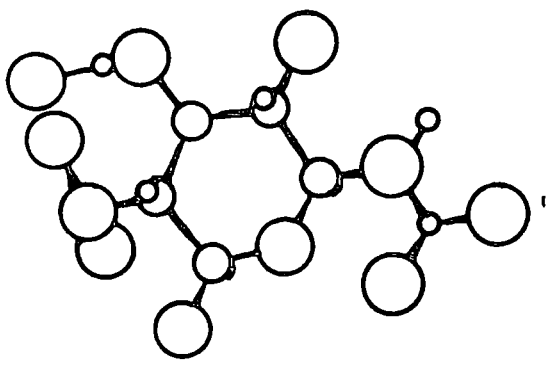

Figure 1.6 The gg, gt and tg conformations of the C_6 primary nitrate ester group

1.5 Surface Studies

1.5.1 ESCA

Many of the important properties of cellulose nitrates may be expected to depend on surface phenomena. Since the initial reaction of any nitrating medium with cellulose fibrils is at the surface and since it is the surface which interfaces with the surroundings, the question of the mechanism of synthesis, of initial burn rate, and of denitration are circumscribed by details of structure and bonding in the outermost few tens of Ångstroms of the surface.

Clark[69] has shown ESCA to be the single most useful technique for surface characterisation of polymer systems.

It is not the subject of this section to explain the basic principles of ESCA, as this will be done in Chapter Two; but to review the pertinent literature of the application of ESCA to cellulose nitrates.

Figure 1.7 shows an example of the type of spectra obtained for a cellulose and from a sample nitrated to a DOS of 2.6 in the acid mix 70% H_2SO_4; 22.5% HNO_3; 7.5% H_2O.

The C_{1s} spectrum shows three distinctive components once a standard lineshape analysis has been carried out. Thus, the central peak at 287.4eV arises predominantly from the carbons at C_2 and C_6 bearing the nitrate ester functionality with contributions from C_4 and C_5. C_1 attached uniquely to two oxygens in the cyclic hemiacetal formulations of the β-D-glucopyranose ring is at the highest binding energy. The component at 285.0eV arises from extraneous hydrocarbon, which

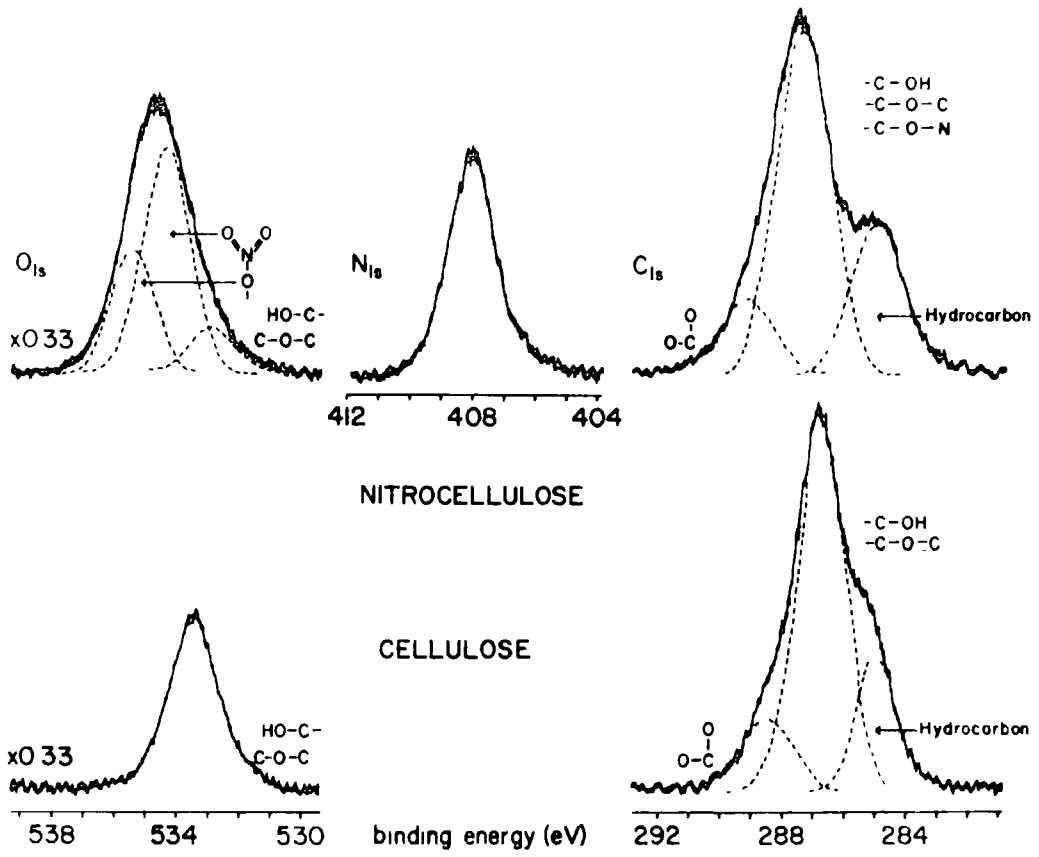

Figure 1.7 C_{1s}, O_{1s} and N_{1s} spectra of a cellulose nitrate and C_{1s} and O_{1s} spectra of a cellulose.

has been shown by Clark[58] *et al* by use of different X-ray sources, to be confined to the very surface of the fibrils. This hydrocarbon is always present irrespective of the source or type of cellulosic material.

The N_{1s} signal consists of an intense high binding energy component consistent with the nitrate ester group. A low binding energy nitrogen signal is often present at ∿406eV which is consistent with the nitrite ester group. The occurrence of the nitrite ester in cellulose nitrates has

not been suggested previously. Their effect on such factors as burn rate is investigated in Chapter Five of this thesis.

The O_{1s} core levels are essentially composed of three peaks which can be identified, but for the purpose of this thesis are left unresolved, as the chemical shifts within O_{1s} core levels are small.

Hence, using these assignments which are supported by theoretical calculations,[79] it is a straightforward matter, once appropriate sensitivity factors are known from model systems, to calculate the DOS.

Hence, monitoring of the N_{1s} signal provides a ready means of following the reaction rate. This study was carried out by Clark and Stephenson[58] over a range of DOS and in each case the N_{1s} intensity remained constant for reaction times of one second to one hour to a depth of $\sim$150Å. It is clear therefore that the equilibrium DOS is rapidly established in the surface regions.

The gross features of the equilibria which are involved in determining the overall DOS at the surface of cellulose fibrils is outlined schematically below for a nitric acid-sulphuric acid mix.

(i) $\sim O\text{-}H + 2HNO_3 \overset{K_1}{\rightleftharpoons} O\text{-}NO_2 + HNO_3 \cdot H_2O$

$HNO_3 \cdot H_2O \overset{K_2}{\rightleftharpoons} HNO_3 + H_2O$

$\sim O\text{-}H + HNO_3 \overset{K}{\rightleftharpoons} O\text{-}NO_2 + H_2O$

$K = \frac{K_1}{K_2}$ Nitration-denitration equilibrium rapidly established?

(ii) Competitive sulphonation

$$\sim O\text{-}H + H_2SO_4 \longrightarrow \sim O\text{-}SO_3H + H_2O.$$

(iii) Work-up procedure-hydrolysis

$$\sim O\text{-}NO_2 + H_2O \longrightarrow \sim O\text{-}H + HNO_3.$$

For mixed acid nitrating mixes, it has been proposed that the sulphuric acid component does not diffuse into the crystalline microfibrils but acts purely as an intrafibrillar swelling agent, and this could lead to differences in DOS for the surface and bulk regions since only in the surface is sulphonation thought to be truly competitive with nitration. Clark *et al*[58] showed that sulphate esters only occur at the very surface (<50Å) of the cellulose nitrate fibrils, although this fact is further discussed in Chapters Four and Five.

Since the initial interaction of any radiation with a solid occurs at the surface, ESCA has also proved invaluable in the study of UV degradation and general weathering investigations of polymers.[60] Hence cellulose nitrates have been studied[59] by ESCA after exposure to controlled doses of UV light of known wavelengths. It has been demonstrated that the surface composition of these materials is altered considerably by such exposure, resulting in a loss of nitrate groups and the introduction of a low binding energy ~400eV nitrogen species under certain conditions. Previously degradation studies have by necessity concentrated on the monitoring of the products by chemiluminescence techniques[61,62] which take no account of the effect at the surface and the interaction

of the degradation products with that surface.

The degradation of cellulose nitrates are further addressed in Chapter Five of this thesis.

1.6 Summary and Areas of Interests

The previous sections of this chapter are necessarily brief but one is left with a number of important questions unanswered.

The interaction of cellulose fibres with reagents (solid-liquid and solid-gas) for example is of immense importance in relation to a number of important reactions and ideas about the possible morphology and fibrillar structure of the fibres. How reagents diffuse into fibrils and the intent of their reaction is a process not yet fully understood. There is also a large gap in knowledge as to the absorption of plasticisers into cellulose nitrates and the sorption of other liquids known not to enter crystalline regions of the fibre. Some of these questions have perhaps been unfruitful because of the lack of a suitable technique such as ESCA, but also a lot of the past work is unrepeatable as chemists tended to treat cellulose as a readily categorised material. It is now widely understood that the type and source of linters is a very important parameter. The whole question of cellulose morphology is poorly understood and the various models proposed rarely fit all the data but are modelled on a particular set of experiments.

The use of ^{13}C solution state n.m.r. has proved invaluable in the elucidation of cellulose nitrates' bulk structure.

Such information has helped to resolve some of the anomalies encountered in the nitration-denitration equilibria. For example, are nitrate groups in particular positions on the chain resistant to denitration and does denitration take place preferentially alongside a residue already partly denitrated? The combination with X-ray diffraction significant advances can be made in structural determinations. Also the d(110) interchain spacing linked with the distribution data may shed light on the complex changes in microstructure which occur in nitrated and denitrated samples.

The application of ESCA to analysis of cellulosic materials promises a great deal in the various degradation of such materials, for example the UV, X-ray, gamma and thermally-induced degradation. Only ESCA or other surface orientated techniques offers any realistic means of monitoring changes at the surface, or surface orientated reactions.

Therefore, there is a wealth of information available from the individual application of ESCA and high resolution solution ^{13}C n.m.r. to more common techniques (*e.g.* X-ray diffraction), giving rise to a greater overall understanding of cellulose nitrates; a polymer whose potential was first realised in the eighteenth century.

CHAPTER TWO

ELECTRON SPECTROSCOPY FOR CHEMICAL APPLICATIONS

2.1 Introduction

Photoelectron spectroscopy was essentially developed during the 1950s and 1960s.[63] However it is only comparatively recently that experimental difficulties in resolution and electron detection have been overcome, which has caused ESCA to emerge as one of the most versatile and potent techniques for the investigation of the structure, bonding and reactivity of material surfaces.

In essence, the ESCA experiment involves the measurement of kinetic energies of electrons emitted from a sample when that sample (gas, liquid or solid) is irradiated with a source of soft X-rays *in vacuo*. A spectrum may be obtained which exhibits a series of discrete bands which reflect the composition and electronic structure of the sample.

Until Siegbahn[63] and co-workers developed a spectrometer capable of hitherto unheard of resolution and accuracy, the full potential of ESCA was not appreciated. This increase in resolution enabled the Uppsala group to observe chemically induced shifts in the binding energies of the emitted core electrons.[64] From this observation, and also the work of Steinhardt *et al*[65] which showed that the photoelectron peak intensities could be treated quantitatively, many more distinct chemical and physical effects have been observed. Thus from analysis of the various aspects of an X-ray photoelectron spectrum, a hierarchy of information levels becomes available (see Figure 2.1).

It is this spread of information levels that makes ESCA such a useful technique which finds application in many areas of chemistry and materials science.

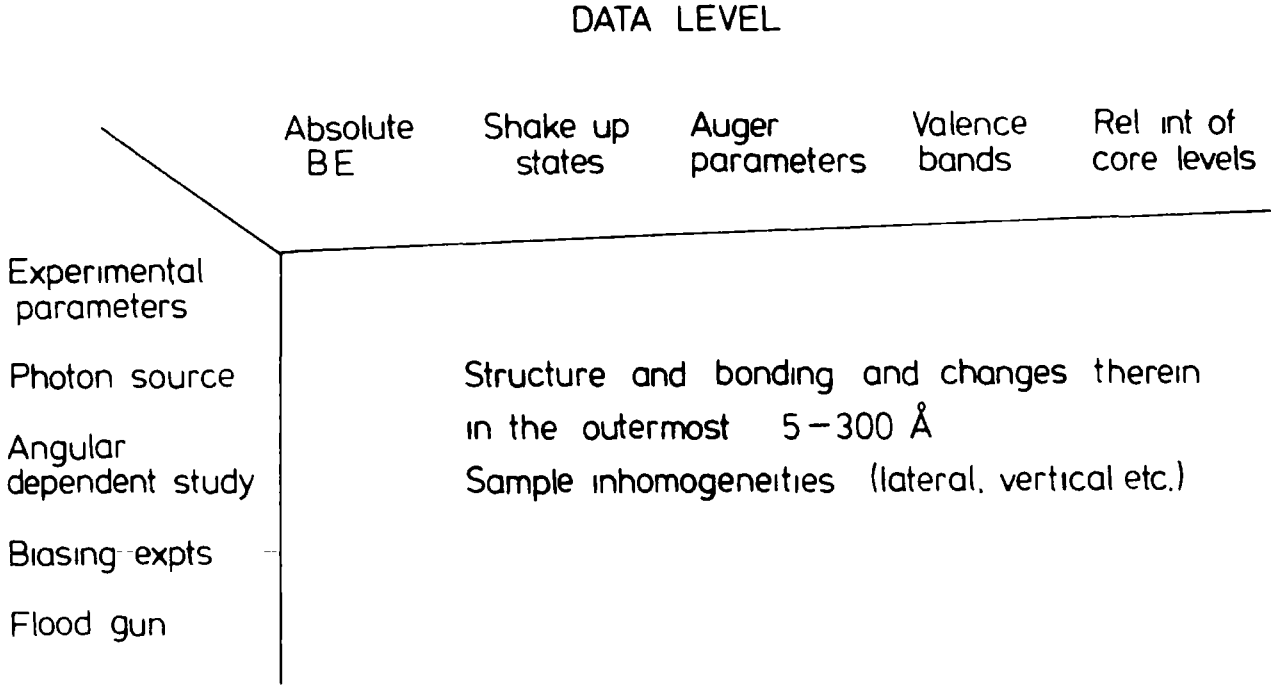

Figure 2.1 Information Levels Available from ESCA

2.2 Fundamental Electronic Processes involved in ESCA

2.2.1 Photoionisation

When a molecule is irradiated with a monoenergetic beam of photons, photoejection of electrons with kinetic energies less than the photon energy results.[66] The total kinetic energy (KE) of the ejected electron is given by equation 2.1

$$KE = h\nu - BE - Er \qquad (2.1)$$

where h = Planck's constant

ν = frequency of incident radiation

B.E. = binding energy of the photoemitted electron. (defined as the positive energy required to remove the electron to infinity with zero kinetic energy).

Er = recoil energy of the atom or molecule.

Using $Al_{k\alpha_{1,2}}$ (1486.6eV), Siegbahn[67] and co-workers have calculated that the recoil energy of atoms decreases with increasing atomic number, *e.g.* H = 0.9eV, Li = 0.1eV, Na = 0.04eV, K = 0.02eV and Rb = 0.01eV. Generally the recoil energy is considered to be negligible for routine studies when using typical X-ray sources, *e.g.* $Mg_{k\alpha_{1,2}}$ and $Al_{k\alpha_{1,2}}$. However, recent studies by Cederbaum and Domcke[68] have shown that modification of the vibrational band envelopes of light atoms may also occur when using high energy photon sources, *e.g.* using $Ag_{k\alpha}$ (~22keV), the recoil energy of Li is 2eV. It is evident that in such cases the Er term must be taken into account. Therefore, routinely equation 2.1 can be reduced to equation 2.2.

$$KE = h\nu - BE \qquad (2.2)$$

The lifetimes of the corehole states formed in such photoionisation events are typically 10^{-13} - 10^{-15} seconds.[69]

It is important to understand the relationship that exists between the experimentally observed binding energies for solids, and those obtained for free molecules as compared with values calculated theoretically in *ab initio* and semi-empirical LCAO-MO-SCF treatments. This relationship depends on the reference level (*e.g.* Fermi level, *etc*)

which differs for conducting and insulating systems. The problem of extracting absolute binding energies is, in practice, avoided by the use of reference standards to calibrate the binding energy scale.

2.2.2 Processes Accompanying the Photoionisation Event

The initial photoionisation event may be accompanied by a variety of processes which may conveniently be divided into two categories depending upon the time scale relative to the photoionisation events. Slow processes such as X-ray fluorescence and Auger electron emission have negligible effects upon the kinetic energy of the photoejected electron.[70] Electronic relaxation processes,[71-73] shake-up, shake-off, and the interaction of conduction electrons with the core hole occur on a similar time scale and result in a modification of the kinetic energy of the photoemitted electron.[74-76] These primary, and secondary decay processes are illustrated schematically in Figure 2.2.

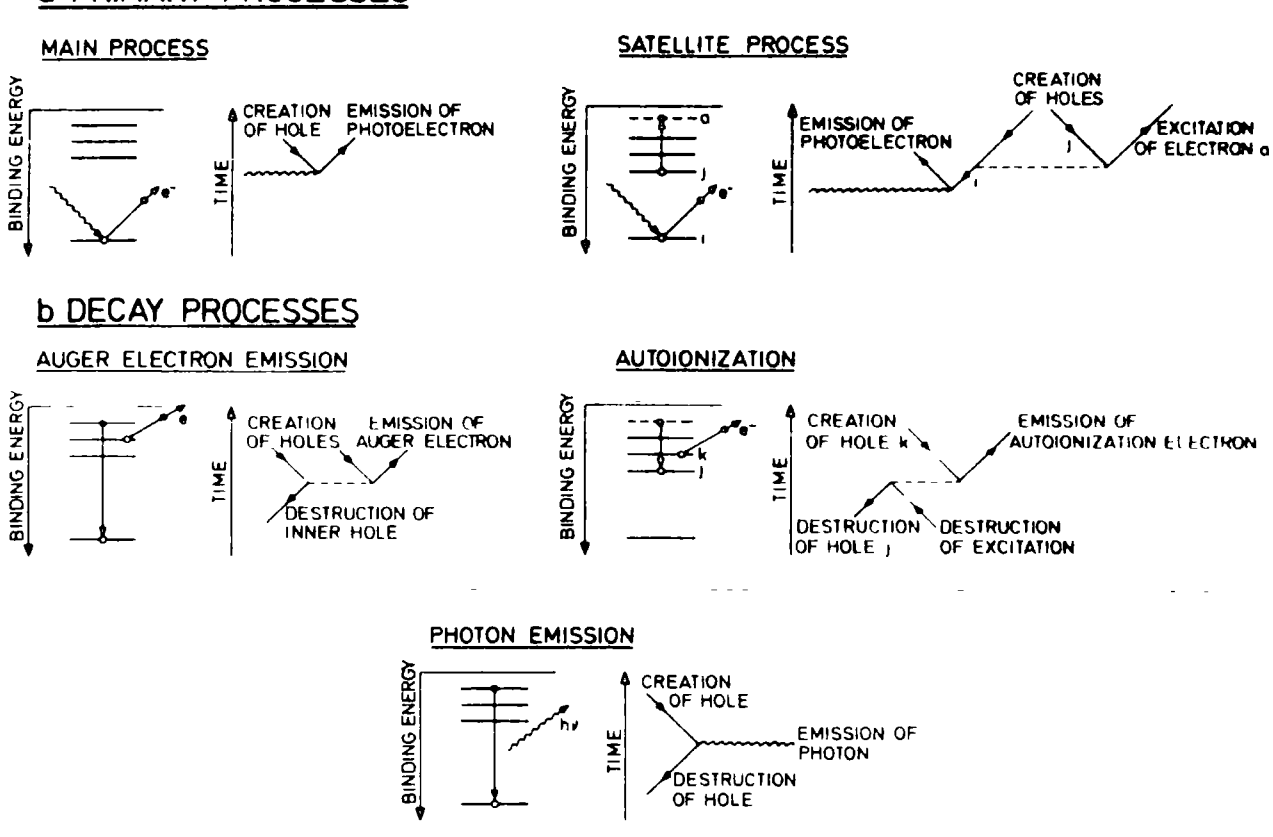

Figure 2.2 The Photoionisation Event and Accompanying Processes

2.3 Features of ESCA Spectra

2.3.1 Chemical Shifts

The binding energies of core level electrons in an atom are essentially characteristic of that particular element.[77] The core level electrons are localised and tightly bound and, as such, do not take part in bonding. They are, however, very sensitive to the local environment of an atom; small changes in the chemical environment of an atom giving rise to measurable changes in the binding energy of the photoemitted electrons. These shifts are characteristic

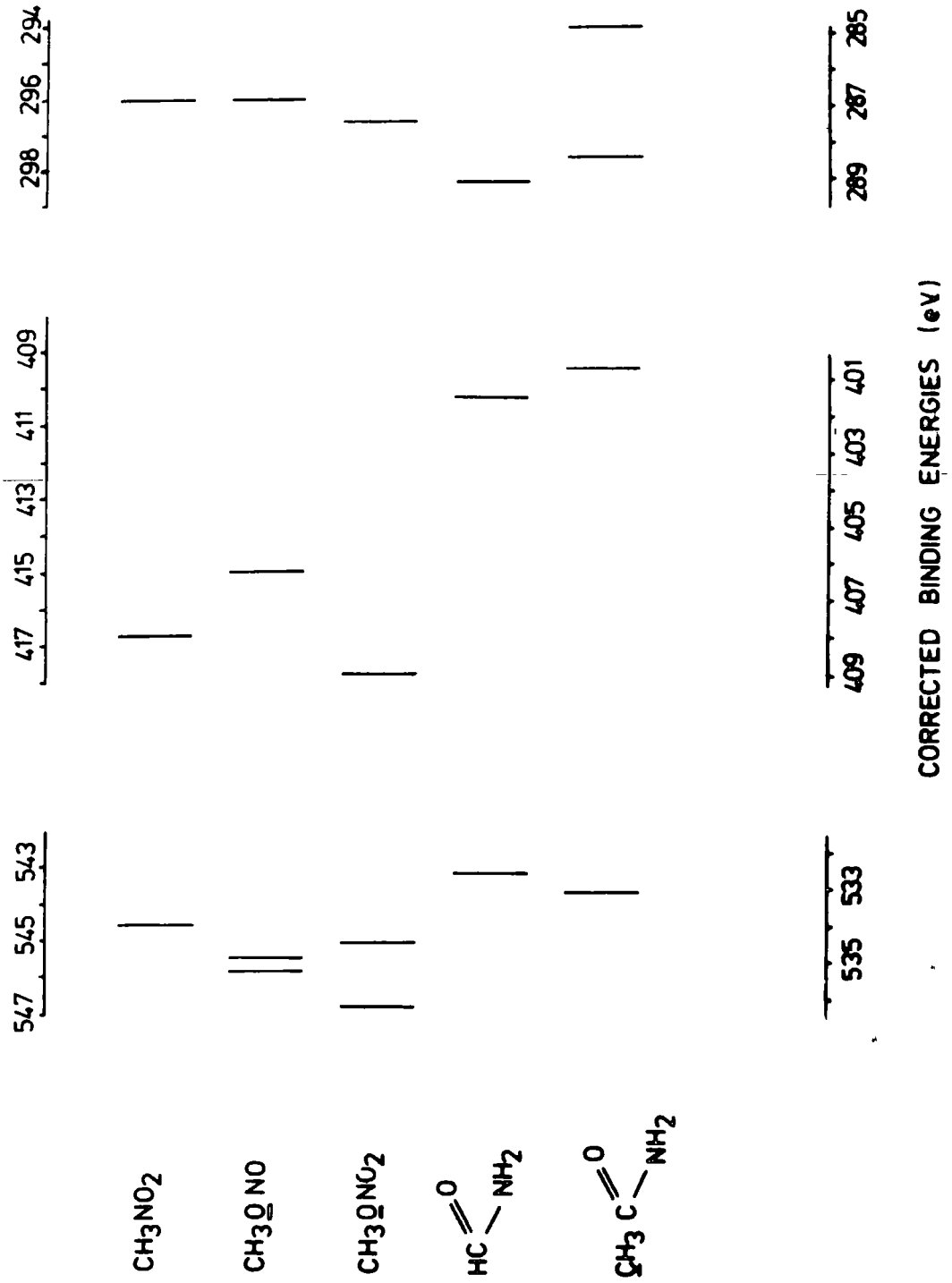

TABLE 2.1 Chemical Shifts of core levels

of the presence of a particular structural feature within the surface of the sample.

A study of the shifts in core levels as a function of substituent for systems pertinent to this thesis are displayed in Table 2.1.

Emphasising the close relationship between theory and experiment in ESCA, a variety of approaches exist for the calculation of chemical shifts, *inter alia*.

(i) Koopmans' Theorem.[78]

(ii) Core Hole Calculations (ΔSCF).[79,80]

(iii) Equivalent Cores Model.[81]

(iv) Madelung Charge Potential Model.[67]

(v) Quantum Mechanical Potential Model.[82-84]

(vi) Many-Body Formalism.

A complete discussion of the theoretical basis of the physical processes involved in photoemission has been given by Fadley.[85]

2.4 Fine Structure

There are three types of splitting that could occur in photoelectron spectroscopy. Each will be considered in turn, although it is only the spin-orbit interactions which are particularly relevant to this thesis.

2.4.1 Multiplet Splitting

The multiplet splitting of core levels results from the interaction of the spin of an unpaired electron resulting from the photoionisation process with the spins

of other unpaired electrons present in the system under study.[66,86] Many examples are to be found in the core level spectra of transition metal compounds.[87,88]

2.4.2 Spin-Orbit Splitting

If photoionisation occurs from an orbital which has an orbital quantum number (l) greater than 1 (*i.e.* p, d and f) then a doublet structure is observed in the ESCA spectrum. This doublet occurs from a coupling of the two magnetic momenta of the spin (S) and the orbital angular momentum (L) of the electrons to yield a total momenta(J).[88,89] When spin-orbit coupling is weak compared to the electrostatic interactions then

$$L + S = J \qquad \text{(Russell-Saunders Scheme)}$$

Where spin-orbit coupling is large with respect to the electrostatic interactions, then

$$j_1 + j_2 = J \qquad \text{(j-j coupling scheme).}$$

where $j_1 = l_1 + s_1$, *etc.*

It can be shown that the Russell-Saunders coupling scheme dominates for the lighter elements (up to the Lanthanides), and the jj coupling scheme for heavier elements.

The intensities of the signals in the doublet structure observed are proportional to the ratio of the degeneracies of the states which is defined quantum mechanically by the (2J+1) rule.

The relative signal intensities of the J states for the s, p, d and f levels are shown in Table 2.2.

TABLE 2.2 Intensity Ratios for Different Levels

	Orbital quantum number	Total quantum number		Intensity Ratio
s	0	J=(l±s)	$^1/_2$	(2J+1)/(2J+1) no splitting
p	1	$^1/_2$	$^3/_2$	1 : 2
d	2	$^3/_2$	$^5/_2$	2 : 3
f	3	$^5/_2$	$^7/_2$	3 : 4.

Figure 2.3 shows an example of the spin orbit splitting in S_{2p} as observed in the ESCA experiment.

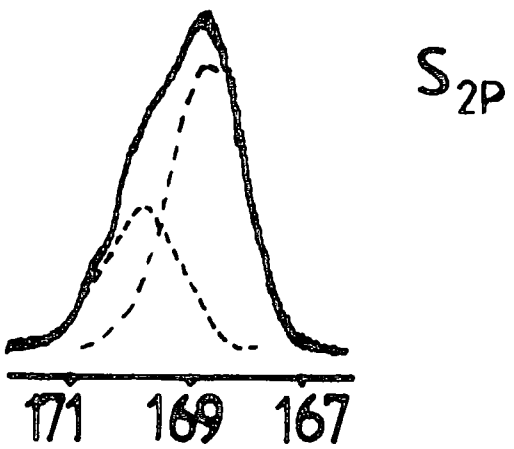

Figure 2.3 Spin-Orbit Splittings in the S_{2p} core level.

2.4.3 Electrostatic Splitting

Some tin, gold, uranium[90] and thorium[91] compounds give rise to this type of splitting which is attributed to the differential interaction between an internal electrostatic field and the spin states of the core level under investigation.[92,93] Since most polymers are inherently amorphous the establishment of such fields is improbable and hence this splitting is unlikely to be seen in polymer systems.

2.5 Sample Charging and Energy Referencing

"Sample charging" arises from the inability of an insulating sample to replace electrons lost by photoemission. An equilibrium situation is established when the photoemission current is balanced by the sample attracting electrons from the sample backing or by the capture of stray electrons from the vacuum system. As a result the sample surface rises to a net positive potential; photoemitted electrons from the sample experience a net retardation and hence appear at higher binding energies.

Charging may be detected by varying the incident electron flux on the sample using a low energy electron flood gun. If charging is present, this extra flux will tend to move the photoelectron peaks to a lower apparent binding energy. The use of flood guns is especially useful in work involving monochromatised X-ray sources;[94] here the secondary electron flux from the adjacent window of an X-ray gun is not present. In its absence, insulating samples may charge dramatically.

An alternative approach to the problem has been to illuminate the sample chamber with UV radiation. Sufficient secondary electrons are generated from the sample chamber walls to reduce charging to a low level.

For insulating samples, or samples not in electrical contact with the spectrometer, energy referencing is not as straightforward as with conducting samples which are in electrical contact with the spectrometer.[70,95] This is because in insulating samples, the Fermi level is not well-defined.

In the case of polymer samples, and indeed, many samples, the most facile method of circumventing the problems of energy referencing caused by sample charging is by the use of a suitable reference peak. The observed shift in this reference peak is then used to correct the binding energies of other peaks observed in the spectra, and thus find their true binding energies. The most commonly used calibration point in polymeric systems is the C_{1s} peak due to ($\underline{C}H_2$) environments, either inherent in the sample or in extraneous hydrocarbon deposited as a contaminant layer in high vacuum at 285.0eV; or the use of the $Au_{4f_{7/2}}$ level at 83.8eV if the sample has been deposited on a gold[2] substrate.

A detailed study of the charging phenomena of polymers has been made by Clark *et al.*[96,97] Sample charging was found to be a very sensitive probe of the outermost few tens of Angstroms of a sample in its own right.

Surface modification of a sample can lead to interesting charging effects. For example, when polytetrafluoroethylene is bombarded with argon ions, loss of fluorine occurs from

the surface and there is a concomitant decrease in charging.[98] Similarly, treatment of cellulose with trifluoroacetic anhydride vapour causes increased charging due to the presence of trifluoroacetate groups at the surface (see Chapter Six).

2.6 Signal Intensities

For an infinitely thick, homogeneous sample, the inelastic photoionisation peak intensity for photoelectrons originating from a core level is given by:

$$dI_1 = F\alpha_1 N_1 k_i e^{-x/\lambda_i} .dx. \quad [99,100] \qquad (2.3)$$

where I_1 = intensity arising from core level 1.

F_1 = exciting incident photon flux.

α_1 = photoionisation cross-section of the core level i.

k_1 = spectrometer factor.

N_1 = number of atoms per unit volume on which the core level is localised.

λ_1 = inelastic mean free path of the emitted electron from core level 1.

Integrating (2.3) gives,

$$I_1 = \int_0^{\infty} F\alpha_1 N_1 k_1 e^{-x/\lambda_1} dx. \qquad (2.4)$$

and $I_i = F\alpha_i N_i k_i \lambda_i$

Examining these parameters further:

F, the X-ray flux depends primarily on the operating power and efficiency of the X-ray gun, α_1, the cross-section for photoionisation[101] for a given core level, i, describes the

probability that a core level will be ionised when irradiated by a given energy, being a function of the core level and the energy of the incident photon. α_i is also dependent upon the angle of detection with respect to the angle of incidence of the incoming photons and is hence weighted to include only those electrons emitted within the solid angle of the analyser lens system. The total photoionisation cross-section, α_i, is given by,

$$\alpha_i = \frac{\alpha_i^{TOT}}{4\pi} \left[1 - \frac{1}{4} \beta_i (3\cos^2\phi - 1\right] \qquad (2.5)$$

where ϕ is the angle between the incident X-rays and the analyser entrance slit (see Figure 2.4).

α_i^{TOT} is the total cross-section of the core level i, and β_i the asymmetry parameter[102] for that level. For a given spectrometer ϕ and hence α_i is normally constant. The cross-sections, α_i, may be calculated from atomic properties or determined experimentally.

k_i, the spectrometer factor is an instrumentally dependent parameter reflecting the efficiency of the detection system and the transmission of analyser to electrons of various kinetic energies, and the solid angle of acceptance of the analyser.

λ_i, the inelastic electron mean free path, is defined as the distance in the solid that electrons of a given energy can travel before $^1/_e$ of them have not suffered energy loss through inelastic collision. λ_i can be determined experimentally,[103] or calculated theoretically.[104]

λ_i, is also a function of electron energy. Hence electrons of energy 80eV have $\lambda_i \simeq 4$Å, and those of energy $\sim$4000eV, $\lambda_i \simeq 40$Å.

ANGULAR STUDIES

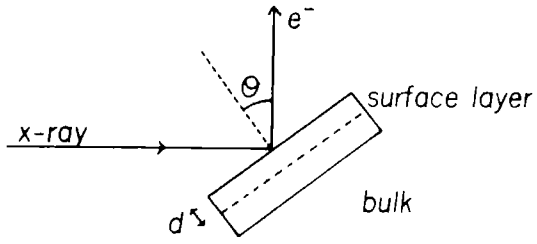

HOMOGENEOUS SAMPLE

$$I = f(\Theta) F \alpha N K \lambda$$

where F is the x-ray flux

α is the cross section for photoionization

N is the number of atoms, on which the core level is localized, per unit volume

K is a spectrometer dependant factor

λ is the mean free path of the electrons

INHOMOGENEOUS SAMPLE

-for the suface layer

$$I = f(\Theta) F \alpha N K \lambda \ (1 - e^{-d/\lambda \cos\Theta})$$

-for the bulk

$$I = f(\Theta) F \alpha N K \lambda \ e^{-d/\lambda \cos\Theta}$$

Figure 2.4 Schematic of sample geometry relative to the X-ray source and analyser.

Another useful quantity is the sampling depth, *i.e.* the depth from which 95% of the signal from a given core level is derived.

$$\text{Sampling depth}_i = -\lambda_i \ln 0.05 \tilde{\sim} 3\lambda_i \qquad (2.6).$$

This is a useful quantity when discussing the surface sensitivity of ESCA data.

Finally, N_i, the number of atoms per unit volume on which the core level is localised. It can easily be seen from equation 2.5, that the relative intensities of core levels will be related to the overall stoichiometry of the atoms in the surface. Hence, for two core levels, i and j

$$\frac{I_i}{I_j} = \frac{F\alpha_i N_i k_i \lambda_i}{F\alpha_j N_j k_j \lambda_j} \qquad (2.7)$$

If i and j correspond to different chemical environments of the same core level, then

$$\frac{I_i}{I_j} = \frac{N_i}{N_j} \qquad (F\alpha_i N_i k_i \lambda_i = F\alpha_j N_j k_j \lambda_j)$$

If, however, $i \neq j$ then,

$$\frac{N_i}{N_j} = \frac{I_i}{I_j} \left[\frac{k_j \alpha_j \lambda_j}{k_i \alpha_i \lambda_i} \right]$$

The bracketed quantity, is known as the sensitivity factor, and can be determined experimentally from samples of known stoichiometry. These quantities are spectrometer dependent.

2.7 Analytical Depth Profiling

It can easily be seen from equation 2.4 that the sampling depth of the sample can be altered by changing θ, (*i.e.* the angle of the escaping electrons with respect to a direction normal to the samples surface - see Figure 2.4). Hence electrons emitted from a point a depth d below the sample's surface thus travel a distance $d/\cos\theta$ in the sample to escape. Due to the short mean free paths of electrons, by varying the "take-off" angle (θ) it is possible to analyse electrons originating from surface and sub-surface regions of the polymer.[105] This relationship only applies to flat surfaces. In this thesis, the majority of the samples are fibrous and hence analytical depth profiling *via* take-off angle measurements is invalid.

To enable depth profiling of fibrous or powder samples a further two techniques can be employed. The first is to use $Ti_{k\alpha_{1,2}}$ X-ray radiation (4510eV). If this radiation is used, the kinetic energies of the emitted electrons from the same levels as studied with the softer $Mg_{k\alpha_{1,2}}$ source (1253.6eV), will be correspondingly higher and hence possess a greater sampling depth (equation 2.6).

Given the same exciting photon energy, the ratioing of two core levels from a given atom (*e.g.* the O_{1s} and essentially core-like O_{2s}) will serve as a measure of the vertical homogeneity of the surface.

Thus from a combination of variable take-off angle measurements over a series of levels and by the use of a variety of X-ray sources, a depth profile of the distribution of various components in a surface may be built up.

Often in the analysis of polymer surfaces by ESCA the situation is encountered where the composition of the surface layers differs from that of the bulk or subsurface; there may be a smooth gradient from a surface composition to the bulk composition with depth, or more commonly, a contamination layer may be present on the surface. The latter case shall now be considered theoretically, from which a treatment of the former may be developed:

Consider the case as shown in Figure 2.4, where an overlayer of depth d, of differing composition to the substrate, is present.

The signal arising from the overlayer alone can be expressed from equation 2.3 on integration between the limits x=0 to x=d.

$$I_1^{over} = F\alpha_i N_i k_1 \lambda_i \ (1-e^{-d/\lambda_1}) \qquad (2.8)$$

By integrating between the limits x=d to x=∞, the signal arising from the substrate is:

$$I_j^{sub} = F\alpha_j N_j k_j \lambda_j \ (e^{-d/\lambda_j}) \qquad (2.9)$$

Equations 2.8 and 2.9 are derived in the case where the photoelectrons escape normal to the surface. From Figure 2.4 it is evident that these equations can become angularly dependent,

i.e. $$I_i^{over} = F\alpha_i N_i k_1 \lambda_i \ (1-e^{-d/\lambda_i \cos\theta}) \qquad (2.10)$$

and $$I_j^{sub} = F\alpha_j N_j k_j \lambda_j (e^{-d/\lambda_j \cos\theta}) \qquad (2.11).$$

Thus, it can be seen that as $\theta \rightarrow \pi/2$, the signals derived from the overlayer come to dominate the spectra. Similarly,

by using a harder X-ray source (*e.g.* $Ti_{k\alpha_{1,2}}$), F and λ increase giving the same effect as changing the angle. Thus the attenuation of a signal derived from the substrate by an overlayer will depend strongly on the kinetic energy of the photoemitted electron. This will be discussed further in Chapter Six.

2.8 Linewidths and Lineshape Analysis

ESCA spectra have large inherent linewidths comparable in magnitude to the magnitude of the chemical shifts in the system.[69] The dominating contribution to broad linewidths comes from the inherent linewidths of the polychromatic X-ray photon source normally used.

The measured linewidth for a core level may be expressed as a convolution of several effects.

$$(\Delta E_m)^2 = (\Delta E_x)^2 + (\Delta E_s)^2 + (\Delta E_{cl})^2 \qquad (2.12).$$

where ΔE_m = observed full width at half maximum (FWHM) of the photoelectron peak.

ΔE_x = the FWHM of the exciting X-ray source *ca.* 0.7eV for $Mg_{k\alpha_{1,2}}$.

ΔE_s = spectrometer contribution to the FWHM (*i.e.* analyser aberrations, slit widths *etc.*).

ΔE_{cl} = natural line width of the core level. This also includes solid state broadening effects not directly associated with the life-time of the core-hole state for solid samples, including variations in chemical shift due to differences in lattice environments.

The inherent broad linewidths necessitates the use of curve-fitting procedures for accurate lineshape analysis to delineate the core level environments within a given envelope. The convolutions to the overall line shape of the X-ray source and the core-level are essentially Lorentzian in character, however the spectrometer resolution function represents a Gaussian contribution[67] to the overall line shape. The convolutions of these factors leads to a hybrid shape which is essentially Gaussian with some Lorentzian character in the tails. For insulators, it has been shown that the assumption of a pure Gaussian lineshape introduces only a small error in the lineshape analysis.

In the analysis of peak profiles both analogue and digital aids are available.[66,70] Such systems allow close control to be exercised over the positions, widths and heights of the component variables. However, such curve-fitting procedures require a sound theoretical background to obtain meaningful results; the solutions produced are rarely unique and must be examined in a chemical content.

In the work in this thesis, curve-fitting has been performed both by analogue simulation (using a Dupont 310 curve resolver) and digitally, (using the data analysis software of the DS300 data system).

The work presented in this thesis was carried out on two spectrometers, an AEI ES200AA/B and a customised KRATOS ES300 spectrometer. Details of these electron spectrometers are presented in Appendix One of this thesis.

2.9 An Appraisal of ESCA

ESCA is an extremely powerful tool with wide ranging applicability. The principle advantages of the technique may be summarised as follows:

(i) The sample may be solid, liquid or gas. The sample sizes are small, *e.g.* 10^{-3}g for solids, 0.1µl for liquids and 0.5 cm^3 for gases at STP.

(ii) The technique is essentially non-destructive.

(iii) The technique is independent of spin properties of the nucleus and can be used to study any element Z>2.

(iv) Materials may be studied *in situ* easily.

(v) ESCA provides a large number of information levels.

(vi) ESCA has a higher sensitivity than many other analytical techniques as shown in Table 2.4.

TABLE 2.4 Sensitivities of Various Analytical Techniques

Bulk Techniques	Minimum Detectable Quantity (g).
Infra-red absorption	10^{-6}
Atomic absorption	10^{-9} - 10^{-2}
Vapour Phase Chromatography	10^{-3} - 10^{-7}
High Pressure Liquid Chromatography	10^{-6} - 10^{-9}
Mass Spectrometry	10^{-9} - 10^{-15}
Surface Techniques	
ESCA	10^{-10}
Neutron Activation Analysis	10^{-12}
X-ray Fluorescence	10^{-7}
Ion Scattering Spectrometry	10^{-15}
Auger Emission Spectrometry	10^{-14}
Secondary Ion Mass Spectrometry	10^{-13}

(vii) The data is often complementary to that obtained by other methods.

(viii) ESCA has the capability of distinguishing surface and subsurface or bulk in solids.

(ix) The information from ESCA relates to the binding and molecular structure of the molecule. This allows a thorough analysis of the electronic structure of the system to be made.

(x) The theoretical basis is well understood. Hence *ab initio* investigations are possible.

The disadvantages of ESCA are few:

(i) The purchasing cost and maintenance are high.

(ii) Spatial resolution is poor; $\sim$0.3 cm^2 is normally sampled.

(iii) If the surface differs from the bulk, it is not possible to say anything about the bulk structure by means of ESCA without sectioning the sample.

CHAPTER THREE

THE NITRATION AND DENITRATION OF CELLULOSIC MATERIALS: A TIME DEPENDENCE STUDY

3.1 Introduction

A considerable volume of literature has appeared over the past eighty to ninety years concerning the technical nitration of cellulosic materials.[4,30] Although both the displacement[8] and "technical" processes[8] have been thoroughly investigated, there still remains a surprising number of important, fundamental questions left unanswered. It is, however, generally accepted that in most conditions employed in the technical nitrations (media, temperature, *etc.*) the final bulk DOS is governed by thermodynamics as opposed to an accessibility argument.

It is not inconceivable that cellulose nitrates of the same degree of substitution prepared by displacement or technical processes may be structurally different according to the nitrating and quenching procedures employed.[4] This has, in fact, recently been suggested by results of Lewis[56] from optical path difference measurements. The role of the quenching and stabilisation procedures in cellulose nitrates will be discussed in Chapter Five of this thesis. As outlined in Chapter One, Clark and Stephenson[43,45] made advances into the structure of nitrocelluloses prepared *via* nitration and denitration, using high resolution ^{13}C nuclear magnetic resonance techniques, ESCA and X-ray spacings. These studies have shown how this combination of techniques has led to additional insight into the kinetics and mechanism of surface *versus* bulk nitration and denitration of cellulosic materials.

The investigation of nitration-denitration reactions of cellulosic materials as a function of time particularly over

extended periods has a long and chequered history. Using classical microanalytical techniques, Berl and Klaye[26] showed that in a mix of composition 60% H_2SO_4, 22.5% HNO_3, 17.5 % H_2O, denitrated material of high starting degree of substitution and unnitrated material reached the same DOS after a period of a few days at room temperature. The DOS decreased with sample disintegration after extended periods of fifteen days or so.

Demougin[28] and Bonnet[29] extended this work and showed that nitration and denitration gave materials with the same DOS after a certain length of reaction, but there was a trend to lower DOS for both the initially unsubstituted and nitrated materials after extended periods of time > 20 days in a mix identical to that employed by Berl and Klaye.[26] The comparison between these two studies emphasizes the dependence of the stability as a function of time on the characteristic molecular weight distribution, physical form (*e.g.*, paper, linters, *etc.*) of the samples employed.

In this chapter, ^{13}C nuclear magnetic resonance spectroscopy, ESCA, scanning electron microscopy, X-ray diffractometry and micro-Kjeldahl analyses are used to investigate the time dependence of the surface and bulk, gross and fine structural features of cellulosic materials exposed to nitration and denitration in a medium of given composition.

3.2 Experimental

In this section the basic procedures for preparation of nitrated and denitrated material used throughout the work

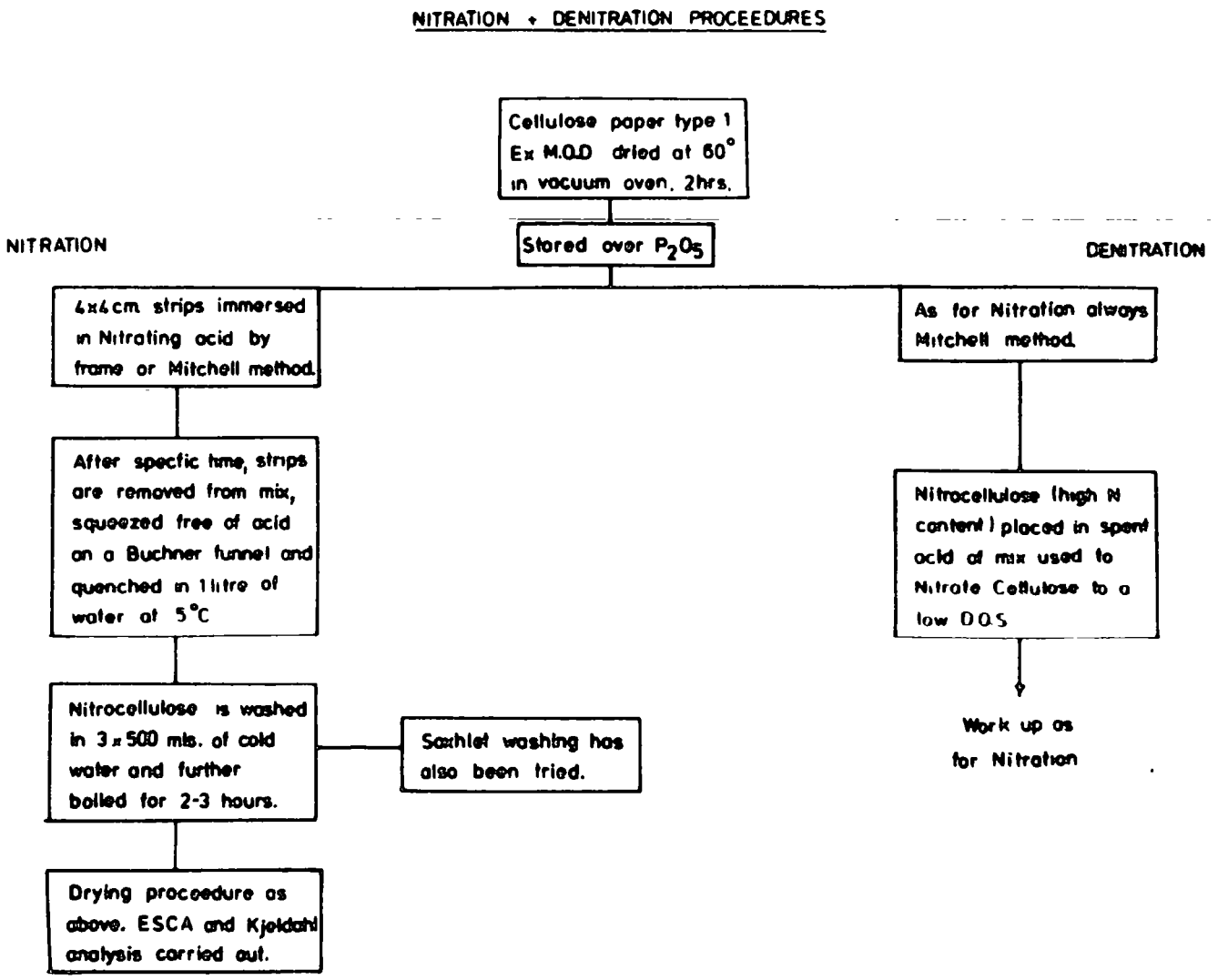

Figure 3.1 Schematic of the preparative methods of nitration and denitration

presented in this thesis are outlined. It is important to specify both the source of raw cellulose and the methods used to nitrate since both can be a major source of variability.[4]

The general procedures are indicated schematically in Figure 3.1.

Commercially produced, (Hercules Powder Company), linters (in the form of linters or papers) were used. The original cotton of American origin was dewaxed and depectinised. A Shirley fluidity of 8.8, and approximate degree of polymerisation 1100 was recorded for the linters which were vacuum dried at 60°C for two hours and stored over phosphorus pentoxide for several days before use. This provides a starting cellulose with <2% water content.

Nitrations and denitrations were accomplished by immersion in the appropriate acid mix of sample strips for a given period of time using an apparatus such as that depicted in Figure 3.2. The starting material for denitration used in this study were prepared in the Mitchell[33] mix and gave a 2.83 DOS cellulose nitrate. The reaction (nitration and denitration) was accomplished in an acid mix of composition 60% H_2SO_4, 22.5% HNO_3 and 17.5% H_2O.

Bulk nitrogen determinations have been carried out using a modified micro-Kjeldahl technique (see Appendix II).

The ^{13}C spectra were recorded on (a) a Varian HL200 spectrometer, proton noise decoupled (75.5 MHz); typical acquisition time of ∿12 hours, or, (b) a Bruker WH-360 spectrometer, proton noise decoupled (90.56 MHz); typical acquisition

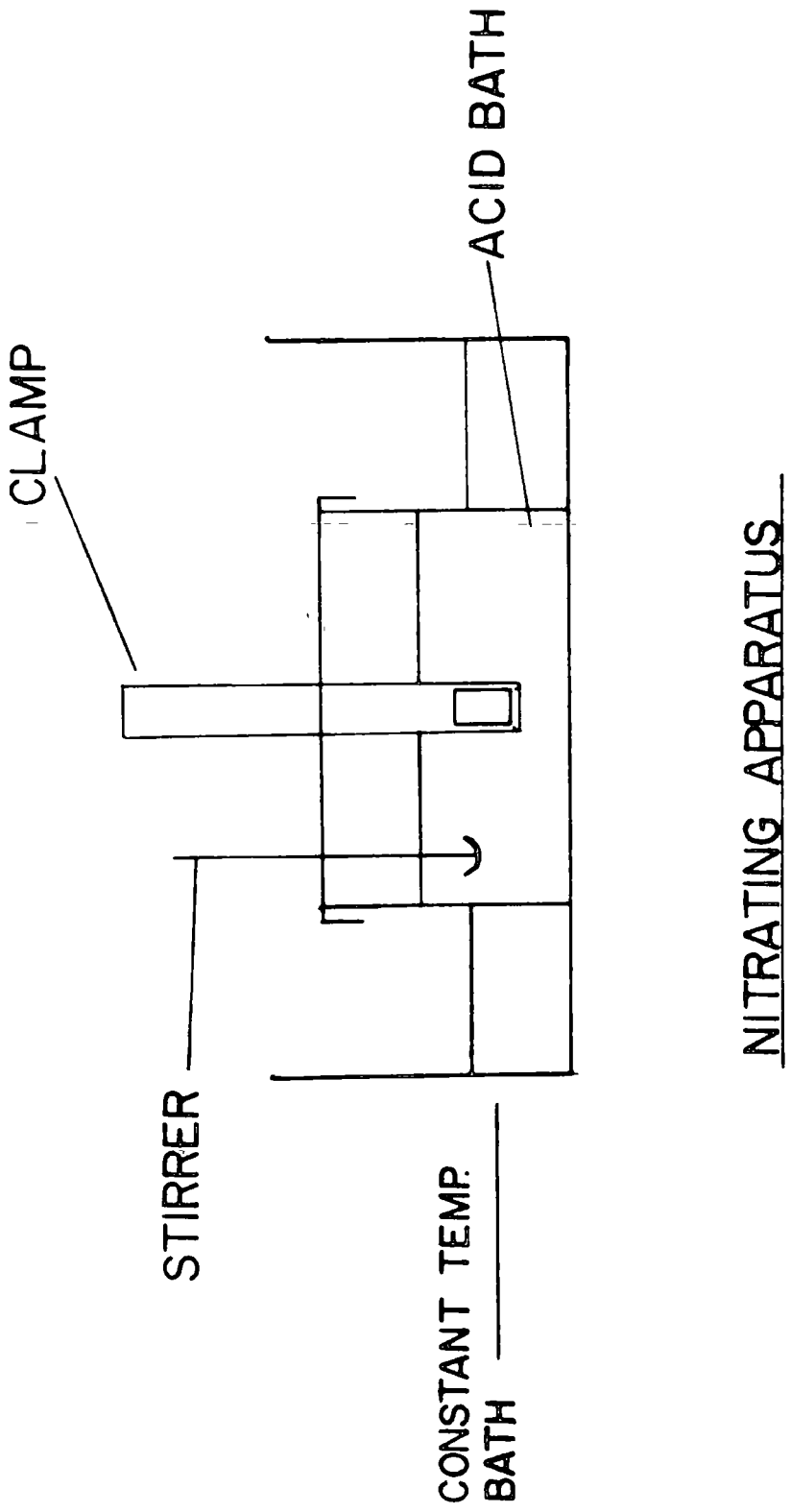

Figure 3.2 Apparatus used for the nitration of cellulose

times of ∿16 hours. In both cases, 10% by weight solutions of the polymer were made up in dimethylsulphoxide-d_6. The carbon chemical shifts are reported with respect to the internal tetramethylsilane (TMS, Me_4Si) reference. Area ratios were determined from the analogue spectrometer outputs by tracing and weighing. Low temperature (25-29°C) n.m.r. spectra were recorded, but were found to be broad and show poor resolution due to the solution's high viscosity. Hence high temperature (∿80°C) conditions as used by Wu[46] were employed. This high temperature gave discoloured solutions and additional small peaks on long acquisition times (*c.f.* data in ref. 46).

The X-ray diffractometer employed was a Phillips P.W.1130 3kW X-ray generator incorporating a P.W.1050 diffractometer assembly (Cu tube operating at ∿40kV, 25mA). The recordings span from 4° in 2θ to 20° in 2θ and the mean d(110) spacing is taken as the centre of the peak occurring at around 12° in 2θ.

The ESCA spectra were recorded on an AEI ES200 AA/B and a customised Kratos ES300 electron spectrometer, employing a Mg anode, as outlined in Appendix I.

3.3 Results and Discussion

3.3.1 Detailed Studies of Surface Nitration and Denitration

In this section two sets of data were taken. The experiments are exactly similar in all respects except the form of cellulose used. In the preliminary experiment cellulose

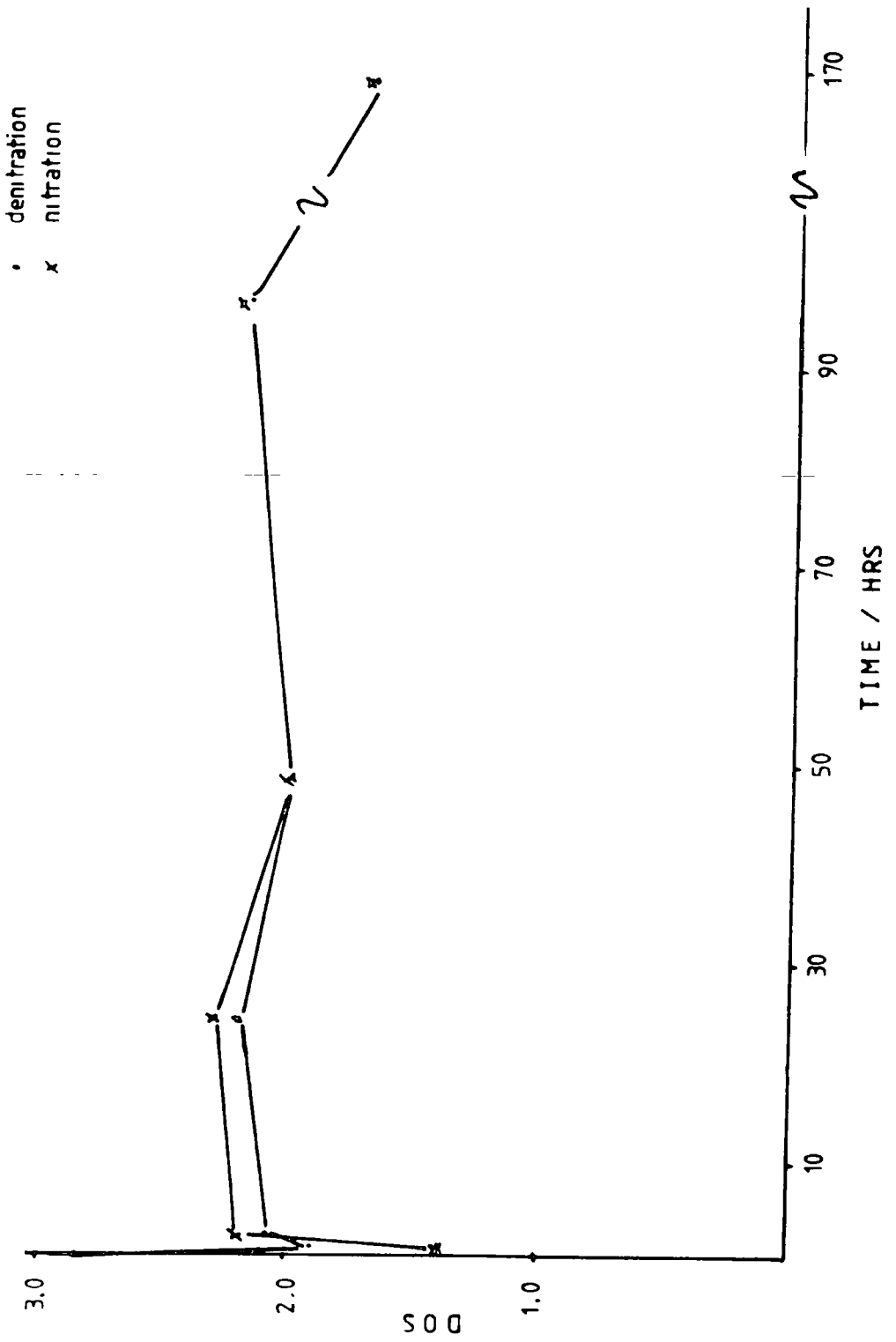

Figure 3.3 Surface DOS *versus* time for nitration and denitration

was taken in the form of papers (type K300 cellulose). In the latter, more precise experiment, cellulose Type K300 linters were used and were pressed into 20 mm discs using a standard Specac press (type 25.011) before analysis *via* ESCA. Figures 3.3 and 3.5 show the dependence of surface DOS against time for both sets of data.

Considering the nitration of cellulose papers shown in Figure 3.3, it is clear that within experimental error, the DOS within the top 50Å is established after one hour at ∿2.2. However after four days there is a drop in the surface DOS. The sample after 168 hours is physically degraded and appears as a powdery material. Figure 3.4 shows spectra after two hours and 168 hours nitration. It is evident from these spectra that the sample's surface chemistry is similar, *i.e.* the sample after 168 hours is not chemically different, but physically different from that at 2 hours.

The sample after one hour nitration time has a particularly low surface DOS. It has been shown by Clark and Stephenson[11] that the surface DOS is reached within one second and is maintained for reaction times up to ∿4 hours. The reaction at one hour was repeated several times, and gave in each case a lower DOS than expected. It was noticed that this sample when taken out of the reaction mixture was brittle and very difficult to mount on a sample probe tip. It must be stressed that this brittleness is not due to localised heating effects that may take place in the quenching and stabilisation procedures, but is a product of this particular acid media and time. The samples at either side of one hour nitration time are normal in respect to their physical characteristics.

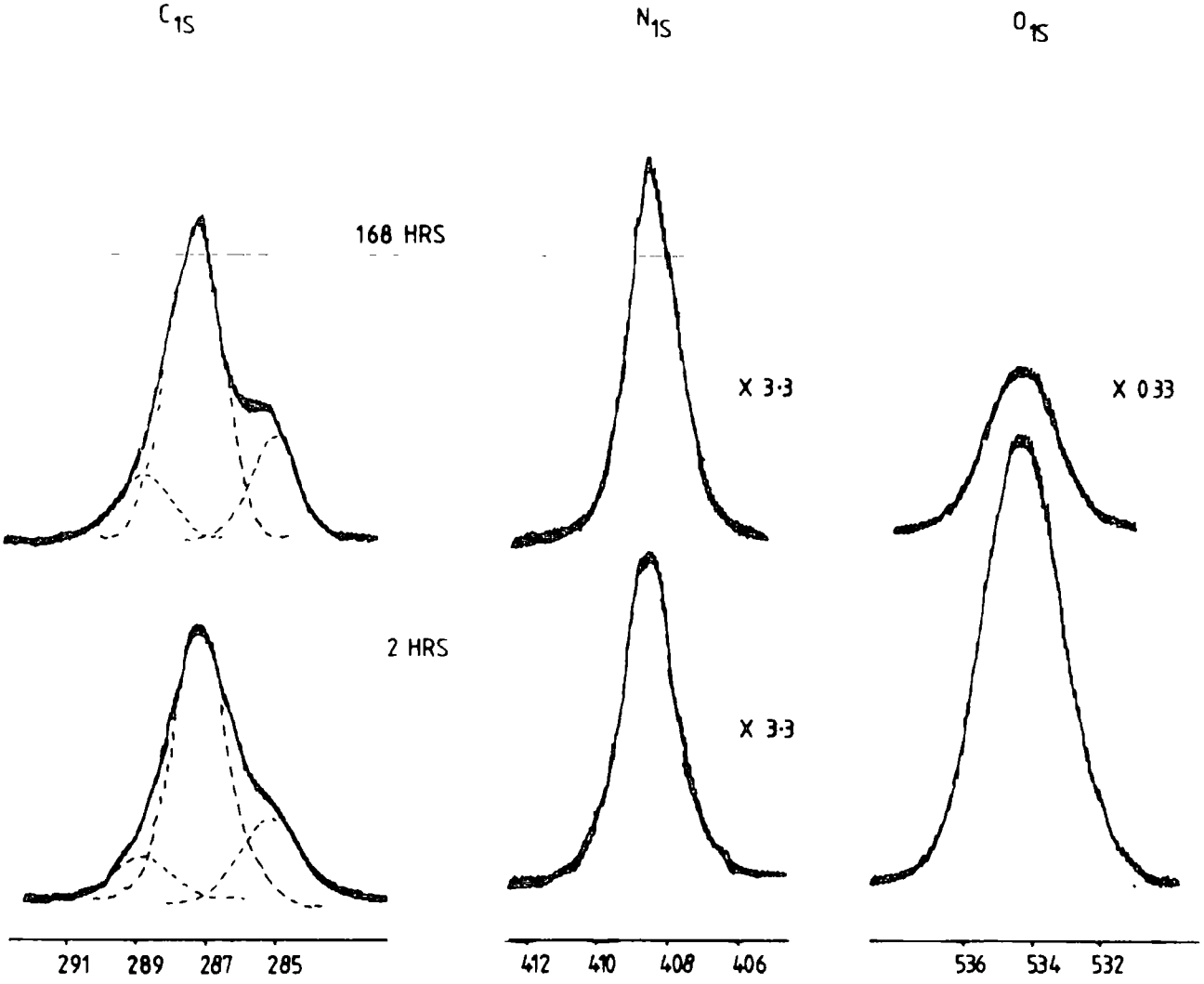

Figure 3.4 C_{1s}, O_{1s} and N_{1s} core level spectra for samples nitrated for 2 and 168 hours

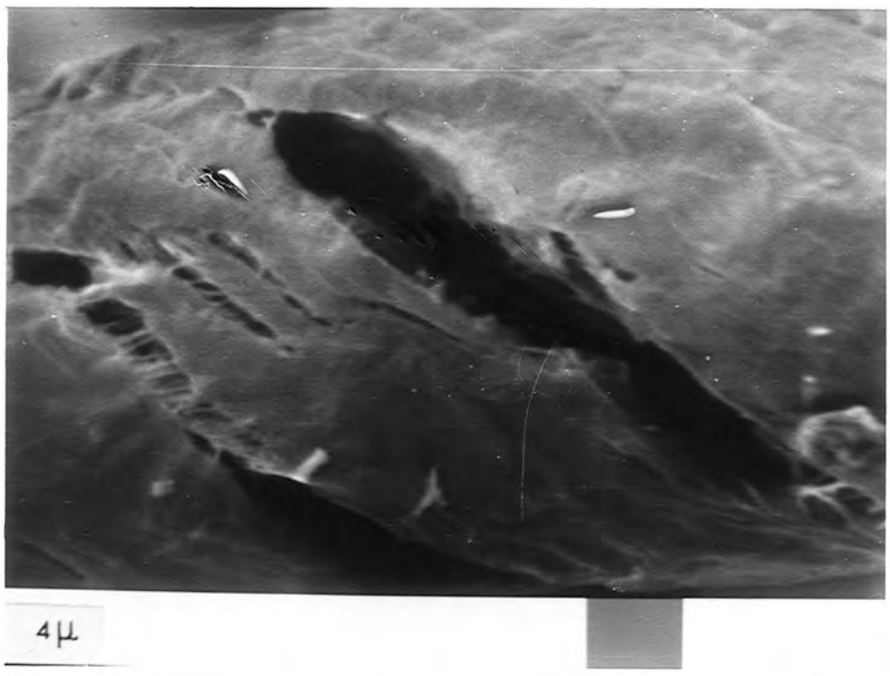

Plate 1 Scanning electron micrograph of the sample nitrated for 1 hour

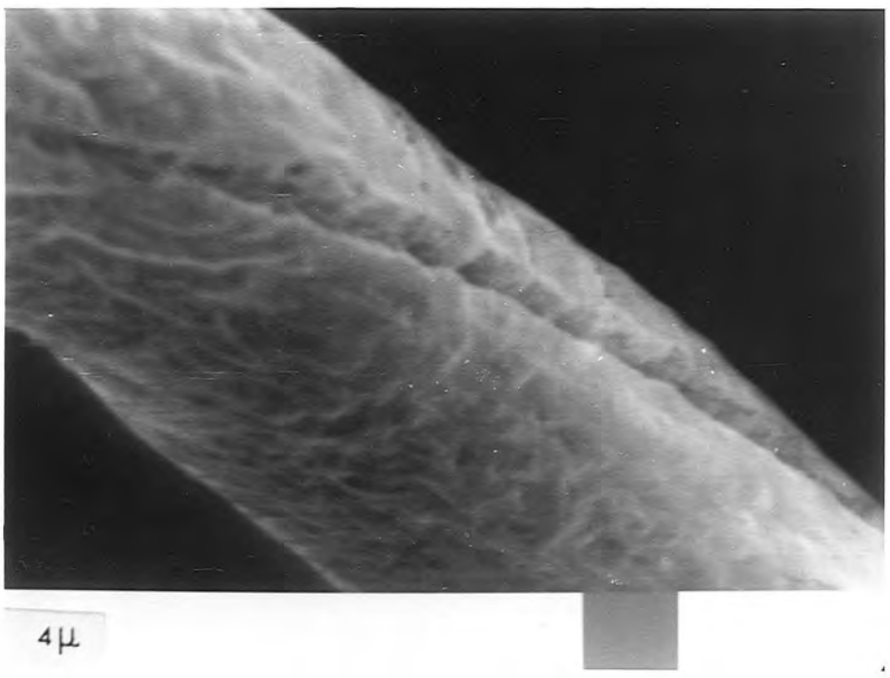

Plate 2 Scanning electron micrograph of the sample nitrated for 2 hours

In the initial stages of the reaction the changes in interchain spacing (see later) in the surface and sub-surface will be different than for the deep bulk. These differences in dimensions could physically be the basis for internal stress and this may be relieved by cracking.

Scanning electron micrographs of the samples after one hour and 2 hours were taken. These are shown in Plates 1 and 2. It can be clearly seen that the sample nitrated for one hour has large crevices normal to the fibre axis. It is these crevices that must lead to the brittleness of this sample. Further discussion of this interesting phenomenon will be addressed later in this chapter.

The denitration reaction in this study is shown in Figure 3.3. It is evident that denitration of a 2.83 DOS cellulose nitrate reaches the same surface DOS as of that produced *via* nitration after 2 hours. From this experiment it may be deduced that the nitration-denitration equilibria involved is thermodynamically controlled in the top 50Å of the surface and that the nitration of cellulose and the denitration of cellulose nitrate is a truly equilibrium reaction. This point will be addressed at a later stage of this chapter.

In a subsequent, more precise experiment the surface nitration-denitration of cellulosic material was performed. The experiment is similar to that previously mentioned, except the physical form of the cellulose is altered (i.e. linters rather than paper). The graphs of DOS *versus* time are depicted in Figure 3.5 for the nitration and denitration reactions.

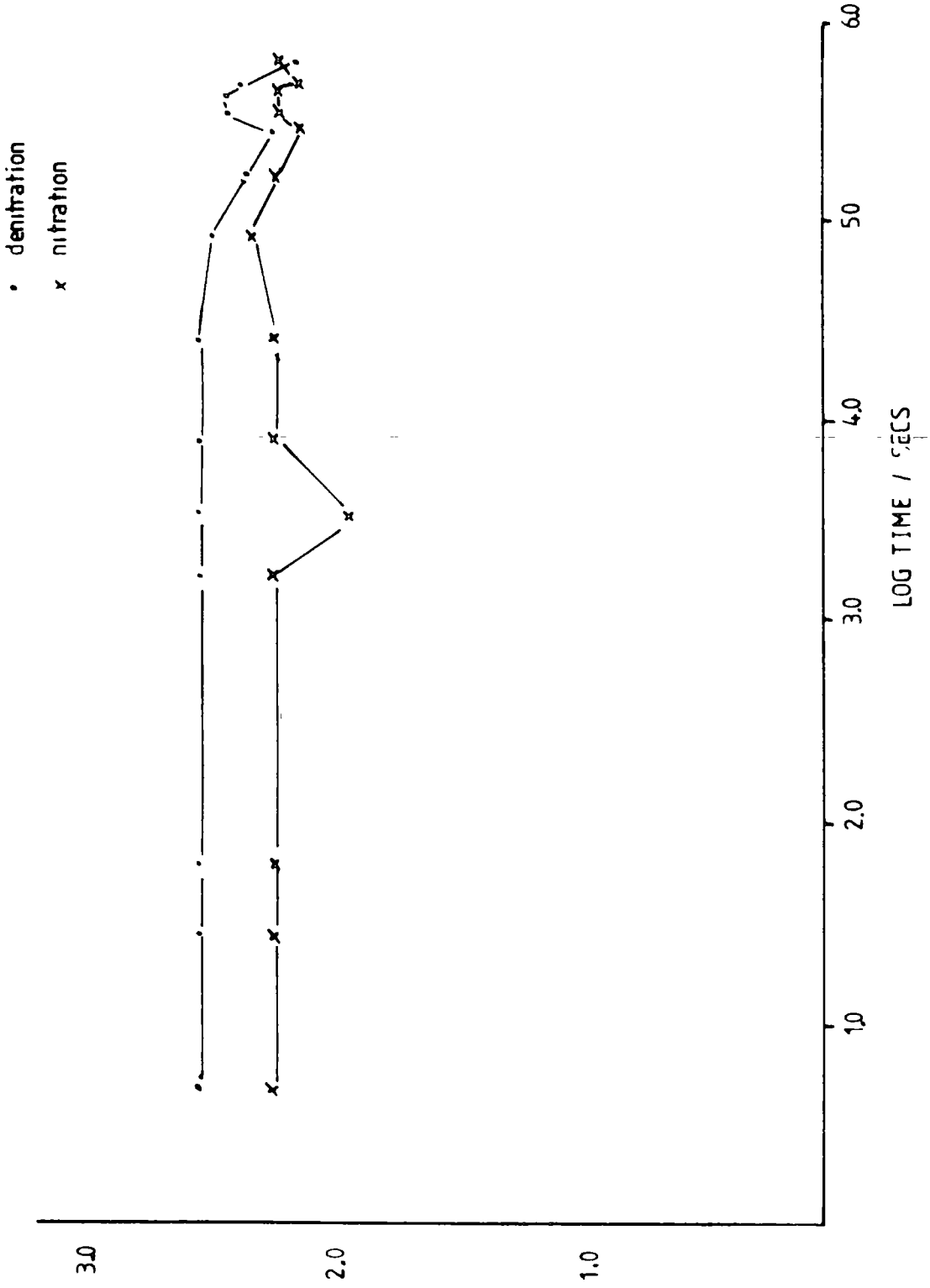

Figure 3.5 Surface DOS *versus* lg. time for nitration and denitration

Clearly the nitration of cellulose graph shown mirrors closely that shown in Figure 3.3. However, it is the denitration cycle that differs markedly, in that the surface DOS plateaus out at a DOS of 2.5 for reaction times less than seven hours. After seven hours the DOS becomes similar to that shown in the previous experiment. The plateau at a DOS of 2.5 must indicate the role of the cellulose physical characteristics, *i.e.* linters, as opposed to paper cellulose, must play a large part in the initial stages of the reaction presumably due to diffusion of the acid media into the cellulose nitrate structure.

Again, the low DOS at one hour nitration time is prevalent and electron micrographs show the crevices within the sample.

Further discussions of these findings are presented in Section 3.3.2.

3.3.2 Detailed Studies of the Bulk Nitration and Denitration

In this section, ^{13}C n.m.r., X-ray diffractometry and micro-Kjeldahl analytical techniques have been used to monitor the bulk nitration and denitration of cellulosic materials. The samples used are those described earlier in Section 3.2.

It is pertinent to review the methods used in analysing the ^{13}C n.m.r. spectra and X-ray d(110) spacings, before considering the data.

As was alluded to in Chapter One of this thesis, one of the most intriguing aspects of the nitration and denitration of cellulosic materials is the substantial change in interchain spacings (d(110)) as a function of degree of substitution.[10] The fact that such spacings differ for materials of the same DOS produced by either nitration or denitration must reflect the detailed differences in chemical microstructure and substitution patterns in individual and sequences of β-D-glucopyranose residues.

The first indication that equilibrium DOS at different sites in the glucose residues were not the same, came from the iodination experiments of Murray and Purves.[108] By specifically displacing primary nitrate esters by iodide, it was shown that the partial DOS for the primary (C6) site in any cellulose nitrate was always greater than that for the secondary sites (C2 and C3). However, with materials of DOS>2, considerable degradation occurs during the reaction.

An important advance in this area has recently been reported by Wu in an n.m.r. study.[46] It has proved possible to assign the components in the region of ∿100 ppm. to the low field of TMS, to the anomeric (C1) carbon in the variously substituted glucose residues. This demonstrated unambiguously that the equilibrium partial DOS is in the order C6>C2 C3. An analysis based solely on the anomeric carbons has certain inherent weaknesses which can largely be eliminated by using the remainder of the ^{13}C data originating from C2-C6 once appropriate assignments of Clark and Stephenson[47] have been made.

PEAK NO.		ASSIGNMENT
1	C1 in	3,6-disub
2	C1 in	6-mono
3	C1 in	2,3,6-tri
4	C1 in	2,6-di
5	C3 in	3,6-di
6	C2 in	2,6-di
7	C3 in	2,3,6-tri
8	C4 in	2,3,6-tri (remains constant)
9	C2 in	2,3,6-tri
10	C2 in	3,6-di
11	C6 & C5	(coincident in frequency and shift insensitive to remaining substitution pattern)

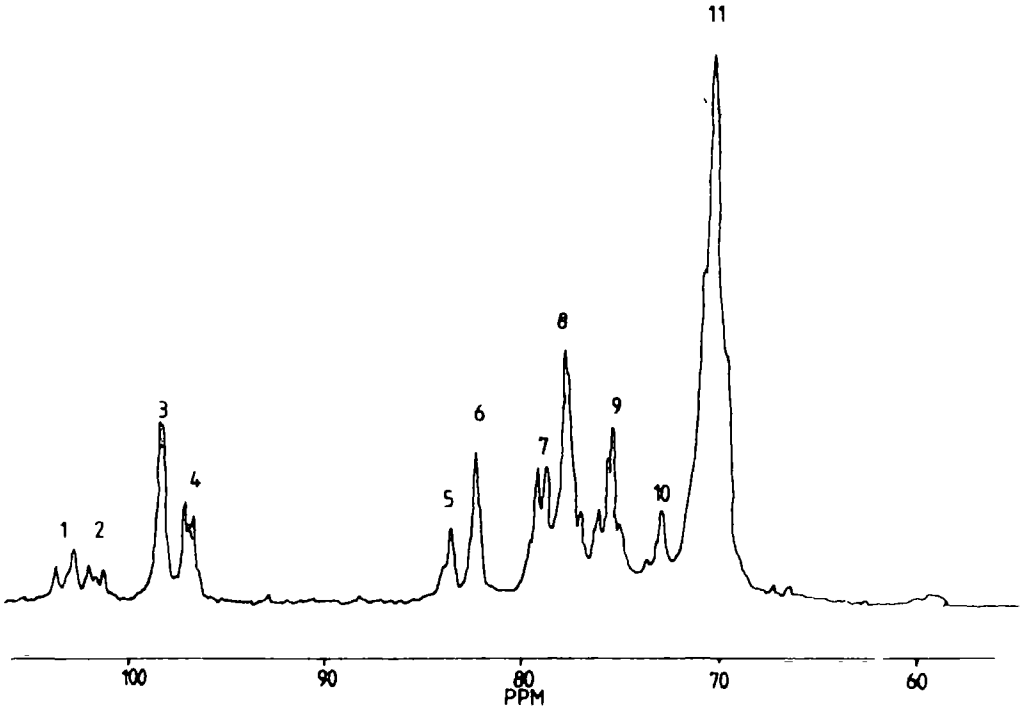

Figure 3.6 ^{13}C n.m.r. (90.56 MHz proton decoupled), spectrum of a nitrated material of DOS 2.2

The spectrum shown in Figure 3.6 (the spectrum is for a nitrated material for 2.5 hours in acid mix 60% H_2SO_4; 22.5% HNO_3; 17.5% H_2O) has been assigned. The components at 99.7 and 98.4 ppm. are well resolved and assigned to the anomeric carbon in trisubstituted and 2,6-disubstituted residues respectively. The component at 85.2 ppm. arises from C3 in 3,6-disubstituted glucose residues whilst the component at 83.2ppm. corresponds to C2 in 2,6-disubstituted glucose residues. As will become apparent, the Nuclear Overhauser Enhancements (NOE) for C1-C5 are essentially the same so that the ratio of the peak areas allows the direct determination of the ratio of disubstituted products. Taken in conjunction with the total integral for the lowest field region for the anomeric carbons and the area ratios for the two higher field components, this allows a partitioning of substitution pattern into tri-, di-, and monosubstituted glucose residues. The intense components at 80.2, 79.1 and 76.9 ppm. are then assigned to C3, C4 and C2 respectively, in the trisubstituted glucose residues. The minor component at 74.5 ppm. arises from C2 in the 3,6-disubstituted residues and its intensity is the same as that of the component at 85.2 ppm. arising from C3 in the 3,6-disubstituted residue as required by this assignment. It should also be noted that the intensity of the component at 83.2 ppm. arising from C2 in the 2,6-disubstituted residues is the same as that of the highest field component of the anomeric carbon region, again as required for a consistent assignment. The intense peak at 71.6 ppm. corresponds to C6 nitrated material (shift insensitive to remaining substitution pattern) and to C5 which

is coincident in frequency. Since one would anticipate that C5 would have a comparable NOEto C2-C4 one may subtract the ratioed intensity of the C5 component from the total integrated intensity for the component at 81.6 ppm, and this provides an estimate of the correcting factor to account for the unexpected difference in NOE for the methylene group of C6. The factor of 1.5 derived from this analysis has then been used to estimate the extent of non-nitrated glucose residues in appropriate cases from an analysis of the component at 60.5 ppm. assigned to C6 ($-CH_2-OH$).

With respect to the anomalous X-ray d(110) lattice spacings it is interesting to address the available data for information pertaining to sequence distribution in cellulose nitrate chains. Trommel[10] has suggested that material prepared by denitration of high DOS material is likely to consist of large chain segments of fully nitrated material adjacent to segments of unnitrated glucose residues. Thus, it was postulated, that denitration is more probable in residues adjacent to those already of low DOS.

Clark and Stephenson[47] addressed this important and interesting question and using a knowledge of the assignment of peaks in the ^{13}C n.m.r. spectra, have modelled the most probable octad sequence distribution patterns. For a sample of cellulose nitrate (1.9 DOS) prepared by nitration in an acid mix 53% HNO_3, 20% H_2SO_4 and 27% H_2O, the distribution data from the ^{13}C n.m.r. analysis is:

Tri	2,6	3,6	Mono	Unsubstituted.
36	23	14	10	17

The analysis can be simplified approximately in terms of decad sequence *viz.* the ratio of tri:2,6:3,6:6:unsubst. is approximately partitioned 4:2:1:1:2. On the basis of a random substitution pattern one would predict a probability of 0.5(5/10) that a 3,6-disubstituted residue in this material would be adjacent to another 3,6- or trisubstituted residue, *i.e.* have a nitrate ester group at the C3′ position. However, the integrated area ratio reveal a probability close to 0.25. The calculation was repeated for the peak at highest field in the anomeric region (∿98 ppm.) due to C1 in 2,6-disubstituted residues. Again the probability due to random substitution did not correlate with the integrated area ratios. Hence Clark and Stephenson[47] concluded that the substitution is far from random, and that the nitrate ester equilibrium favours short blocks of fully substituted residues with short blocks of lower DOS residues. This is not unreasonable since Clark *et al*[45] have previously argued that the rate constants for nitrate ester formation at a given site in a glucose residue must increase as the DOS increases in that residue. By the same token, substitution in adjacent residues may well therefore increase the rate of nitration such that a block structure develops.

In this section, we shall consider a ^{13}C n.m.r. investigation of the time dependence of the gross and fine structural features of cellulosic materials exposed to nitration and denitration in a medium of given composition.

Figure 3.7 shows typical high resolution ^{13}C n.m.r. spectra for cellulose papers (K300), nitrated and denitrated for one hour (a) and 48 hours (b) respectively. The spectra

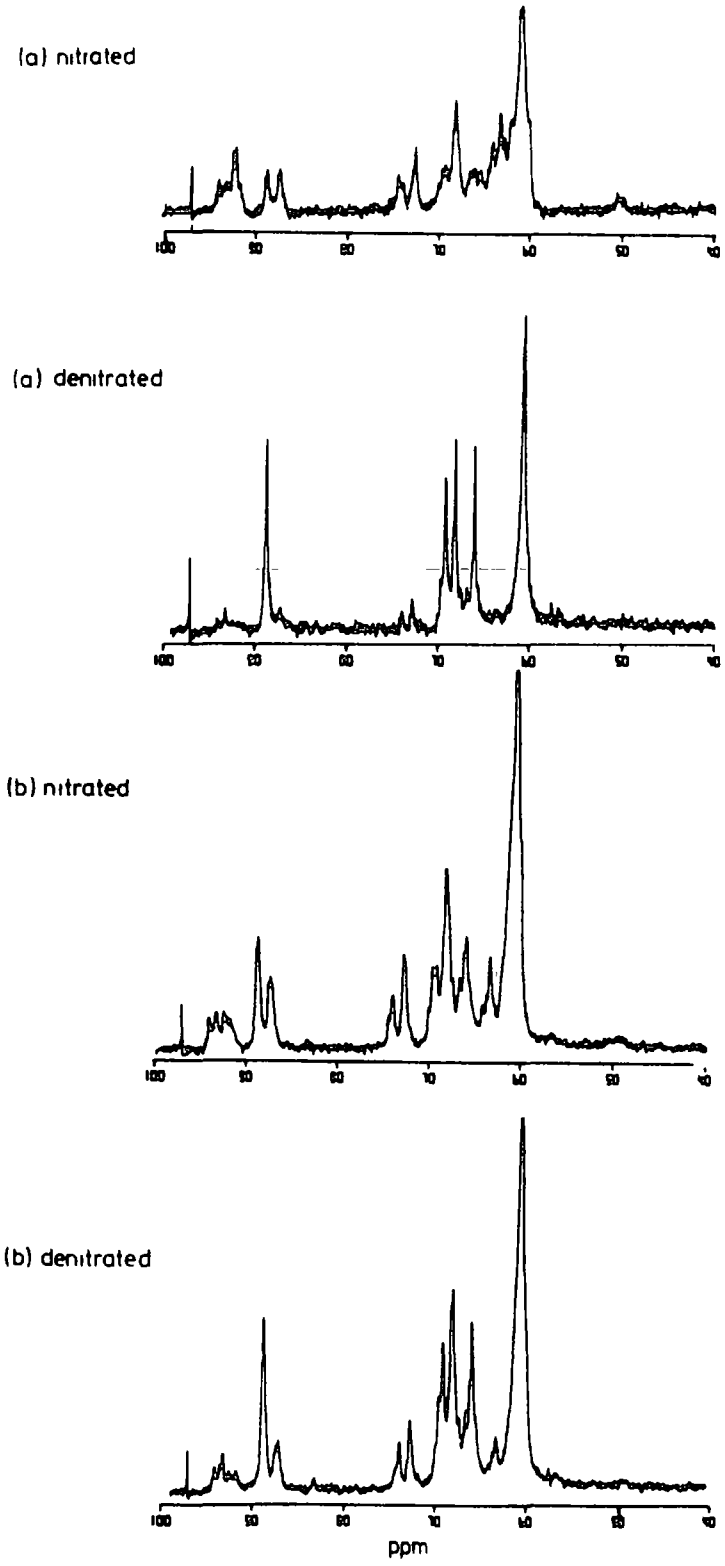

Figure 3.7 ^{13}C n.m.r. (75.5 MHz) solution spectra of samples denitrated and nitrated for (a) 1 hour, and (b) 48 hours.

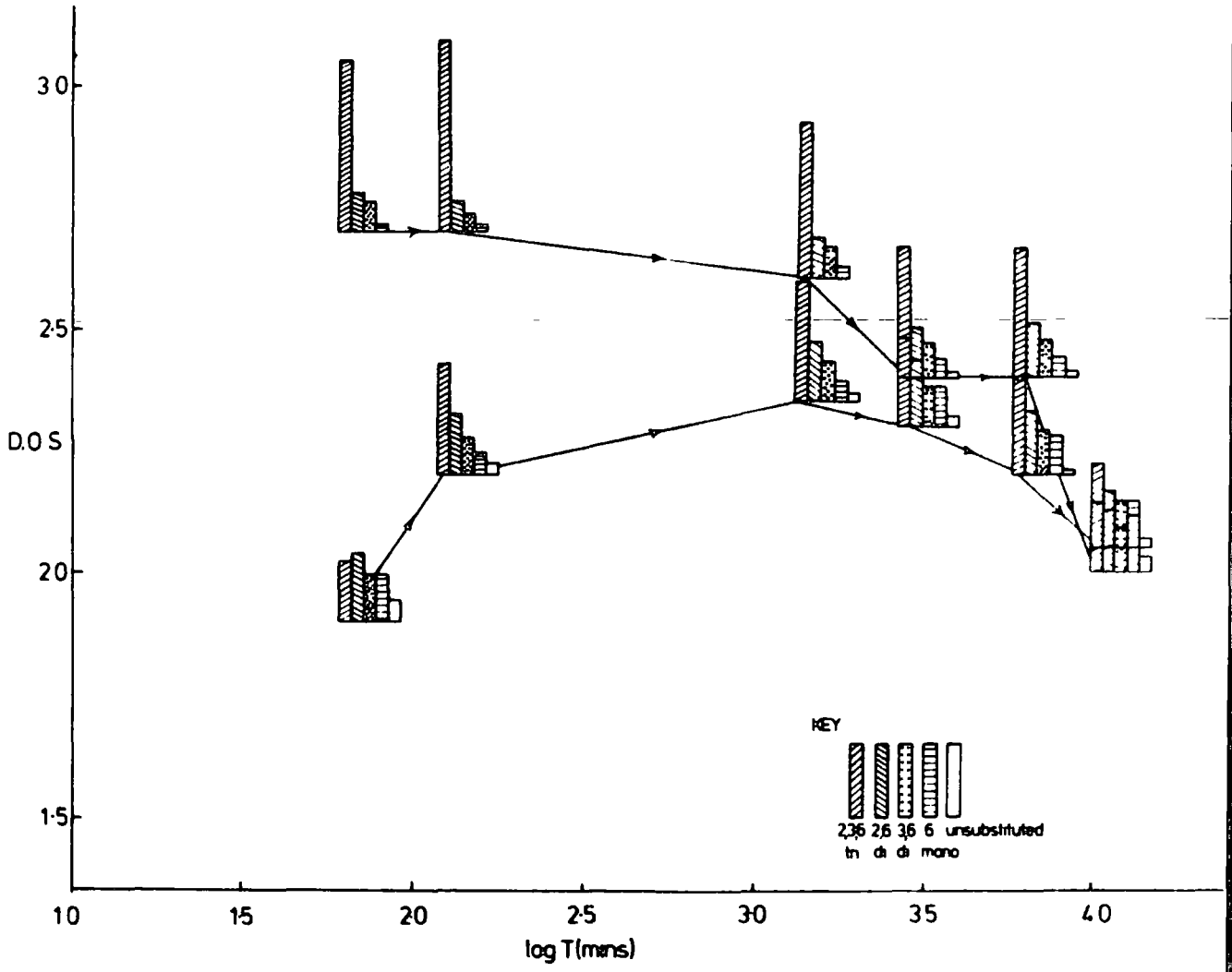

Figure 3.8 Block Histogram of nitrate ester formation by nitration or denitration over long periods of time

(a) after one hour of reaction clearly shows the much higher DOS for the denitrated material, and even after 48 hours when the DOS are closely similar (2.4 denitrated *versus* 2.3 nitrated), the spectra clearly reveal significant differences in microstructure.

The analysis of the spectra provides the information displayed in Figure 3.8 where the contribution to the various substitution patterns are noted. Denitration is seen to involve the conversion of 2,3,6-trisubstituted residues into 2,6-, 3,6-, and 6-monosubstituted residues. However, after extended periods of exposure some unsubstituted residues appear. It has previously been concluded that denitration of the 6-mononitrate ester is kinetically quite slow and hence for short periods of reaction the unsubstituted glucose residues are not observed for denitrated material.

In contrast to this behaviour, it has previously been alluded that in nitration the presence of a nitrate ester residue activates the hydroxyl groups in the same glucose residue towards nitrate ester formation. In consequence, there is a slow reduction in the contribution to the overall ^{13}C n.m.r. signal from the unsubstituted glucose residues.

In denitration, the samples appear to reach a plateau in composition after ~2-4 days' exposure with a marked decrease in DOS for those samples exposed to the acid mix after one week. The nitrated samples also show a plateau after 1-2 days and these exhibit a steady decrease in DOS over a period of a week. The samples (either nitrated or denitrated) retrieved from the acid mix after one week were extensively degraded and were powdery in form as opposed to the original fibrous papers.

Also, in comparison with Figure 3.3, the denitration is seen to differ markedly in the bulk than the surface data over the first few hours. This fact has been noticed previously by Stephenson[109] when using mixed acids.

It is also clear that the bulk DOS after one hour nitration, is again lower than expected and must reflect the different physical characteristics of this material.

The identical experiment was conducted with cellulose (K300) linters, and the ^{13}C n.m.r. analyses compared with a consideration of the X-ray d(1$\bar{1}$0) spacings and micro-Kjehdahl analyses.

The component analyses are shown in Table 3.1 for the nitration and denitration of the cellulosic material, and the X-ray spacings and Kjehdahl analyses in Table 3.2.

It is clearly seen from Tables 3.1 and 3.2 that the bulk DOS measured *via* a micro-Kjehdahl analytical technique (see Appendix II) is identical to that calculated from the component analysis of the ^{13}C n.m.r. data.

Consideration of the samples prepared *via* denitration shows some very interesting features. Again it is seen from Table 3.1 that denitration involves the conversion of the 2,3,6-trisubstituted glucose residues to 2,6-di; 3,6-di and 6-monosubstituted residues. It is interesting to note the rapidity with which denitration is seen to occur. Within the first 5 seconds of immersion in the acid mix, the equilibrium DOS is established. The initial sample containing 85% of trisubstituted glucose residues has reached a value of 63% within five seconds, with the large increase of 0% to 9%

TABLE 3.1 Component Analysis from ^{13}C n.m.r.

Nitration

Time	2,3,6-tri	2,6-di	3,6-di	6-mono	unsubst.	DOS.
30 min.	0.30	0.28	0.21	0.14	0.07	2.0
1 hr.	0.34	0.28	0.21	0.12	0.05	2.1
2.5 hr.	0.41	0.27	0.17	0.12	0.03	2.2
7 hr.	0.46	0.26	0.16	0.09	0.03	2.2
24 hr.	0.48	0.25	0.14	0.10	0.03	2.3
48 hr.	0.41	0.23	0.17	0.16	0.03	2.2
72 hr.	0.33	0.31	0.18	0.13	0.05	2.1
96 hr.	0.42	0.28	0.16	0.11	0.03	2.2
120 hr.	0.42	0.27	0.15	0.13	0.03	2.2
144 hr.	0.33	0.25	0.18	0.23	0.01	2.1
168 hr.	0.42	0.29	0.15	0.12	0.02	2.2
Denitration						
0	0.85	0.10	0.05	0.00	0.00	2.8
5 sec.	0.63	0.14	0.11	0.09	0.03	2.5
30 sec.	0.60	0.18	0.12	0.07	0.03	2.5
60 sec.	0.61	0.17	0.12	0.07	0.03	2.5
30 min.	0.68	0.11	0.10	0.08	0.03	2.5
1 hr.	0.62	0.14	0.13	0.09	0.02	2.5
2.5 hr.	0.64	0.16	0.13	0.05	0.02	2.5
7 hr.	0.62	0.18	0.13	0.02	0.05	2.5
24 hr.	0.59	0.19	0.12	0.07	0.03	2.46
48 hr.	0.51	0.19	0.17	0.09	0.04	2.3
72 hr.	0.46	0.22	0.15	0.11	0.06	2.2
96 hr.	0.57	0.20	0.13	0.06	0.04	2.4
120 hr.	0.57	0.20	0.14	0.06	0.03	2.4
144 hr.	0.52	0.22	0.13	0.10	0.03	2.35
168 hr.	0.41	0.20	0.20	0.12	0.07	2.1

TABLE 3.2

	Nitration		Denitration	
Time	Kjehdahl DOS	X-ray d(110) Spacing	Kjehdahl DOS	Xray d(110) spac.
0	-	-	2.83	-
5 sec.	-	-	2.5	-
30 sec.	-	-	2.5	-
60 sec.	-	-	2.5	7.56 - 7.62
30 mins.	2.1	7.14 - 7.25	2.5	6.91 - 7.02
1 hr.	2.2	6.91 - 7.02	2.5	7.13 - 7.19
2.5 hr.	2.2	7.08 - 7.13	2.5	7.43 - 7.49
7 hr.	2.2	7.02 - 7.13	2.5	7.43 - 7.49
24 hr.	2.2	7.16 - 7.20	2.4	7.19 - 7.25
48 hr.	2.2	7.19 - 7.25	2.3	7.02 - 7.08
72 hr.	2.1	7.49 - 7.56	2.2	6.91 - 6.97
96 hr.	2.2	7.02 - 7.13	2.4	7.09 - 7.14
120 hr.	2.2	7.02 - 7.08	2.4	7.09 - 7.14
144 hr.	2.1	6.91 - 6.97	2.35	7.02 - 7.08
168 hr.	2.1	7.02 - 7.08	2.1	6.86 - 6.97

of the 6-monosubstituted glucose residues. Also, contrary to the work of Stephenson[47] the appearance of unsubstituted residues is very rapid. This could be due to two reasons: (a) the denitration studies of Stephenson were conducted in nitric acid: water mixes, and (b) cellulose in the form of papers was used.

In comparison with the initial experiment shown in this chapter, unsubstituted glucose residues were not apparent until >48 hours exposure to the acid mix. Therefore it must be concluded that the physical form of cellulose used plays a large rôle in the bulk chemistry of these materials.

It can also be clearly seen from Table 3.1 that discontinuities occur in the component analysis patterns at 30 minutes and 48-72 hours denitration time. It appears that before 30 minutes and after 30 minutes that a quasi-steady state is established with an approximate component analysis of:

62% 2,3,6-tri, 16% 2,6-di, 12% 3,6-di.

However at 30 minutes there is an increase in the 2,3,6-trisubstituted residues and decreases in the 2,6-di- and 3,6-trisubstituted glucose residues, although the bulk DOS is very closely similar.

Similarly, at 48 and 72 hours the component analyses of the sample show a relative decrease in the 2,3,6-trisubstituted residues. Classical thermodynamics cannot explain changes such as these, without invoking a change in structure. This is possible since in both cases the d(110) X-ray spacings are dissimilar than those at straddling times of reaction. It can also be noticed that a times of 30 minutes, 48 hours and

168 hours the percentages of 2,6-di and 3,6-disubstituted residues are closely similar, a fact that is difficult to interpret in the simple analyses put forward by Wu,[46] and also by Clark *et al.*[47]

^{13}C n.m.r. spectra of samples denitrated for 1 minute, 30 minutes and one hour clearly show differences in the component analyses. It is obvious that the sample denitrated for 30 minutes has a different sequence distribution than those after 1 minute, or one hour, although in all cases the bulk degree of substitution is similar.

From Tables 3.1 and 3.2 it is clearly seen that the DOS determined from the micro-Kjehdahl analysis is similar in all cases to that calculated from the ^{13}C n.m.r. component analyses. The time taken to reach the equilibrium DOS value of 2.2 is seen to be ∿2 hours; a time which has been quoted before as the time to reach the equilibrium DOS throughout the bulk of the material.

^{13}C n.m.r. spectra were not run for samples nitrated for times less than 30 minutes, as the material before this time is not completely soluble in the dimethylsulphoxide-d_6 solvent. This is a consequence of the bulk of the material still being cellulosic as opposed to nitrated material.

It is evident from Table 3.1 that nitration is seen to involve the conversion of unsubstituted, 6-mono, 2,6-di and 3,6-di-substituted residues into the 2,3,6-trisubstituted glucose residues. It has already been mentioned that in nitration, the presence of a nitrate ester residue activates the hydroxyl groups in the same residue, and therefore there is

a slow reduction in the contribution to the overall ^{13}C n.m.r. signal from the unsubstituted glucose residues.

As in the denitration reaction, discontinuities occur in the nitration reaction at 72 and 144 hours' exposure time with a concomitant lowering in the d(110) X-ray spacings. Clearly some morphological change must be occurring within the sample to account for these anomalies.

The anomalous degree of substitution at 1 hour nitration time, as seen in previous experiments is not really evident from the bulk ^{13}C n.m.r. component analysis, although the d(110) X-ray spacing is slightly lower than expected.

The possibility of morphological transformations to account for the distinct discontinuities present will now be discussed further. However, it is important to stress that the nitration/denitration of cellulosic materials is, indeed, very complex. From the data presented in this chapter, it is clear that although an equilibrium DOS has been attained, the individual reactions have not attained an equilibrium position. The nitration/denitration reactions of cellulosic materials must depend on the physical characteristics (*e.g.* physical form, molecular weight distributions, previous history, *etc.*) of the samples employed.

Consideration of what is currently known about the physical structure of cellulose leads one to conclude why cellulose (and chitin) serve as load-bearing components of major groups of natural composite tissues- cellulose[110-112] in many plant-cell walls and chitin in the skeletal materials of many lower animals. Their chemical structures are very

similar: cellulose is a poly-β(1→4)-D-glucose and chitin is its 2-acetomido derivative; not surprisingly this leads to similar structures and morphologies. The β(1→4)glucan chain is inherently stiff and extended and must be judged ideal for the formation of fibrous structures.[113,114]

At least four different crystalline forms of cellulose (celluloses I-IV) are recognised on the basis of their X-ray diffraction patterns and infra-red spectra.[120,121] In each structure, the chains have approximately the same backbone conformation, with two glucose residues repeating in approximately 10.3Å. The structures differ in terms of the packing of adjacent chains.[122] Cellulose I (native cellulose) is the naturally occurring form in plant-cell walls.[115,116] Regeneration of cellulose from solution,[117] *e.g.* in the manufacture of rayon fibres, leads of cellulose II. This structure can also be produced by the process of mercerization,[4,118] which involves swelling in caustic soda followed by removal of the swelling agent. This process is used to modify the properties of cotton fibres.[117] The cellulose I→II transformation is irreversible, which implies that cellulose II is the stable form and that cellulose I is a metastable structure. Cellulose III can be produced by treatment of either cellulose I or cellulose II with liquid ammonia. However, the structures obtained depend on the parent material and are distinguished as celluloses III_I and III_{II}.[119] The unit cells of these structures are approximately the same, but the infra-red spectra show that they have different hydrogen-bonding networks.[119] Washing with water restores the parent cellulose I or II indicating that the forms III_I and III_{II} retain a memory of their

original structure. Likewise, cellulose IV_I and IV_{II} can be prepared from celluloses I and II by treatment in hot glycerol (*e.g.*, at 270°C); these structures can also be restored to their original structures. Treatment of cellulose I and II with concentrated acids has been reported to produce a fifth form, designated cellulose X, which is similar to, but not identical to, cellulose IV.[124]

With regard to the conversion from cellulose I to cellulose II, (*i.e.* a change from parallel to antiparallel polarity) it is easy to see how this can be achieved in solution, but the mercerization process presents more difficulty. In principle, reversal of polarity in the solid state could be achieved either by regular chain folding or by rearrangement of extended chains. Morphological and mechanical studies are against any extensive chain folding, and the most reasonable mechanism appears to be rearrangement of extended chains. In mercerization, the individual chains are separated and on removal of the swelling agents will be more likely to unite with antiparallel mates, since the cellulose II structure is thermodynamically more stable.

It should be noted that the mercerization change to cellulose II usually requires several swellings and deswellings to achieve maximum conversion, and there is always some residue of unconverted cellulose I. It is difficult to see why the change should be so difficult unless there is a major structural rearrangement.

It is plausible, therefore to account for the discontinuities in component analysis and sequence distribution

from the ^{13}C n.m.r. spectra, by proposing that since cellulose has a series of polymorphs, then cellulose nitrates could conceivably have various polymorphs. These polymorphs could account in part for the anomalous X-ray spacings and properties inherent in this material. Atkins *et al*[44] have investigated the molecular conformations and packing considerations in cellulose nitrates by X-ray diffraction and computer-modelling. The X-ray diffraction diagrams suggested some type of 5-fold helix in a highly nitrated cellulose (13.9% N). They investigated the stereochemical feasibility of a number of models exhibiting 5-fold helical symmetry, and also the packing of such helices in several unit cells, with reference to the work of Mathieu and Happey.[126] Sathyanarayana and Rao[127] showed that the 5_1 and 5_4 conformations are impossible for a molecule with a (1→4)-linked-β-D-glucose backbone. It is possible to build 5_3 helices but these gave unacceptable close contacts between some atoms in the chain backbone. It was only in the 5_2 helix that satisfactory models could be constructed. Consideration of the packing leads Atkins[44] to adopt an antiparallel structure, since it is this proposed model where there is most room available.

Therefore, there does seem some evidence to suggest that morphological changes within the cellulose nitrate structure could take place depending on the sequence distribution of the nitrate ester groups along the chain. It must be emphasized that the sequence distribution appears, from the data, to be time dependent.

The data suggests possible other experiments to help in the diagnosis of these phenomenon. For example the dynamic properties of these structures could be undertaken experimentally using dielectric relaxation. Pethrick *et al*[128-131] have studied the dielectric properties of cellulose and its derivatives and have indicated that significant differences in these properties exist as a function of the nature of the side group and the preparation of the sample prior to investigation. Certain features of the dielectric behaviour of these polymers appear to be associated with macroscopically observed changes in density incurred in the material as a result of physical or chemical modification, and as such may be expected to arise as a consequence of molecular reorganisation in the polymer.

Another possible technique is positron annihilation.[132] Positron lifetime measurements provide a method of examining and characterising the distribution of cavities at a molecular level, and in this way can indicate the nature of the free volume in the sample.[133,134] In view of the significant differences which exist in the relaxation characteristics of cellulose and its derivatives, positron annihilation was used to correlate this behaviour with the possible influences of cavity distribution in these systems. It was found that significant differences exist in the lifetimes of positrons in cellulose and its derivatives which can be interpreted as evidence for changes in the free-volume distributions in these materials.[135]

Therefore, a complete study of the nitration/denitration reactions of cellulosic materials as a function of time clearly requires the use of a barrage of techniques. Knowing sequence distribution data from ^{13}C n.m.r., correlation with morphological changes as determined by relaxation methods, *etc.*, may become probable.

Until such a time when this work is undertaken, one must again state that the chemistry of cellulosic materials is very complex, and requires a lot more innovative and exciting research.

CHAPTER FOUR

THE NITRATION OF CELLULOSIC MATERIALS - A TEMPERATURE DEPENDENCE STUDY

4.1 Introduction

The nitration of cellulose to produce the highly inflammable cellulose nitrates used in a range of applications including explosive formulations, surface coatings and photographic films is an extremely well documented reaction.[4,30]

The wide ranging nature of both the technological and academic investigations of the cellulose and nitrocellulose field over the past century, however, posed certain difficulties since relevant data is dispersed over a number of disciplines leaving many important questions unanswered.

As pointed out earlier, the main point of interest in the technical nitration in mixed acids, for example, is the question of the degree of substitution and how this relates to the acid mix composition. The question of the limiting degree of substitution could *a priori* be rationalized in terms of two extreme models.

The first can be attributed to the micro and macroscopic structure of the cellulose. Thus, inhomogeneities in the bulk structure could give rise to accessible and inaccessible regions. Since nitration must depend on the diffusion of reagent throughout the bulk structure a further consideration is that there may well be a concentration profile throughout the structure. On this basis the less than maximum degree of substitution is attributable to an inhomogeneous bulk structure corresponding to regions of completely nitrated material and unreacted inaccessible regions.

A more plausible alternative is that since nitration is a reversible esterification process, then the ∿2.8 degree of

substitution typically observed represents the equilibrium situation.

In a recent series of papers, Clark and Stephenson[11,43,54] had shown how ESCA may be used to follow the initial stages of nitration and denitration of cellulosic materials. The great surface sensitivity of the technique has been used to good effect to follow the changes in surface chemistry in the outermost few tens of Angstroms, and this has provided valuable new information on the initial reactions at the heterogeneous interface between the cotton fibrils and the reaction medium. Previous studies by Clark and Stephenson[54] showed that the heterogeneous reactions involved in the nitration of cellulose linters in the form of papers with mixed acids is extremely rapid and at room temperature the equilibrium DOS is established to a depth >100Å on a time scale of seconds.

Since the reactions are so rapid at room temperature it has not proved possible to study the approach to the equilibrium DOS as a function of time since it is not technically feasible to expose samples to the nitrating medium and quench and stabilize the samples on a time scale shorter than a second or so.

In order to study the initial stages of the surface reaction, ESCA studies on samples of cotton linters (in the form of papers) have been carried out, in various nitrating mixes for 30 seconds over the temperature range -25° to $+22^{\circ}C$.

The effect of low temperature nitrations in the bulk required times of nitration of 1 hour and the use of ^{13}C n.m.r. and X-ray methods.

4.2 Experimental

The starting cellulose used in this study was Holden Type II cotton linters (in the form of papers) as described previously. All experimental procedures are those outlined in Section 3.2 of this thesis.

Nitrations were accomplished by immersion in the acid mix which was cooled by means of acetone/dry ice slush baths. The acids: cellulose weight ratio was never less than 100:1. Samples were cut to probe tip size (8 x 22 mm) and mounted using double sided scotch tape.

^{13}C n.m.r. (90.56 MHz, proton noise decoupled) spectra and X-ray d(110) spacings are as described in Section 3.2.

ESCA spectra were run on a Kratos ES300 electron spectrometer. All Raman spectra were run on a Varian Cary 82 Raman spectrophotometer using an Argon gas laser (514.5 nm, 200 mW).

4.3 Results and Discussion

4.3.1 Temperature Dependence of Nitration in Various Acid Mixes

(a) Nitration in 60% H_2SO_4, 25% HNO_3, 15% H_2O for 30 seconds. It has previously been described how analysis of the C_{1s} and N_{1s} core levels allows the direct determination of the DOS by means of ESCA, and the relevant data are displayed in Figure 4.1.

The convolution of rate processes (differing activation energies for nitration and denitration at different sites, and for diffusion) are such that for a 10°C lowering in temperature below ambient (22°C) the degree of substitution in the surface

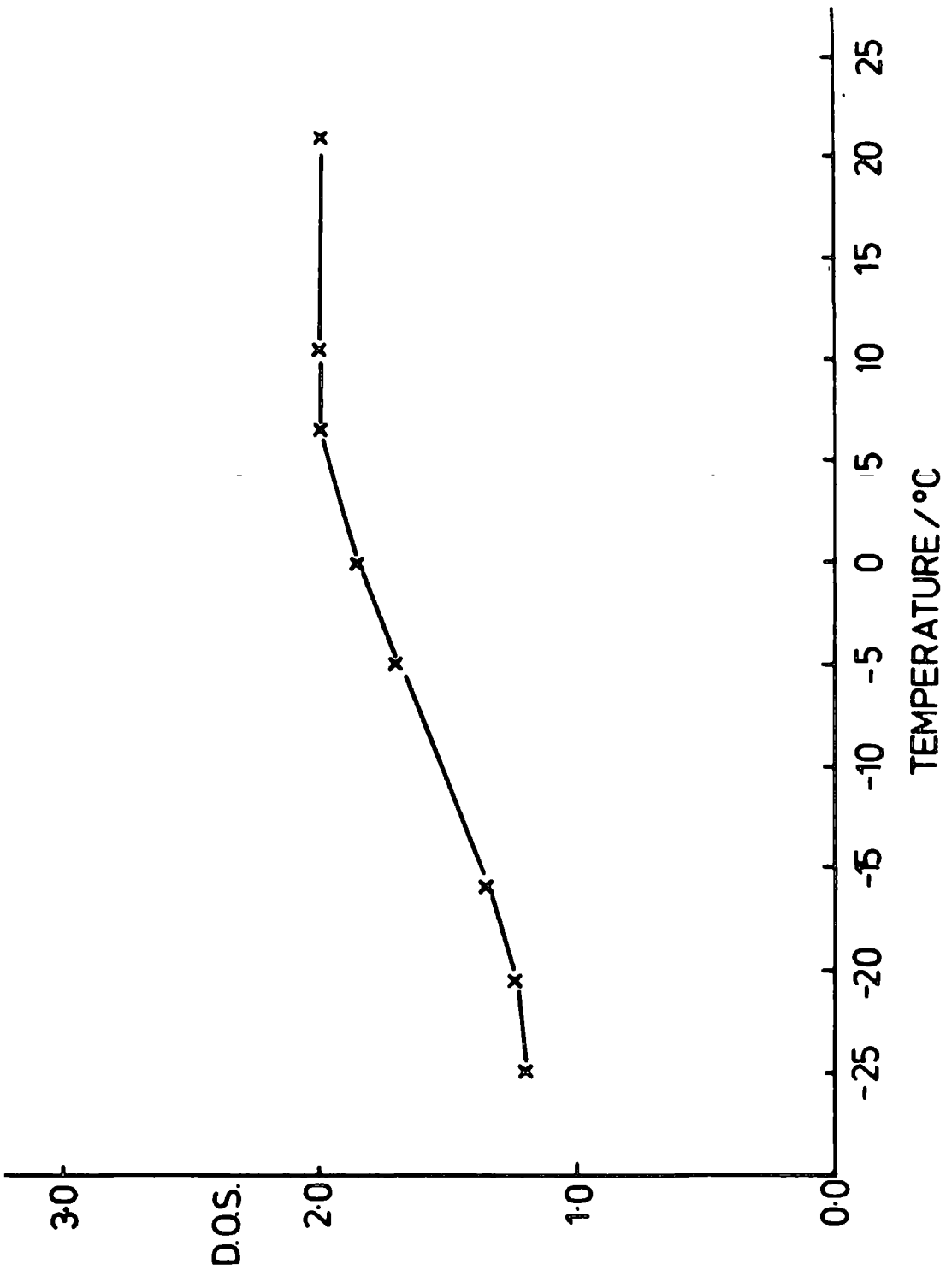

Figure 4.1 Graph of DOS *versus* temperature for the acid mix 60% H_2SO_4, 25% HNO_3, 15% H_2O

region (using $Mg_{k\alpha_{1,2}}$ the effective sampling depth for the C_{1s} core levels is $\sim$50Å) remains essentially constant.

At -25°C the DOS of $\sim$1.2 indicates that nitration has proceeded rapidly even at that temperature to the mononitrate. Previous discussion[54] has indicated that formation of the 6 substituted mononitrate must involve a significantly lower activation energy than for formation of the 2 or 3 monosubstituted derivatives and correspondingly that the activation energy for denitration is higher for the 6 site than for the 2 or 3 substituted derivatives.

At intermediate temperatures there is a gradual increase in surface DOS until at $\sim$8°C the equilibrium DOS remains essentially constant.

(b) Nitration in 70% H_2SO_4, 22.5% HNO_3, 7.5% H_2O for 30 seconds

The relevant data are displayed in Figure 4.2.

The convolution of rate processes are such that for a 13°C lowering in temperature below ambient (20°C) the DOS in the outermost top 50Å of the material remains essentially constant.

At -38°C the DOS of $\sim$1.5 suggests rapid reaction at the surface.

At intermediate temperatures there is a gradual increase in surface DOS until at $\sim$7°C the equilibrium DOS remains essentially constant.

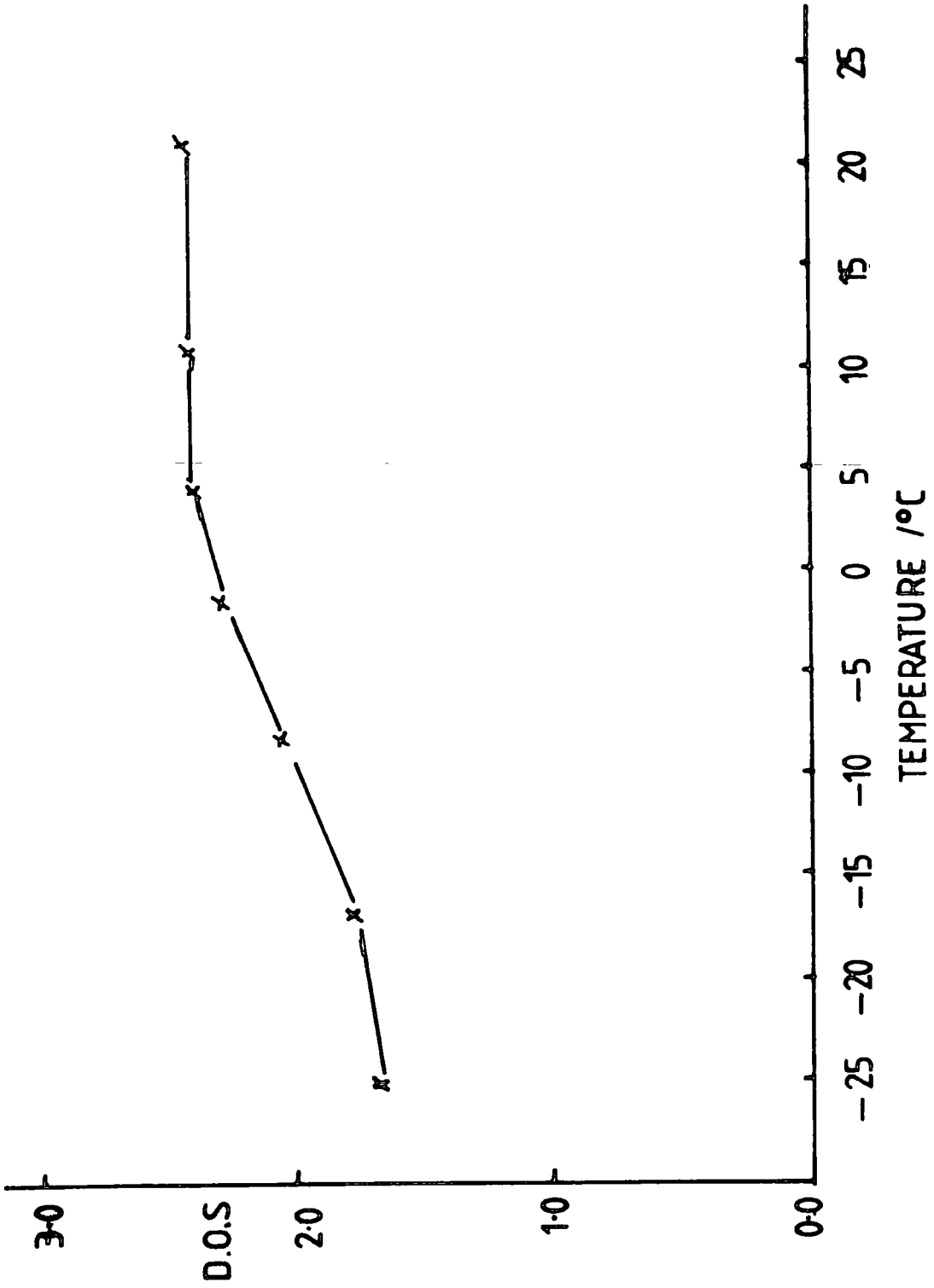

Figure 4.2 Graph of DOS versus temperature for the acid mix 70% H_2SO_4, 22.5% HNO_3, 7.5% H_2O

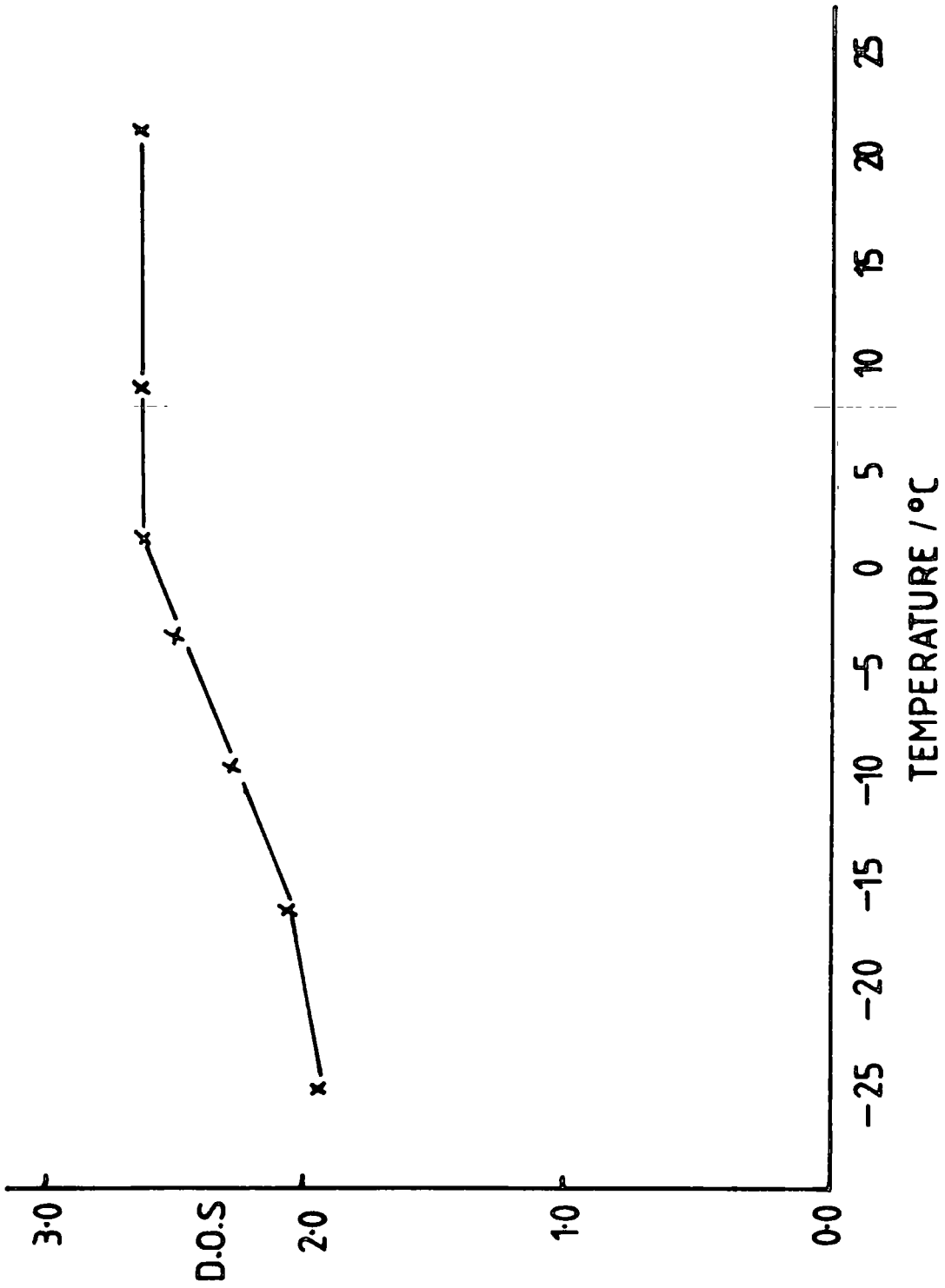

Figure 4.3 Graph of DOS *versus* temperature for the acid mix 75% H_2SO_4, 22.5% HNO_3, 2.5% H_2O

(c) Nitration in 75% H_2SO_4, 22.5% HNO_3, 2.5% H_2O for 30 seconds

The relevant data are displayed in Figure 4.3.

For a 16°C lowering in temperature from ambient (21°C) the DOS in the surface regions remains essentially constant. At -30°C, the surface DOS has reached a value of ∿1.9. At intermediate temperatures there is a gradual increase in DOS to a value of ∿5°C where the equilibrium DOS is achieved and maintained.

4.4 Comparison of data

To draw a clearer comparison of the data presented in earlier sections of this chapter, it is pertinent to superimpose Figures 4.1, 4.2 and 4.3. The resultant graph of degree of substitution *versus* temperature is shown in Figure 4.4.

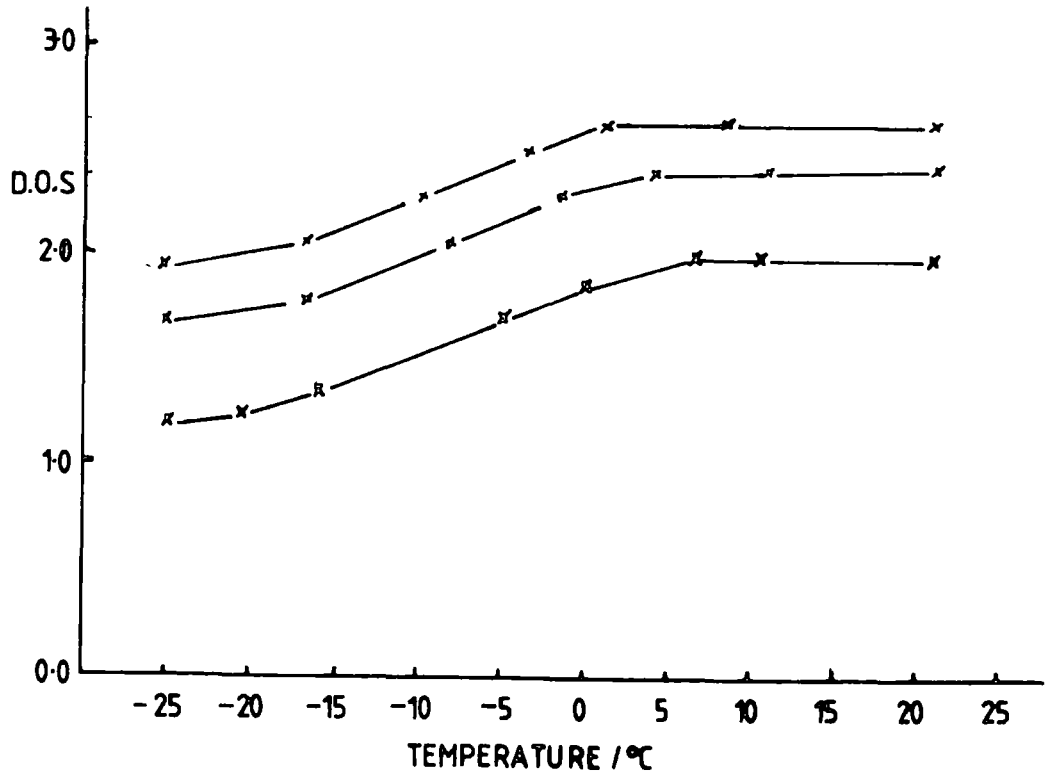

Figure 4.4 Graphs of DOS *versus* temperature for all acid mixes used.

It is clear from this figure that all the curves are closely parallel to each other. There are various probable explanations for these effects which will be outlined below.

(a) Rate of nitration decreases with temperature, *i.e.* a purely time dependent effect.

(b) Diffusion of the acids into the fibrils decreases with temperature - *i.e.* as the viscosity of the acid mix decreases.

(c) The equilibrium constant for the formation of the nitrating agent is temperature dependent; or the equilibrium constant for the reaction of the nitrating agent with the hydroxyl groups is temperature dependent.

If the effect shown in Figure 4.4 is due to a time dependent phenomenon, as in point (a), then this can be quickly and easily resolved.

The initial aim of the low temperature nitration reaction of cellulosic materials was to physically slow down the reaction so as to monitor the initial stages of nitration - since at room temperature the equilibrium DOS is attained within one second.

Sulphate ester groups were also monitored at the surface as a function of temperature; the C_{1s}/S_{2p} area ratios for these materials is essentially constant over the temperature range investigated.

As an aside, Clark and Stephenson[109] could not detect the presence of sulphate ester groups at ~130Å using $Ti_{k\alpha}$ radiation.

Calculations of relative core level signal intensities by Munro[217] have shown that when using $Ti_{k\alpha}$ radiation, it is the S_{1s} core level (BE ∿2472 eV) which should be monitored, not the S_{2p} core level (BE ∿169 eV). By monitoring the S_{1s} core level with $Ti_{k\alpha}$ it is found that sulphate esters are present in the sub-surface for a series of cellulose nitrates prepared in mixed acids where the sulphuric acid percentage ranges from 60-75%.

To ascertain the rôle of kinetics in the reaction, identical experiments were carried out but the time of reaction was increased to one hour. Thereby, if the viscosity of the acids is not so great at -25°C, then the bulk DOS and partial DOS of the material could be monitored as well as the surface chemistry. Also, if the reaction is purely time dependent then reaction at -25°C for one hour should result in a higher surface DOS to that after 30 seconds exposure time.

Table 4.1 below lists the data for all three nitrating mixes as used previously in this work.

As is clearly seen from Table 4.1 the surface DOS at -25°C is not time-dependent.

TABLE 4.1

	Surface DOS		Bulk DOS ^{13}C nmr (Kjeldahl)		X-ray d(110) spacing	
Temp/^{o}C	-25	+20	-25	+20	-25	+20
70% H_2SO_4 22.5% HNO_3 2.5% H_2O	1.9	2.6	-	2.6(2.6)	5.98	7.44
70% H_2SO_4 22.5% HNO_3 7.5% H_2O	1.65	2.3	-	2.3(2.3)	5.95	6.73
60% H_2SO_4 25% HNO_3 15% H_2O	1.2	2.0	-	2.0	5.98	7.13

The materials nitrated for one hour at -25^{o}C would not dissolve in solvents for the nmr spectroscopy and were not digestible for the micro-Kjeldahl analyses. This is due to the fact that nitration has only occurred at the surface, probably due to the viscosity of the acid mixes at this temperature. The d(110) X-ray spacing also confirms this, in that the materials nitrated for one hour have essentially cellulose-type d(110) spacings.

There is no reason to believe that the nitration reaction at the surface will be influenced by diffusion or viscosity.

Therefore, it may be concluded that in lowering the temperature, one has not just slowed down the nitration process,

but clearly equilibria have been altered, so that even after 30 seconds exposure to the nitrating acids the equilibrium DOS of these materials at the surface has been reached.

One must therefore try to explain the curves in Figure 4.4 in terms of thermodynamics rather than kinetics.

If one considers the central linear part of each curve, this may be treated thermodynamically *via* the Van't Hoff Isochore,[149] and values for the heat of formation may be determined. Therefore assuming the activities of the acids and water are unity and temperature independent and that D.O.S. can be treated as activities or concentrations of the products at various temperatures, then a plot of ln. DOS/3-DOS *versus* 1/T (see below) gives a slope equal to $-\Delta H/R$, where R is the gas constant.

This analysis has been effected in all three cases and values of +1.44, +1.31 and +1.20 kJ mol^{-1} for the 2.6-2.0 DOS cases respectively. It is clear from these values that the curves appear to represent an endothermic process. This is also alluded to by using the simple Le Chatelier's Principle which states that if the reaction is endothermic, then there would be an increase in the products as the temperature is increased.

If one requires to treat the nitration of cellulose as an equilibrium then one must know the nitrating species that attacks the hydroxyl groups to form the nitrate esters.

In Miles' review[4] in 1955, various workers [150,151] had tackled this problem assuming certain reaction equilibria for instance, if the reaction is:

$$\text{cell - OH} + HNO_3 \overset{K}{\rightleftharpoons} \text{cell - } ONO_3 + H_2O$$

then $$K = \frac{[\text{cell-}ONO_3](H_2O)}{[\text{cell-OH}][HNO_3]}$$

Various activities for the acids and water were determined, all of which were poor.[152,153] However, if a_w and a_n are the relative activities for water and nitric acid respectively and s is the number of hydroxyl groups which are nitrated then

$$K = \frac{a_w}{a_n} \cdot \frac{s}{3-s}$$

Previous kinetic work[154] showed that the water present at equilibrium does not act on its own, but in union with a nitric acid molecule. Therefore the equilibrium must be:

$$\text{cell - OH} + 2HNO_3 \rightleftharpoons \text{cell-}ONO_2 + HNO_3.H_2O$$

Therefore $$K_1 = \frac{[\text{cell-}ONO_2][HNO_3.H_2O]}{[\text{cell-OH}][HNO_3]^2}$$

and also, since the nitric acid hydrate must itself be in equilibrium with its components, one also has

$$K_2 = \frac{[HNO_3.H_2O]}{[HNO_3][H_2O]}$$

Therefore, still the controlling factor would be the ratio of the two activities (a_w/a_n), although water is not an immediate reactant.

In mixed acid nitration the situation is yet more complex, but however incorrect.

From calorimetry[155] and calculations[156] the heat of formation of cellulose nitrate assuming

$$\text{cell - OH} + HNO_3 \rightleftharpoons \text{cell-}ONO_2 + H_2O$$

is $\sim$-1.17 kcal mol^{-1}.

All the above treatments could not explain experimental results at the time, and this was assumed to be because the equilibria involved were too complex, and not just a simple reversible reaction.

Elegant ^{18}O labelling work by Klein and Mentser[157] showed that the esterification reaction of cellulose was attained by breakage of the O-H bond, not the C-OH bond. From a knowledge of the plausible equilibria in nitric acid: sulphuric acid: water mixes, one would tentatively conclude from:

$$HNO_3 + 2H_2SO_4 \rightleftharpoons NO_2^+ + H_3O^+ + 2HSO_4^-$$

that the nitrating species is either molecular nitric acid, or the nitronium ion, NO_2^+.

It has been stated in the literature[109] that NO_2^+ ion cannot be the effective esterification agent since this only occurs in sulphuric acid concentrations greater than 80%. However, we feel that it is a misunderstanding of the terminology that has led to this discrepancy.*

Miles[4] believes also that the nitronium ion is not the effective nitrating agent for two reasons:

Footnote:

The elegant work of Ingold *et al*[161-173] proposed correctly that when using mixed acids to nitrate aromatic systems *via* the nitronium ion, >80% sulphuric acid was required. However, this assumes that the acid is <u>diluted</u> by water, *i.e.* 100% H_2SO_4 diluted to 80% H_2SO_4 with water; not as is the case with nitrating mixes, weight percentage of the H_2SO_4 in a ternary mix. Clearly, in the regime of the technical nitration mixes employed in this study the concentration of sulphuric acid using Ingolds scheme is always above 80%.

The first is that nitration can take place in the vapour of nitric acid at low pressures, where no liquid can be present, and the formation of this or any other ion is improbable. However, if condensation of the vapour onto the fibril occurs before reaction then the self autoionisation of the acid, as shown below, may occur.

$$2HNO_3 \rightleftharpoons H_2NO_3^+ + NO_3^-$$

$$H_2NO_3^+ \longrightarrow NO_2^+ + H_2O$$

and secondly, the knowledge we now have of the range of compositions in which the nitronium ion can exist. Chédin[160] has been able to divide the ternary acid diagram into two parts by a line, now called the Chédin line. To the right of this line, in the direction of low dilution, the ion is present to an increasing extent. It is noticed that the technical acid mixes used in this study also fall to the right of the Chédin line, and as such the nitronium ion is present.

To investigate this further, aliquots of technical nitration mixes were taken and studied by means of laser-excited Raman spectroscopy. 200-2000 cm^{-1} Raman scans were taken of 95% fuming nitric acid, 98% concentrated sulphuric acid, and two technical nitration mixes of 75% H_2SO_4, 22.5% HNO_3, 2.5% H_2O and 65% H_2SO_4, 22.5% HNO_3, 12.5% H_2O and are displayed in Figures 4.5 and 4.6.

It is evident from Figure 4.5 that in the acid mixes employed in the technical nitration of cellulose, the line at 1400 cm^{-1} is present and is known to be due to the nitronium ion, NO_2^+. It is also apparent that the acid mix which

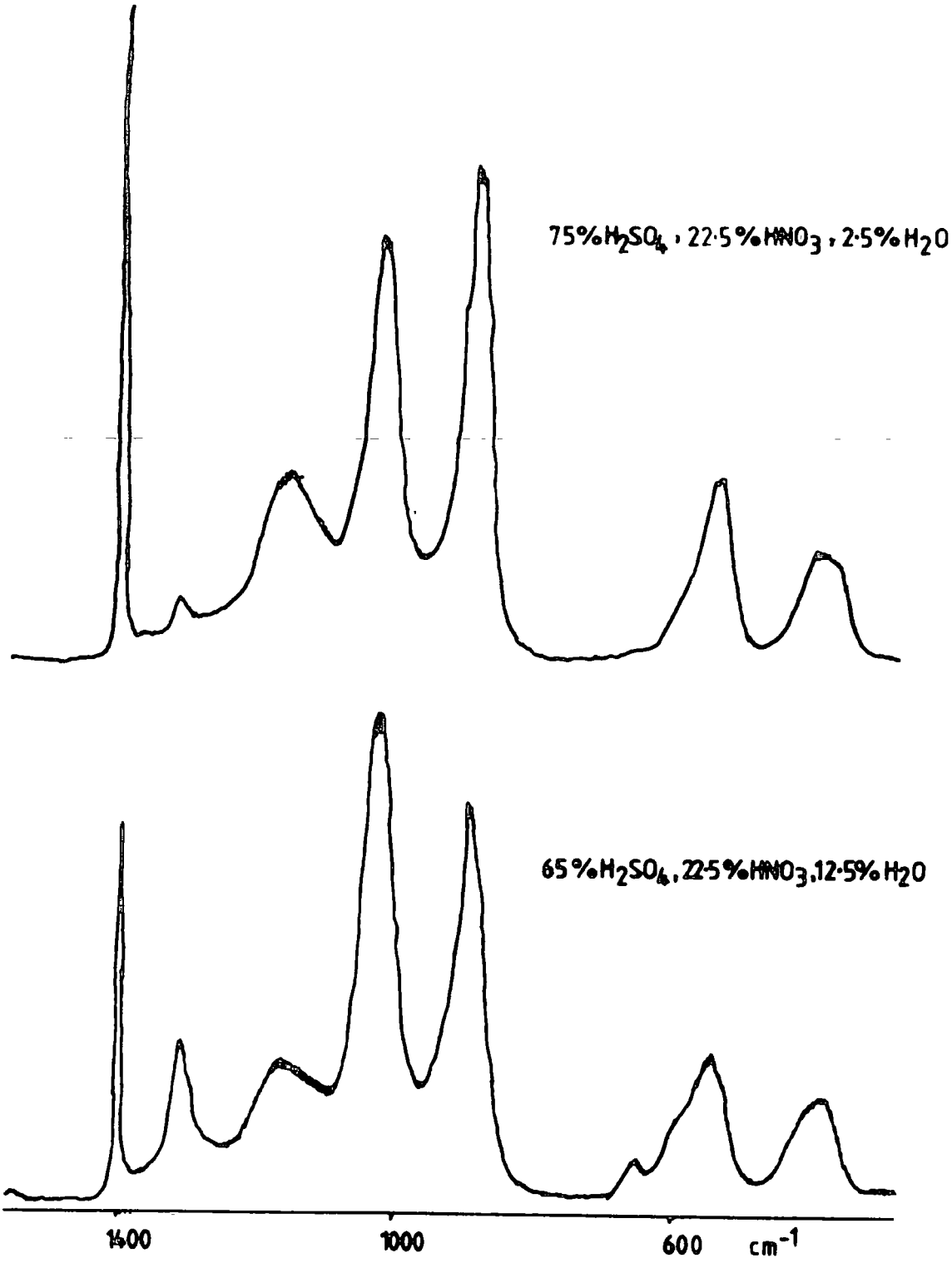

Figure 4.5 Raman spectra of technical acid mixes

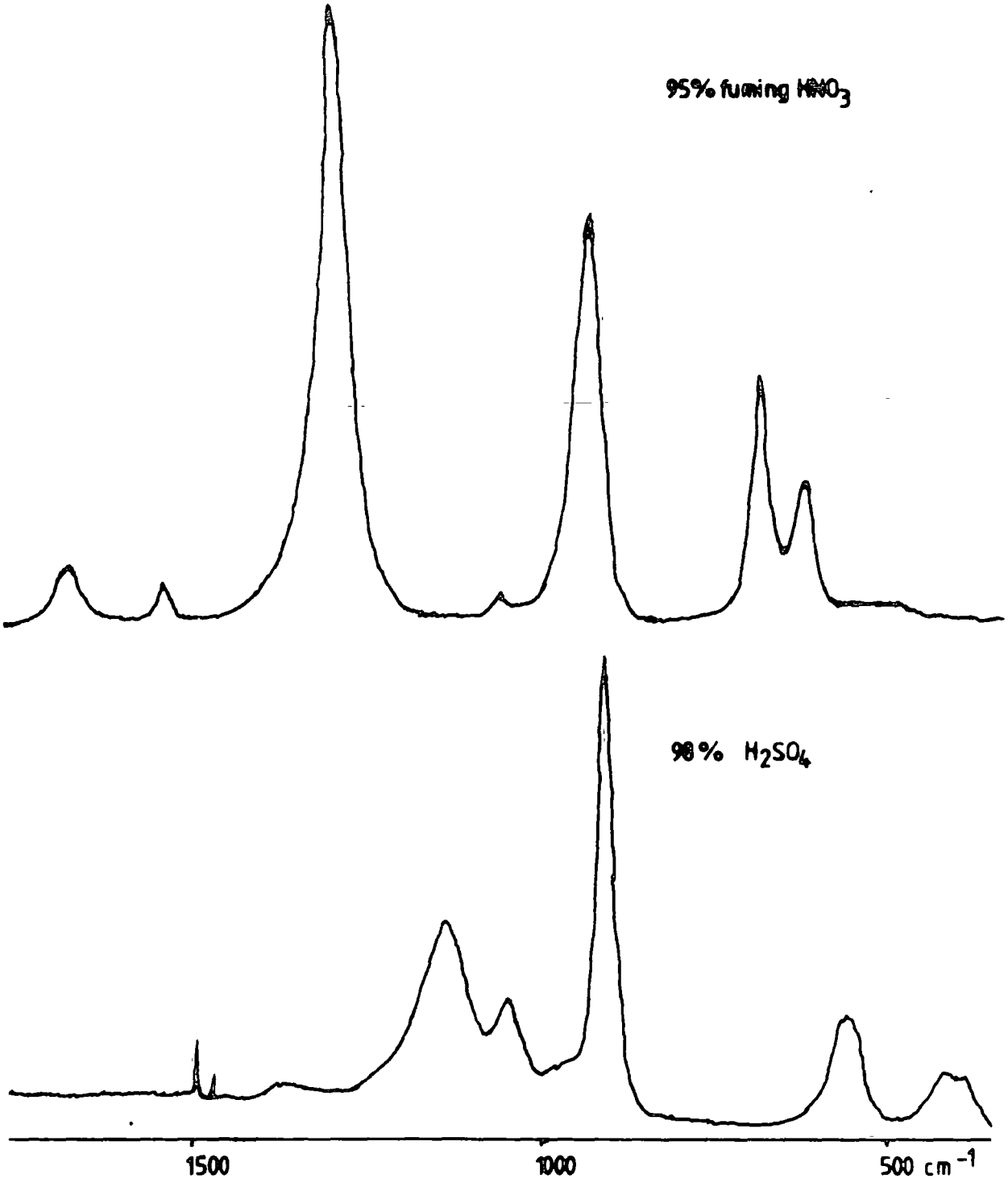

Figure 4.6 Raman spectra of fuming HNO_3, 98% H_2SO_4

produces a high DOS material (75% H_2SO_4, 22.5% HNO_3, 2.5% H_2O) has a relatively larger amount of NO_2^+ present than the other, lower DOS attaining acid mix.

From the evidence outlined above, it is clear that the nitronium ion plays a major part in the technical nitration of cellulose. Therefore clearly the equilibrium, which has been much studied by cryroscopy, titrimetry, *etc.* is an essential part in the technical nitration of cellulose. This equilibrium is:

$$HNO_3 + 2H_2SO_4 \rightleftharpoons NO_2^+ + 2HSO_4^- + H_3O^+$$

Another acid mix commonly used in the laboratory is the nitric/phosphoric mix. A Raman spectrum of a nitric/phosphoric mix has been run and evidence for formation of the nitronium ion is shown in the spectrum.

In 1963, Bayliss and Watts[158] studied the nitrogen species involved in potassium nitrate solutions in various concentrations of sulphuric acid by uv-visible spectrophotometry. It was concluded that the nature of the species present in these solutions depend on the concentration of sulphuric acid as tabulated in Table 4.2.

TABLE 4.2

% wt. H_2SO_4	Species present in solution.
0 - 15%	NO_3^-
15 - 70%	NO_3^- and HNO_3
72 - 82%	HNO_3
82 - 100%	NO_2^+

Therefore this data suggests that whatever is nitrating cellulose should be present in these mixes. An experiment was carried out whereby a 12% sulphuric acid, 75% sulphuric acid and 98% sulphuric acid solutions were prepared by standard procedures. To these solutions ∿5 grms. potassium nitrate was added, which in all cases gave a saturated solution. Cellulose in the form of Whatman-1 filter papers was added to these solutions for two minutes each. This time was chosen, since exposure times longer than this dissolved the cellulose. This was avoided as a heterogeneous reaction was needed. $Mg_{k\alpha}$ core level spectra were run on each of the three samples and these spectra are displayed in Figure 4.7.

It is clear that in the 98% sulphuric acid/KNO_3 mix, a N_{1s} core level is evident at a binding energy of ∿408eV indicative of a O-$\underline{N}O_2$ ester group. Although the $K_{2p_{3/2}}$ level is also evident at a binding energy of ∿292.9 eV, this is not sufficient to account for the level of nitration. The DOS of the cellulose nitrate formed is ∿0.6.

Although the level of nitration is low, nevertheless the nitration of cellulose in a 98% sulphuric acid/KNO_3 mix is possible, and from Table 4.2 there is clear evidence for NO_2^+, the nitronium ion, being the effective nitrating agent.

Raman spectra were run on all three solutions and are shown in Figure 4.8.

The peak at 1400 cm^{-1} [159] is due to the nitronium ion, NO_2^+, and is present only in the 98% H_2SO_4/KNO_3 acid mix.

Clearly therefore in the acid mixes employed in this study, *i.e.* technical acid mixes, the nitronium ion appears

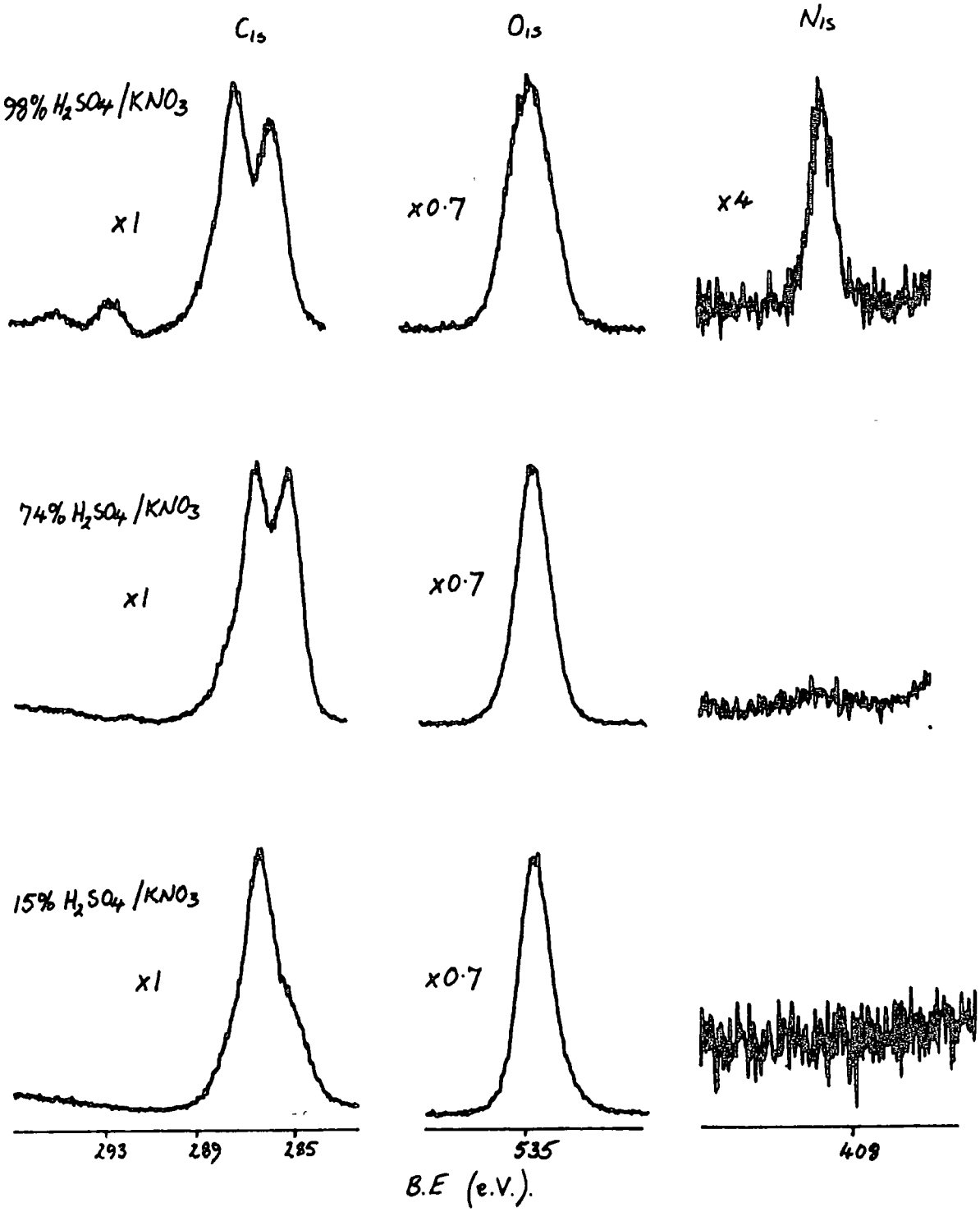

Figure 4.7 $Mg_{k\alpha}$ C_{1s}, O_{1s} and N_{1s} core level spectra for various concentrations of sulphuric acid with potassium nitrate.

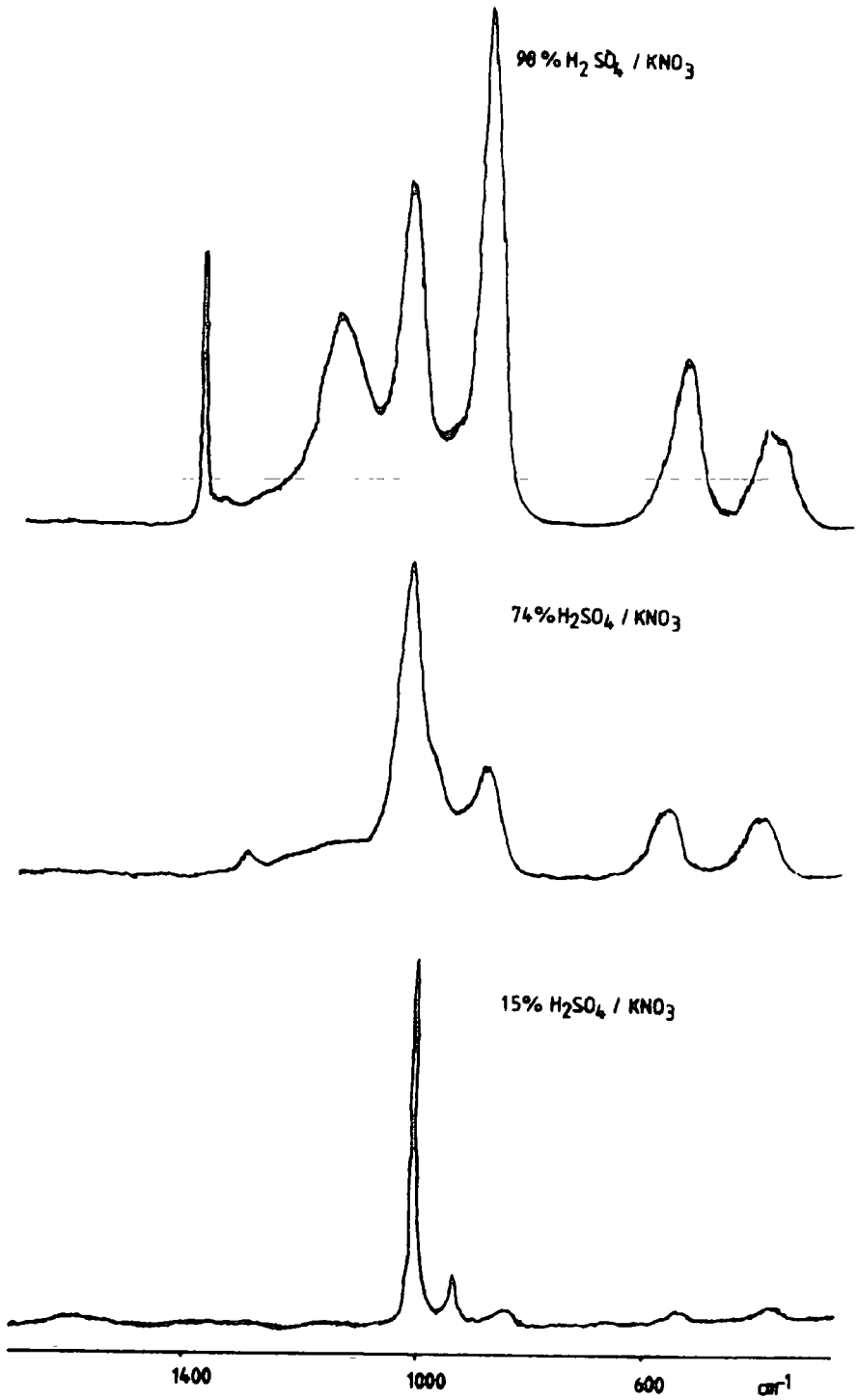

Figure 4.8 Raman spectra for the various concentrations of H_2SO_4 with KNO_3.

to play a major rôle in these nitrations of cellulose.

To further understand the reactions to account for the curves of DOS *versus* temperature in an earlier section of this chapter, one requires a knowledge of the temperature dependent behaviour of these acid mixes. Unfortunately, equipment to monitor the NO_2^+ concentration by Raman spectrophotometry is not readily available. However tenative conclusions can be drawn as to the type of reactions taking place in technical nitrations, *e.g.*

$$HNO_3 + 2H_2SO_4 \longrightarrow NO_2^+ + 2HSO_4^- + H_3O^+.$$

$$\text{cell-OH} + NO_2^+ \longrightarrow \text{cell-O-}NO_2 + H^+.$$

The function of the sulphuric acid in technical acid mixes appears to give a strongly acidic medium towards which the nitric acid acts as a base to form the nitronium ion, NO_2^+.

Although the nitration of cellulose can be explained *via* the two main reaction steps shown above, it is difficult to appreciate how denitration occurs mechanistically. Further research must be done in this very interesting area. One technique which may be particularly fruitful is the use of labelled $H^{15}NO_3$ and ^{15}N nmr. For example, if a sample of cellulose nitrate prepared in unlabelled nitric acid, is then denitrated in ^{15}N labelled nitric acid, any ^{15}N-labelled nitrate esters present in the final substrate should be detected by ^{15}N n.m.r. This approach should therefore reveal if a transesterification reaction occurs during denitration.

The author has tried this approach, but as yet, a ^{15}N n.m.r. spectrum has not been attained.

CHAPTER FIVE

ESCA STUDIES OF THE SURFACE CHEMISTRY OF CELLULOSE NITRATES WITH PARTICULAR REFERENCE TO THEIR DEGRADATION BY X-RAY AND THERMALLY-INDUCED TREATMENTS

5.1 Introduction

The stability of cellulose nitrates to a wide range of conditions (*e.g.* heat, uv light, *etc.*) is of great interest. Over extended periods of time, factors such as exposure to solar radiation, heat and humidity affect the chemical and physical characteristics of cellulose nitrates.

Previously, the degradation of cellulosic materials has been determined by monitoring changes in the viscosity or tensile strength,[4] brought about by a chain scission reaction, which in cellulose is considered to be the major photolytic mechanism. However, the typical quantum yields for chain scission reactions in cellulose and cellulose nitrates (0.001 and 0.01 respectively) are substantially smaller, by at least an order of magnitude, than that reported for the photolysis of nitrate ester groups[137] and it therefore can be expected that the loss of nitrogen oxides from the photolysis of such groups will be the major preliminary degradation pathway in cellulose nitrates.

Published work in this area is relatively small, but there is evidence for three primary processes, where the quantum yields for these processes are in the order (1)>(3)>(2).

$$R - CH_2 - O - NO_2 \xrightarrow{h\nu} R - CH_2 - O\cdot + NO_2 \quad (1)$$

$$\longrightarrow R - CHO + HONO \quad (2)$$

$$\longrightarrow R - CH_2 - ONO + O\cdot \quad (3)$$

Phillips and co-workers[138] have studied the thermal degradation of alkyl nitrates and reported that the initial reaction (1) was followed by:

$$R\text{-}CH_2\text{-}O\cdot + R\text{-}CH_2\text{-}O\text{-}NO_2 \longrightarrow R\text{-}CH_2\text{-}OH + R\dot{C}H\text{-}ONO_2 \quad (4)$$

$$\downarrow$$

$$RCHO + NO_2\cdot$$

Clearly what is known about the possible degradation pathways is slim, and it is therefore not surprising that recent studies of the thermal degradation of cellulose nitrates have concentrated on monitoring the rate of evolution of nitrogen oxides at elevated temperatures as determined by chemiluminescence NOX analyser[139] techniques. In such measurements the loss of nitrogen oxides is monitored continuously, giving direct information on rates, but no information is available on the reaction of degradation products with other constituents. For example, the emphasis recently has concentrated on the volatile degradation products rather than the material which remains.

In order to understand the mechanism of degradation further, such information is essential and, since it is the very surface of these materials which interacts initially with its environment, it is of great importance to study the nature and rate of accumulation of degradation products in the outermost few tens of Ångstroms of cellulose nitrate fibres.

The lack of such information in the literature can be directly related to the lack of a suitable technique, and it is the advent of ESCA (X-ray Photoelectron Spectroscopy) in the last few years that such information is potentially available. Recent ESCA studies of simple model systems[79] and detailed investigations of the surface nitration and denitration of cellulosic materials[11] have yielded important

information, not only on relative rates of reaction but also on the nature and environment of functional groups. The use of ESCA in studying the degradation of polymeric materials was pioneered by Clark and co-workers,[60] and recently Clark and Stephenson[59] have published a paper on the u-v degradation of cellulose nitrates in dry oxygen and nitrogen environments. This initial study of the surface aspects of the uv degradation of cellulose nitrates showed some interesting conclusions. It is apparent that a low DOS nitrocellulose has an increased rate of degradation compared with more highly substituted residues, perhaps as a result of the increased levels in sulphate esters in the surface regions.[11] The nature of the low binding energy nitrogen component observed is dependent upon the atmosphere present during irradiation. Irradiation in dry oxygen atmospheres gives no evidence for the formation of a low binding energy nitrogen species. Therefore it was concluded that, in the presence of oxygen, the free radical sites which would, in a nitrogen atmosphere, react to produce the low BE nitrogen, react rapidly with free oxygen to form peroxides or other oxidised species.

During an early study of the surface chemistry of cellulose nitrate fibres it was noticed that a degradation reaction took place in the surface regions as a result of exposure[109] to a $Mg_{k\alpha_{1,2}}$ X-ray source for prolonged periods of time (>5 hrs.).

It is the purpose of the work, outlined in the following pages, therefore, to carry out a detailed analysis of the surfaces of cellulose nitrates, and to study the degradation occuring in the outermost few tens of Angstroms in these materials on exposure to X-rays and heat.

5.2 Experimental

All cellulose nitrates used were prepared by standard laboratory procedures outlined in Chapter Three of this thesis, from dried Whatman-1 cellulose papers.

For the X-ray induced degradation, samples were cut to probe tip size (8x22mm) and mounted using double-sided Scotch tape. They were analysed using a Kratos ES300 electron spectrometer with a dual anode X-ray source. Due to the configuration of the dual anode, the sample may be irradiated simultaneously with $Mg_{k\alpha}$ and $Ti_{k\alpha}$ X-rays, thus allowing $Mg_{k\alpha}$ spectra to be obtained concomitantly with $Ti_{k\alpha}$ irradiation (250 watts).

Samples used in the thermal treatment were placed in an oven at 130^{o}C in air and dry cylinder nitrogen for fixed periods of time.

Spectra were peak fitted using a Kratos-DS300 data system, hence satellite substraction was possible automatically.

5.3 Results and Discussion

5.3.1 X-ray induced degradation of cellulose nitrates

During an early study of Clark *et al*[59] of the surface chemistry of cellulose nitrate fibres it was noticed that a degradation reaction took place in the surface regions as a result of exposure to a $Mg_{k\alpha}$ X-ray source for prolonged periods of time[109] (>5 hrs.). This degradation was characterized by a reduction in intensity of the N_{1s} core level corresponding to a nitrate ester group at 408.3 eV and the growth of a peak at ~400 eV, presumably corresponding to the products of this degradative process.

It has been reported previously[11] that the extraneous hydrocarbon component is present only at the very surface from using the depth-profiling facility of the Kratos ES300 electron spectrometer with its dual anode capability ($Mg_{k\alpha}$ and $Ti_{k\alpha}$).

From the work of Clark *et al*[59], on cellulose nitrates, it was found that degradation of cellulose nitrates under $Mg_{k\alpha}$ exposure did not occur at the surface within the normal time scale of the ESCA experiment. However, when using $Ti_{k\alpha}$ X-rays this may not be the case due to

(i) greater X-ray flux,

(ii) greater energy, and

(iii) to enable good counting statistics, the acquisition time is generally larger when using $Ti_{k\alpha}$ X-rays.

It is worth emphasizing here that due to the wavelength dependence of typical unmonochromatised X-ray sources it is probably the longer wavelength Bremstralung which is responsible for the degradation, rather than the characteristic X-ray radiation.

The following five sections will discuss the following experiments.

(a) Irradiation of cellulose nitrate (DOS=2.0) using $Mg_{k\alpha}$ X-rays as a function of time.

(b) Irradiation of cellulose nitrate (DOS=2.83) using $Ti_{k\alpha}$ X-rays as a function of time.

(c) Irradiation of cellulose nitrate (DOS=2.2)) using $Ti_{k\alpha}$ X-rays as a function of time.

(d) Irradiation of cellulose nitrate (DOS=2.6) using $Ti_{k\alpha}$ as a function of time.

(e) The power dependence on the degradation of cellulose nitrates (DOS=2.6) as a function of time on exposure to $Ti_{k\alpha}$ X-rays.

5.3.2 Irradiation of cellulose nitrate (DOS=2.0) using $Mg_{k\alpha}$ X-rays as a function of time.

The degradation of 2.0 DOS material *in vacuo* is shown schematically in Figure 5.1 which depicts the C_{1s}, N_{1s} and O_{1s} core levels of irradiated materials. The X-ray power is ∿96 watts (12kV, 8mA). Significant signs of decomposition require irradiation periods of >3 hours, (*i.e.* the induction period is taken as the appearance of the low binding energy nitrogen component at ∿400eV BE).

The main reaction appears to be a photoreduction. Reference to Figure 5.2 shows that the N_{1s}/C_{1s} area ratios for this material (excluding in all cases the hydrocarbon peak at 285.0eV and relevant sensitivity factors) decreases slowly corresponding to a slow loss of nitrogen species from the surface regions. There is also some evidence from the C_{1s} profiles for increased C-O and aldehydic groups. It is also worth noting that throughout these irradiations the amount of nitrite ester (appearing as a peak at ∿406eV), which is known to be formed in similar photolytic reactions of simple alkyl nitrates (*c.f.* introduction) remains at a relatively constant value of ∿5% of the main nitrate ester peak.

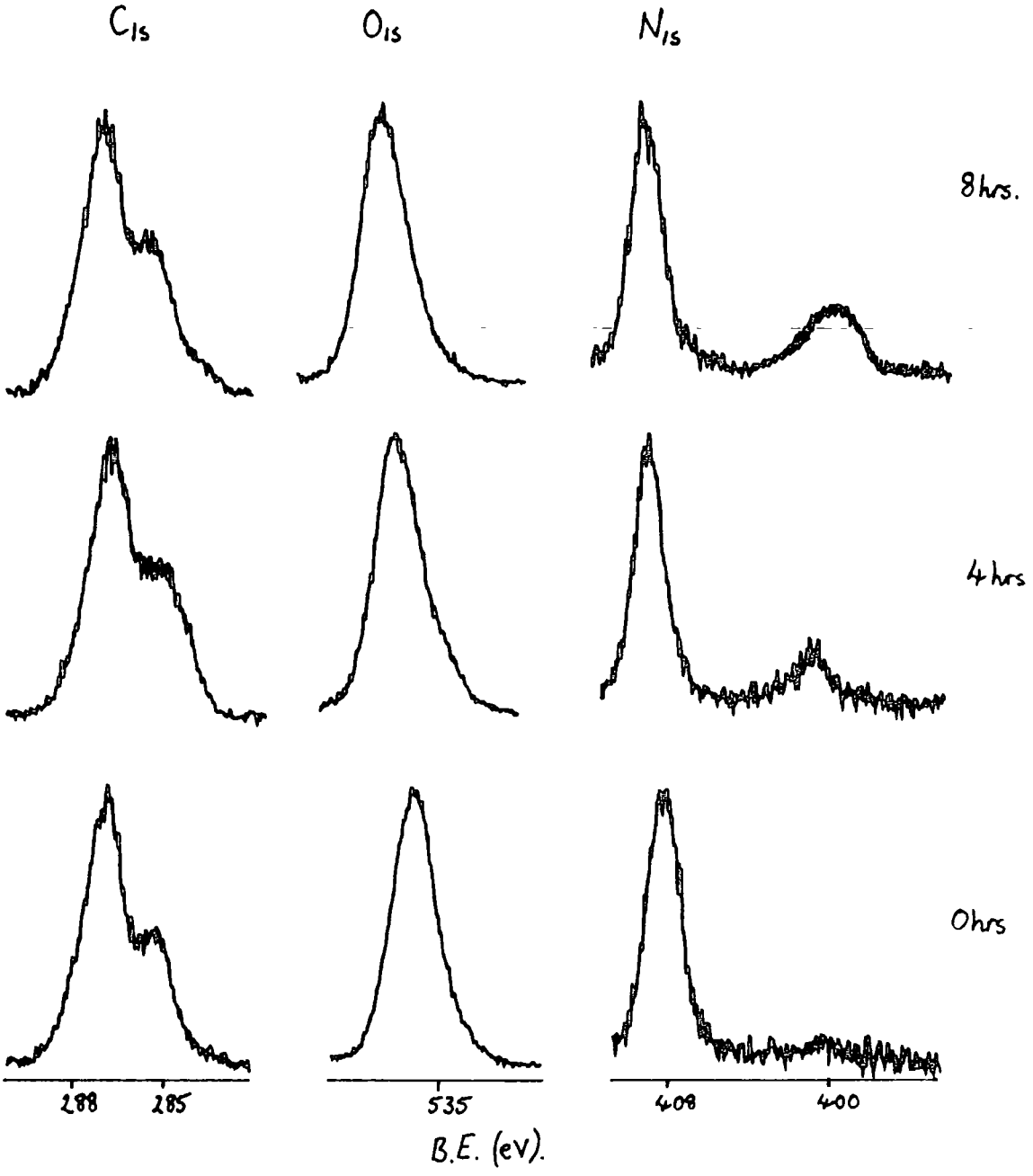

Figure 5.1 C_{1s}, O_{1s} and N_{1s} core level spectra as a function of exposure time

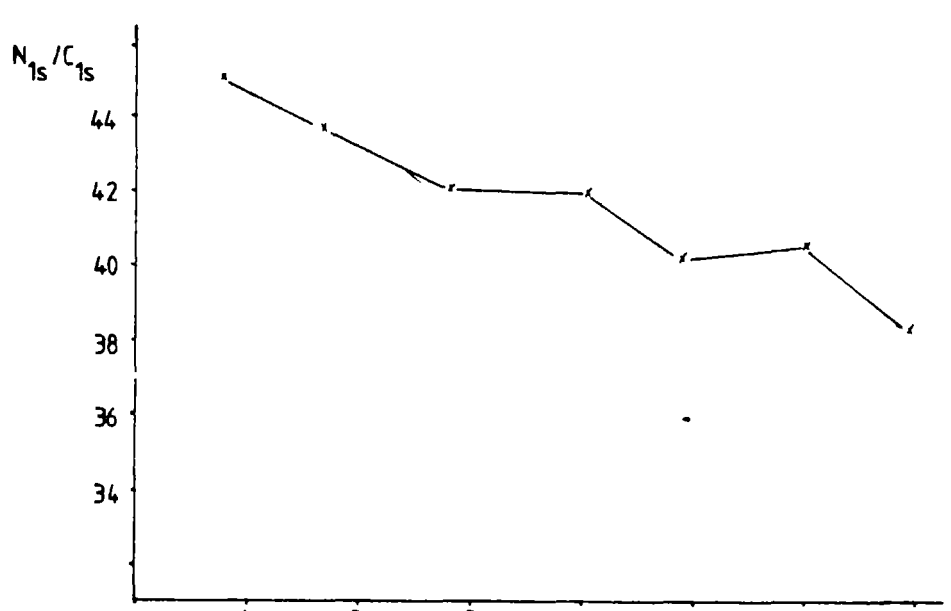

Figure 5.2 N_{1s}/C_{1s} area ratios as a function of exposure time.

5.3.3 Irradiation of 2.83 DOS cellulose nitrate using $Ti_{k\alpha}$ X-rays as a function of time.

The cellulose nitrate used in this study is prepared *via* the Mitchell method using an acid mix of 26% H_3PO_4, 10% P_2O_5, 64% HNO_3 at ambient temperatures for two hours. The resultant material has a bulk and surface DOS of 2.83. This type of material is considered to be highly stable, as much of the literature pertains to the degradation of cellulose nitrates as being due to either sulphate esters, or free sulphuric acid which has not been removed during washing and stabilisation procedures.

The method of exposure to X-rays and the subsequent analysis of the surface by ESCA is slightly different in this experiment than previously nentioned. Here, samples are exposed to $Ti_{k\alpha}$ radiation for fixed periods of time and then sampled

by using only $Mg_{k\alpha}$ radiation, *i.e.* it is a cyclic procedure rather than a continuous one.

Figure 5.3 depicts the decrease in N_{1s}/C_{1s} area ratios as a function of time of exposure to $Ti_{k\alpha}$ X-rays only. That is, the area ratio falls from a value of 0.64 (DOS=2.83) to 0.30 (DOS=1.3) in ∿100 minutes, *i.e.* approximately 50% of the nitrate groups in the cellulose nitrate have reacted to form nitrogen oxides or degradative products. Evidence for C-O and C=O moieties is evident from the C_{1s} profiles, and the low binding energy nitrogen species is evident after a time of ∿40 minutes exposure to $Ti_{k\alpha}$ radiation.

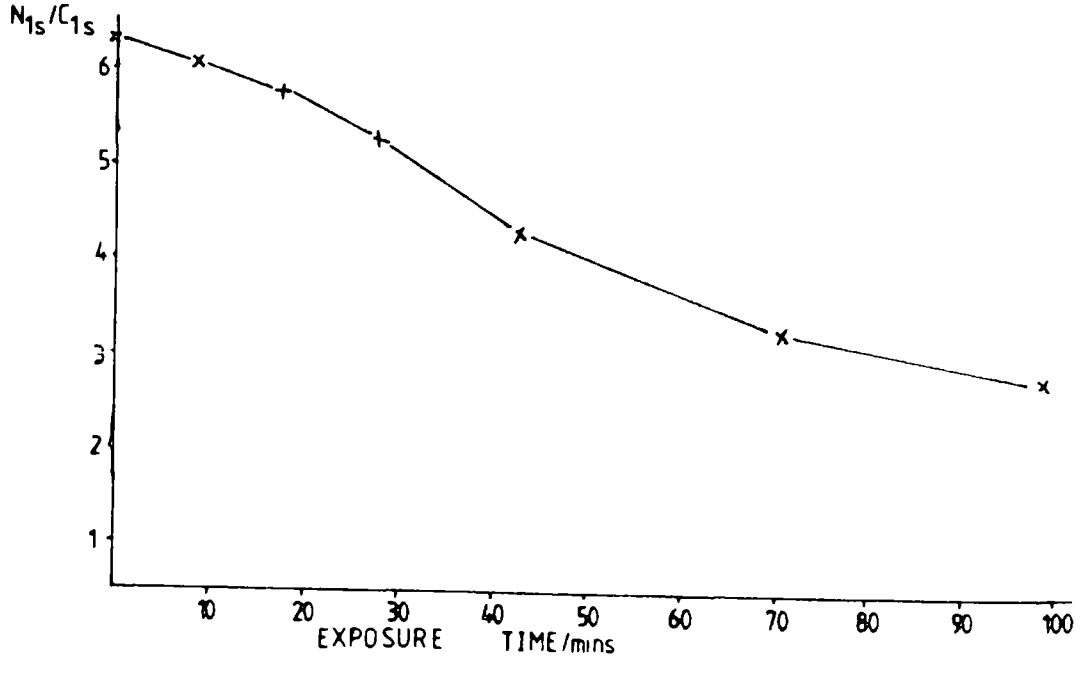

Figure 5.3 N_{1s}/C_{1s} area ratios as a function of exposure time to $Ti_{k\alpha}$ radiation

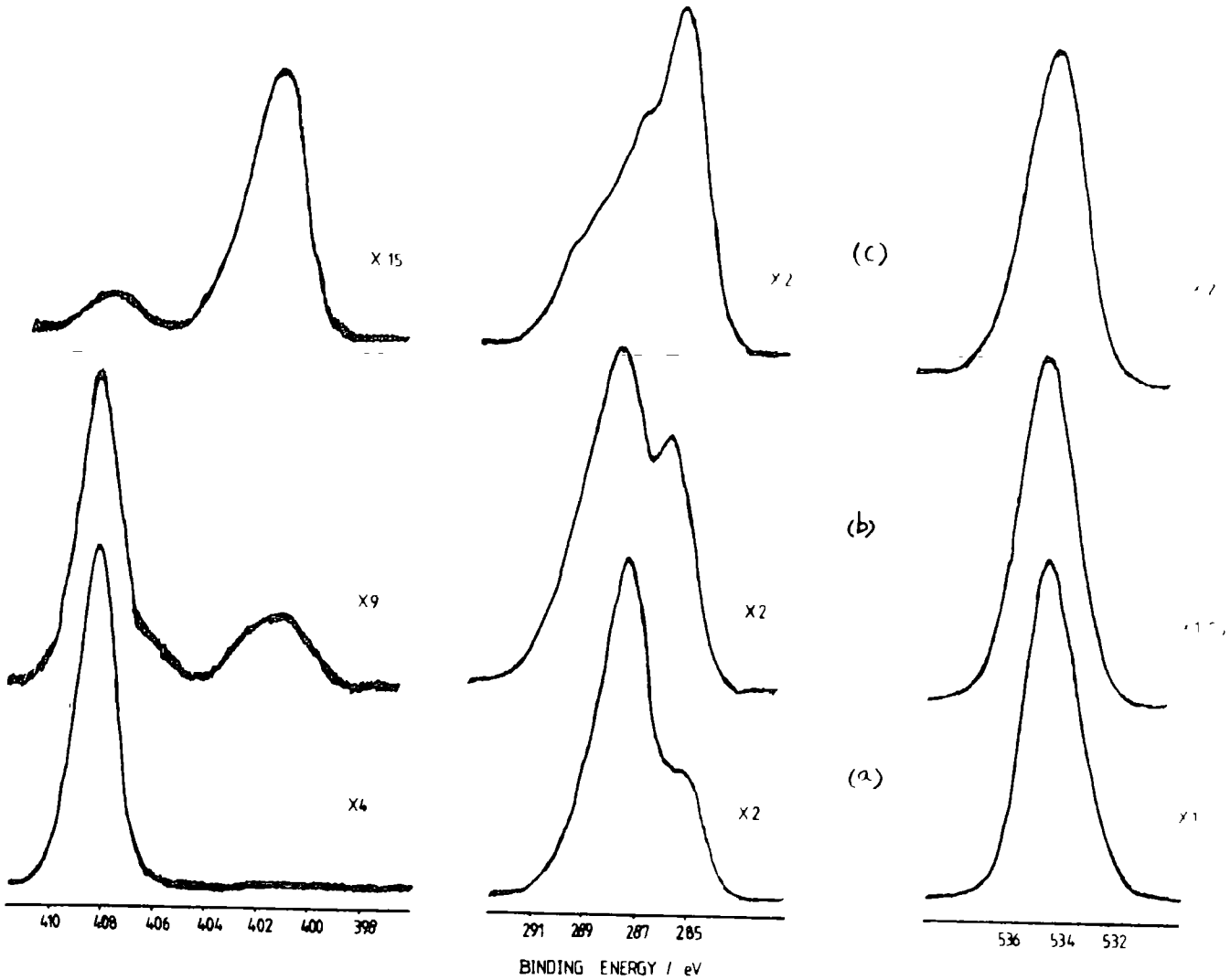

Figure 5.4 C_{1s}, O_{1s} and N_{1s} core level spectra as a function of exposure time

5.3.4 Irradiation of 2.2 DOS cellulose nitrate using $Ti_{k\alpha}$ X-rays as a function of time

Consideration of the changes occurring within the $Mg_{k\alpha}$ sampling depth during $Ti_{k\alpha}$ irradiation are shown schematically in the C_{1s}, O_{1s} and N_{1s} core levels spectra in Figure 5.4.

Typical spectra obtained after 0 hours, ∿3 hours and ∿12 hours exposure are depicted.*

Component analysis of these core level spectra reveal interesting trends which are displayed graphically in Figure 5.5.

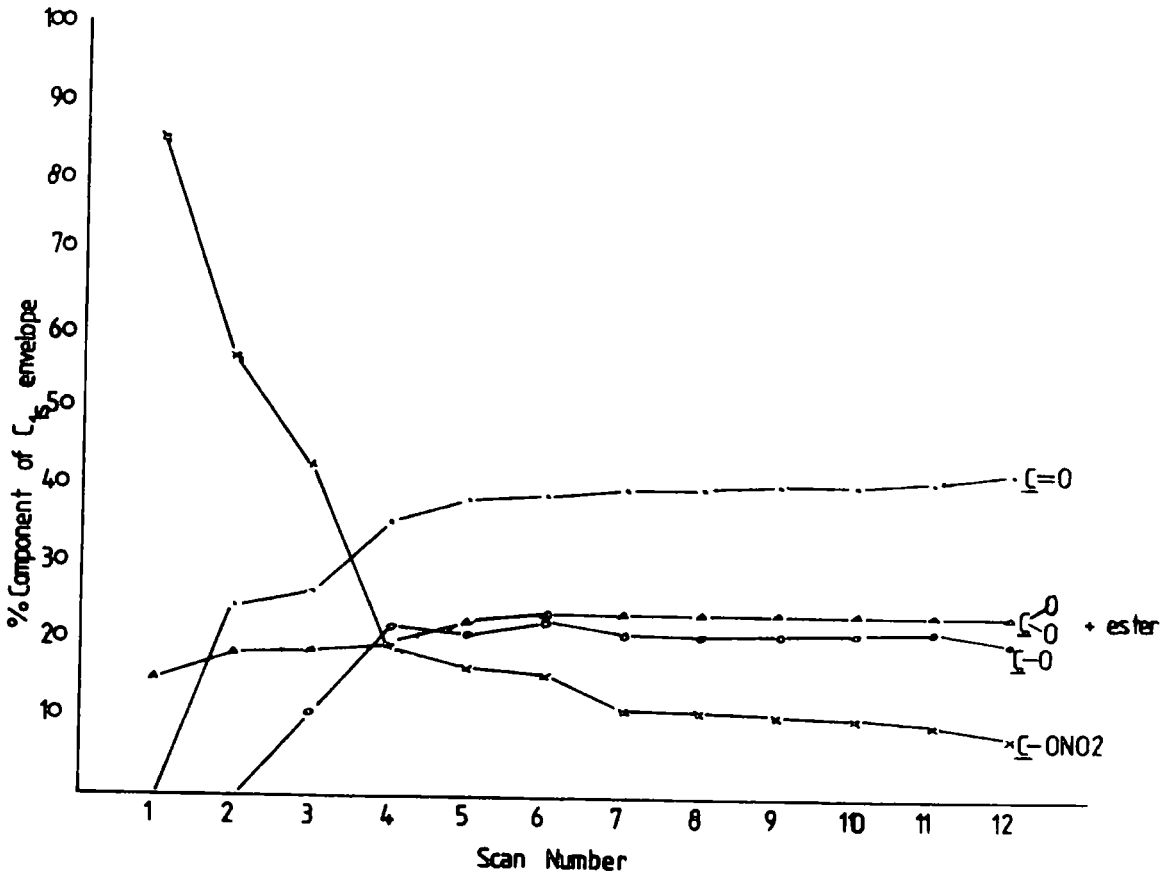

Figure 5.5 Graph showing component analysis of core level spectra as a function of exposure time.

* One scan here is equivalent to 60 minutes.

Consideration of the C_{1s} envelope reveals major changes apparent from a detailed knowledge of binding energies and full width at half maxima for the component peaks. Firstly there is a decrease in the $\underline{C}\text{-}ONO_2$ component at 287.4 eV over the first four hours with the growth of peaks arising from $\underline{C}$-O, $\underline{C}$=O and ester functionalities. The hemi-acetal and ester functionalities are coincident in binding energy, however, as the relative increase in this component is unlikely to arise from an increase in the number of hemi-acetal groups, the growth is assigned to carboxylate groups.

It is worth emphasizing here that due to the wavelength dependance of typical unmonochromatical X-ray sources it is probably the longer wavelength Bremstralung which is responsible for the degradation, rather than the characteristic X-ray radiation.

Changes in the area ratio as a function of time are shown in Figure 5.6.

The N_{1s}/C_{1s} ratio has decreased overall with an approximate exponential decrease in the N_{1s}/C_{1s} ratio due to loss of nitrate functionalities. A small component due to nitrite is evident in all the spectra and is essentially constant throughout the entire exposure. The O_{1s}/C_{1s} area ratios also decrease (but is shown as a C_{1s}/O_{1s} increase). The low binding energy nitrogen component at ~400 eV increases. This is labelled as arising from an oxime for reasons which will be discussed in a later section. The induction period seen in X-ray degradation studies using $Mg_{k\alpha}$ sources is not readily evident in these studies.

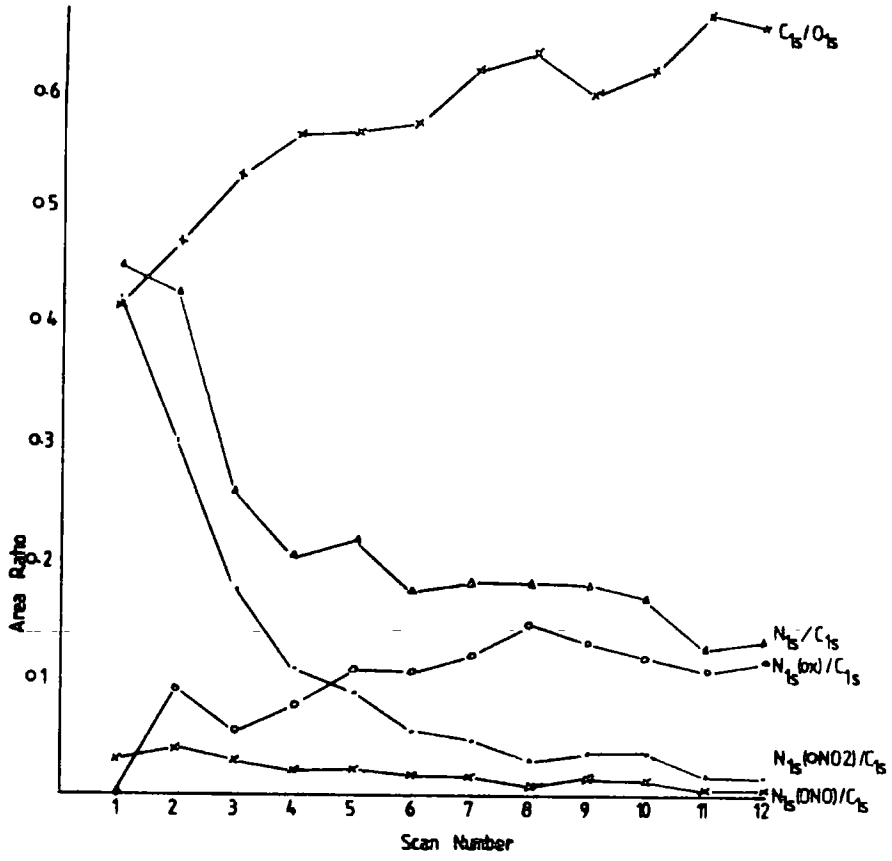

Figure 5.6 Area ratios as a function of exposure time.

The X-ray degraded sample after ∿12 hours (power ≈250 watts) shows changes in its physical characteristics. The sample shows slight yellowing and there is a loss of fibrous character to the sample. This is shown in sample 2 of Plate 5.1, (see page 133).

5.3.5 Irradiation of a 2.6 DOS cellulose nitrate using $Ti_{k\alpha}$ X-rays as a function of time

Data pertaining to 2.6 DOS material are shown in Figures 5.7 and 5.8.

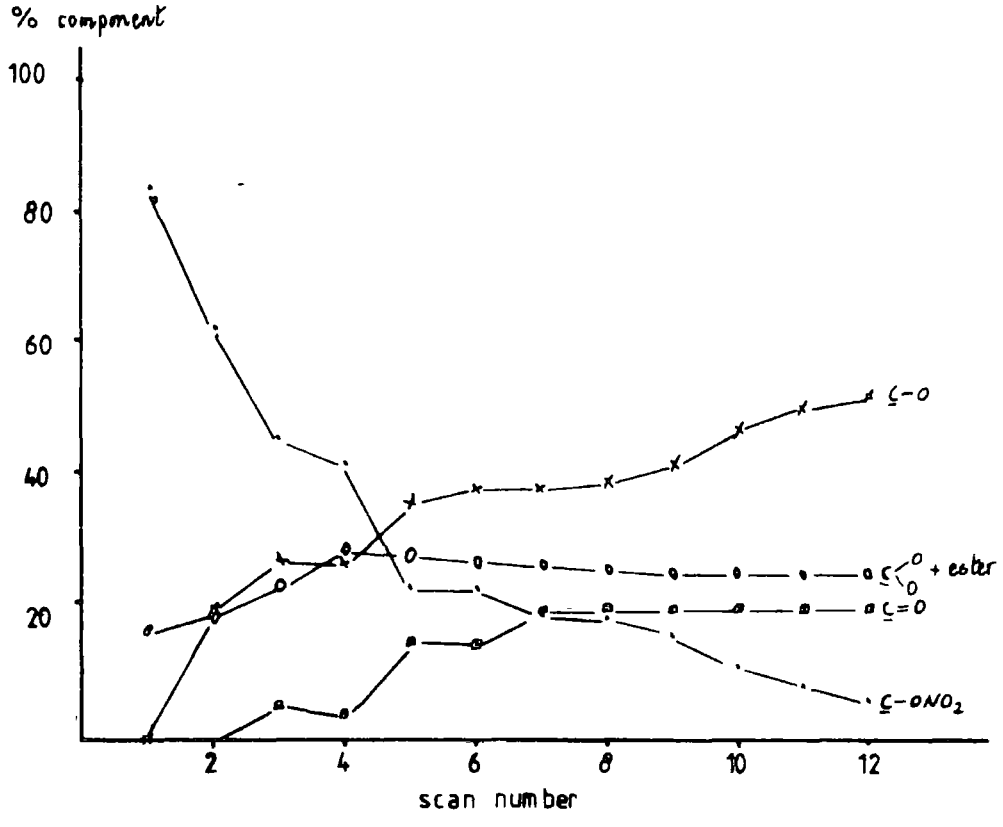

Figure 5.7 Graph showing component analysis of core level spectra as a function of exposure time

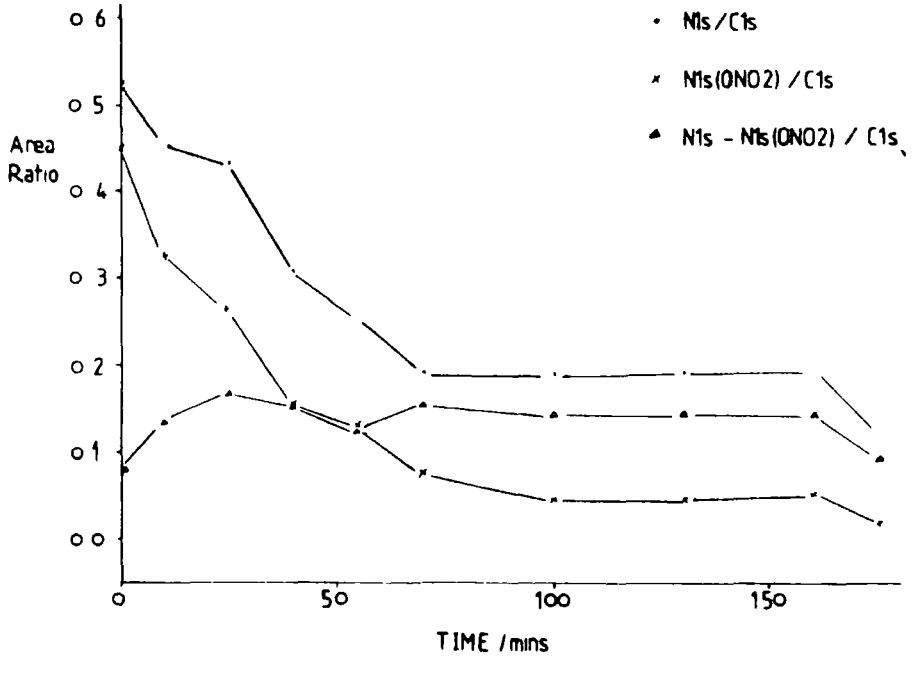

Figure 5.8 Area ratios as a function of exposure time

It is clear that the rate of decomposition under identical conditions is considerably reduced with a much slower loss of nitrogen and comparable decline in oxygen levels. This difference in rate is interesting and may be explained in terms of the difference in preparation of the two cellulose nitrate samples. The low DOS material prepared by nitration in a high sulphuric acid content acid mix is known to have small level of residual sulphate ester groups which have resisted hydrolysis, whereas the high DOS cellulose nitrate prepared in a low sulphuric acid content mix is essentially free of such groups. It is not inconceivable that such groups may act as a photo-initiator and promote the degradation. Another interesting observation is that cellulose nitrates prepared in mixes with a high percentage of sulphuric acid are particularly difficult to stabilise, and without prolonged boiling and washing procedures will rapidly yellow and decompose.

An alternative explanation of the degradation of cellulose nitrates will be discussed in a later section of this chapter.

5.3.6 Power Dependence on the degradation of a Cellulose Nitrate

It is not inconceivable that the power of X-rays incident upon the sample will have an effect on the kinetics of the degradation processes.

It can clearly be seen from Figure 5.9 that the rate of decrease of the N_{1s}/C_{1s} area ratio is dependent on the

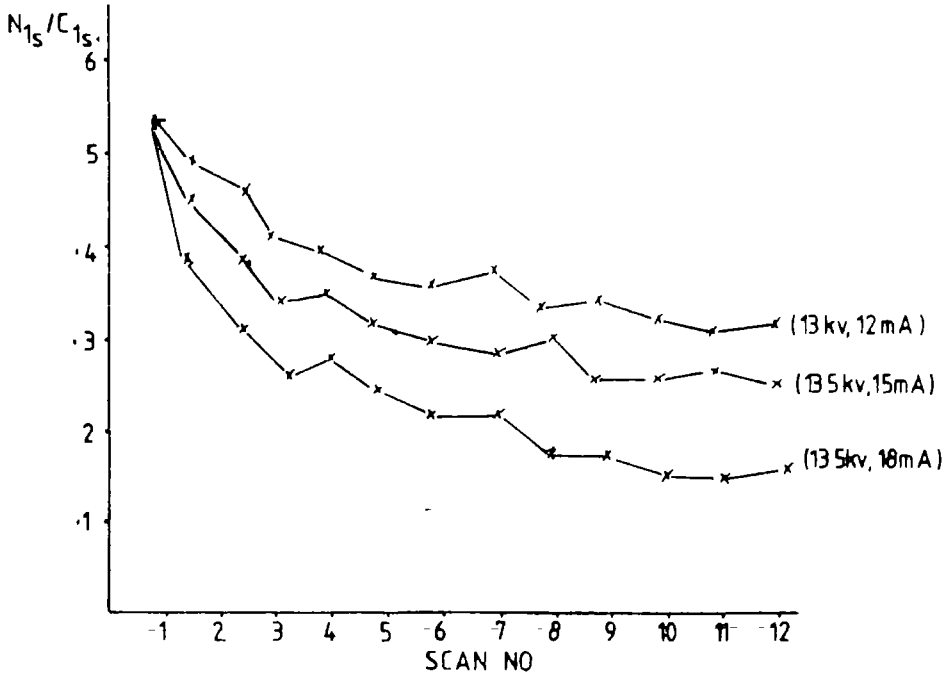

Figure 5.9 N_{1s}/C_{1s} area ratios as a function of time

incident $Ti_{k\alpha}$ X-rays. The lower the incident power, the lower the decrease in N_{1s}/C_{1s} area ratio of the 2.6 DOS cellulose nitrate samples.

Also the relevant increases in C-O, C=O and ester functionalities from the C_{1s} profiles are also, as expected, dependent on power.

5.4 Proposed Mechanisms of degradation in Cellulose Nitrates

From the previous discussion it is obvious that the X-ray induced degradation of cellulose nitrates is extremely complex, and it is not a simple procedure to postulate a complete, complex formalism to account for the formation of a low binding energy nitrogen species and the formation of C-O, C=O and ester functionalities.

However, it is worth considering possible routes to

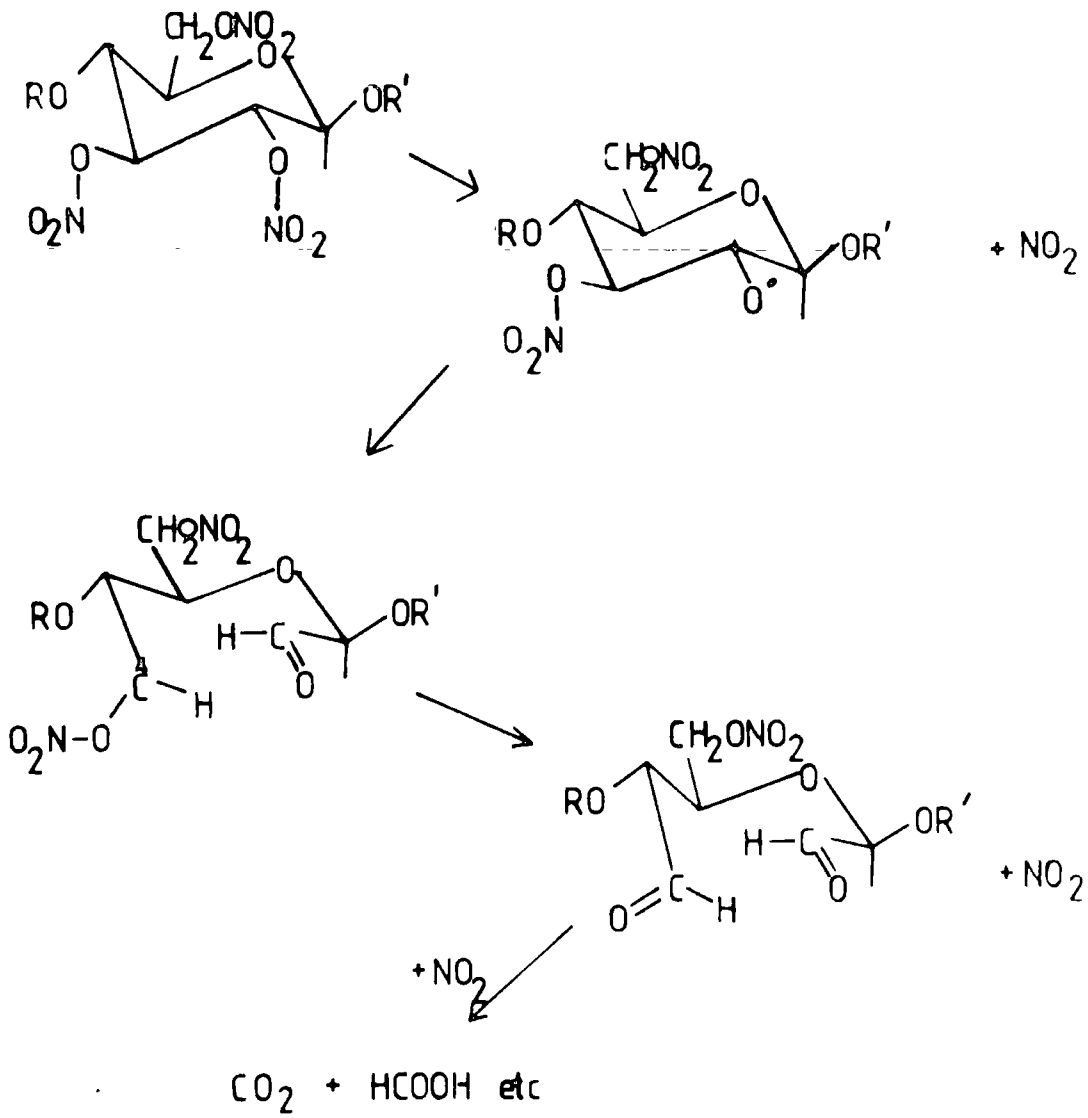

Figure 5.10 Schematic pathway to the formation of carbonyl functionalities and ring cleavage

carbonyl functionalities and the nitrogen moiety formed. From bulk thermal degradation studies[140] it has been proposed that the initial stage of degradation involves the loss of NO_2, and in Figure 5.10, a schematic pathway which results in the formation of carbonyl groups and ring cleavage is shown.

The low binding energy component in the N_{1s} core level spectra appears at first to be inconsistent with the available bulk data in the literature in that the formation of a stable nitrogen functionality within the residue during degradation has not been observed. It therefore is apparent that this is a product present only in the surface regions. However, after long periods of exposure to $Ti_{k\alpha}$ X-rays, a Ti anode spectrum of the N_{1s} core level (see Figure 5.11) is also different.

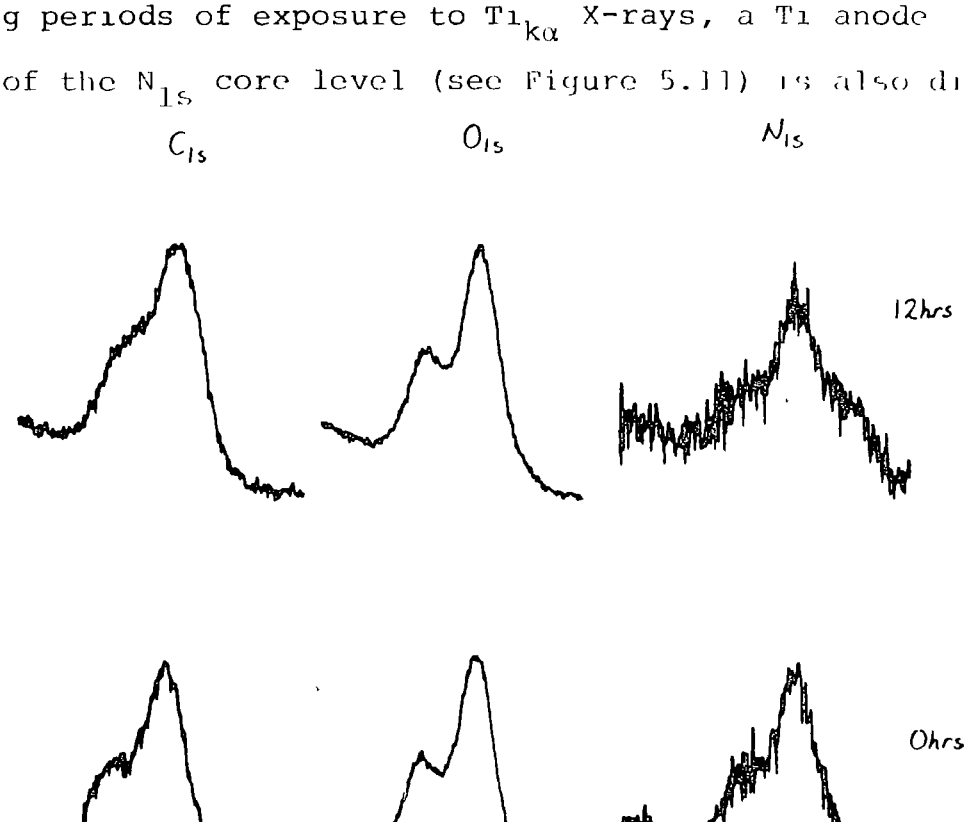

Figure 5.11 $Ti_{k\alpha}$ core level spectra as a function of time (a) 0 hrs., and (b) 12 hrs. exposure time.

By comparison of the two spectra in Figure 5.11, it is clear that a third peak is apparent in the degraded sample. This must be due to the low binding energy nitrogen moiety. Therefore it is noticed that the X-ray degradation of cellulose nitrates is a surface phenomena, which after long exposure times is evident within the Ti sampling depth of ~130Å *i.e.* the subsurface.

The origin of the low binding energy nitrogen peak is uncertain at this stage, in that many nitrogen groups have N_{1s} binding energies of ~400 eV. However, on consideration of known degradation reactions of nitrites and nitrates in solution, a possible assignment is that of an oxime.

The Barton Reaction,[141-142] for nitrites in particular, which leads to the formation of an oxime, is well documented in the literature and it is not inconceivable that a similar type of reaction occurs on the surface regions of cellulose nitrate fibrils during X-ray degradation. A schematic pathway for the formation of an oxime in a cellulose nitrate is shown in Figure 5.12.

Although the Barton Reaction is normally favoured by the formation of a 5- or 6-membered transition state, this is not readily feasible in a β-D-anhydroglucopyranose ring system. For the schematic shown, a 7-membered transition state is proposed which would invoke a 1,7-hydrogen shift. Evidence for this shift has recently been proposed,[144] although it is not inconceivable that due to the material being a polymer, certain of its degrees of freedom must be restricted and perhaps in this case, a 7-membered transition state is not too improbable.

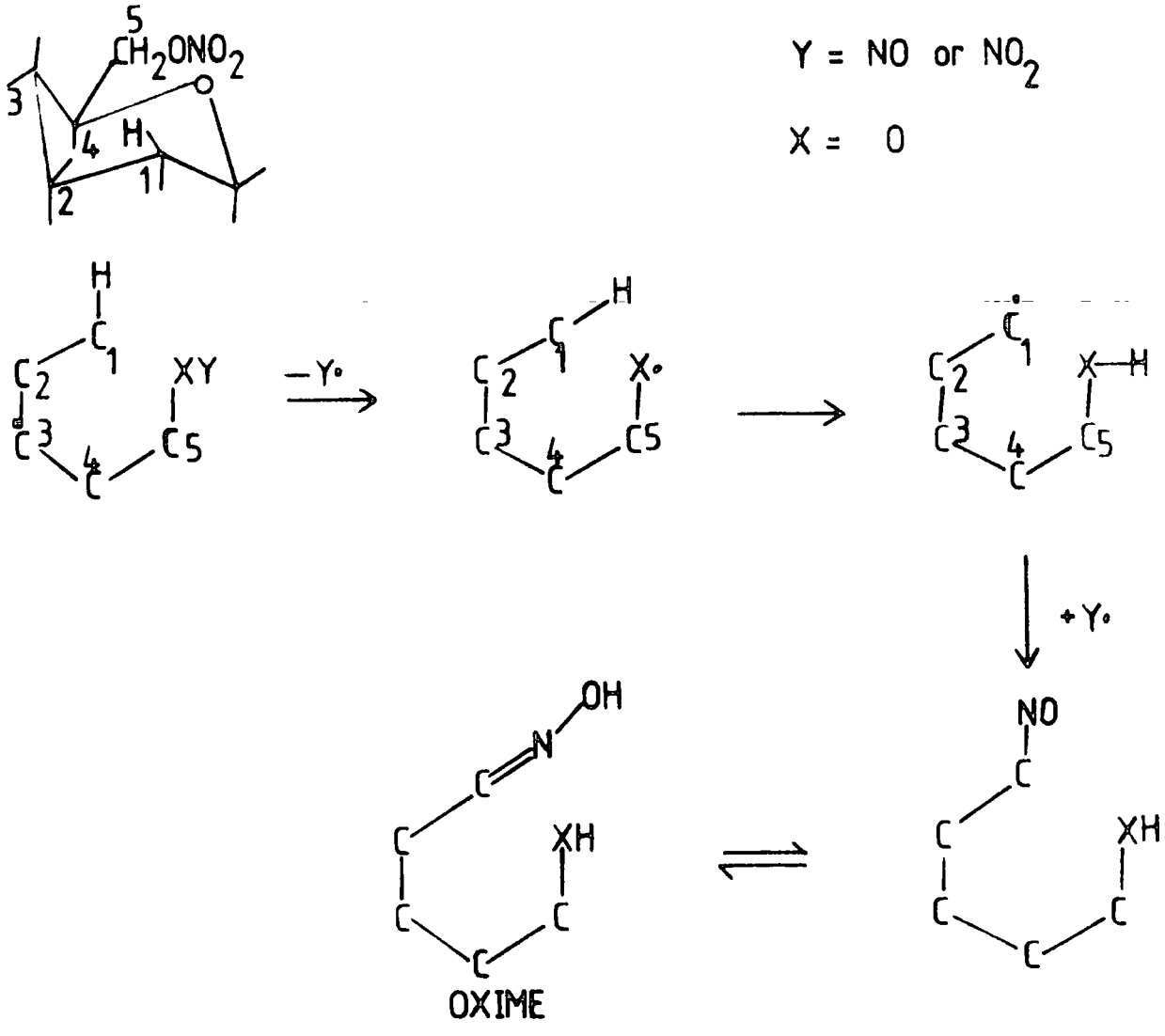

Figure 5.12 Schematic pathway for the formation of an oxime

Other possible "advantages" of a Barton type reaction are that it is catalysed by H_2SO_4, H_3PO_4, P_2O_5, *etc.* A repeat of a previous experiment of an X-ray induced degraded 2.2 DOS material, where the sulphate ester group was monitored at the surface showed that the amount of sulphate ester present remains approximately constant throughout the exposure. Hence the presence of sulphate esters may act in a catalytic or photosensitising rôle.

If photolysis of a nitrite is effected in the presence of oxygen, the product of rearrangement is not a nitroso compound or an oxime but a nitrate, which is easily converted into the corresponding alcohol by mild reduction.[145] The reaction is believed to take a pathway in which the initial carbon radical is captured by oxygen instead of nitric oxide.

This may account for results in the work of Clark *et al*, where when a sample of cellulose nitrate was degraded by uv light in a dry oxygen atmosphere, there was no evidence for a low binding energy nitrogen peak.

5.5 The Thermally-Induced Degradation of Cellulose Nitrates

The thermal degradation of cellulose nitrates is obviously of more technological interest than that induced by X-rays. Recent studies of the thermal degradation of cellulose nitrates have concentrated on monitoring the rate of evolution of nitrogen oxides at elevated temperatures as determined by chemiluminescence NOX analyser techniques.[139] In such measurements the loss of nitrogen oxides is monitored continuously, giving direct information on rates, but no information is available on the reaction of degradation products with other constituents.

Since it is considered that all degradation processes occur initially at the surface, because it is this surface which interfaces with the environment, then ESCA is potentially capable of monitoring the degradation process within the outermost few tens of Ångstroms of such systems.

In this study two cellulose nitrates of differing degrees of substitution were used, and placed in a thermostatically controlled fan circulating oven at 130°C in air. 130°C was chosen as this is the temperature used in the Abel Heat Test.[62]

5.5.1 Thermal Degradation of a 2.2 DOS cellulose nitrate

This material was prepared in mixed acids as described elsewhere in this thesis. $Mg_{k\alpha}$ core level spectra are shown in Figure 5.13 for times of 0, 2, 5 and 17 hours at 130°C in air.

It is evident from Figure 5.13 that very little change has occurred in the surface regions of the sample. There is no evidence from the C_{1s} core level envelope to suggest the appearance of carbonyl or carboxylate functionalities, and the N_{1s} core level suggests no evidence for the formation of a low binding energy nitrogen peak at a binding energy of ∿400 eV.

Figure 5.14 shows graphically the slight decrease in the N_{1s}/C_{1s} area ratio against time at a temperature of 130°C.

Detailed visual inspection, however, of a sample thermally degraded for 17 hours and then compared with the starting material and a sample exposed to X-rays for 100 minutes

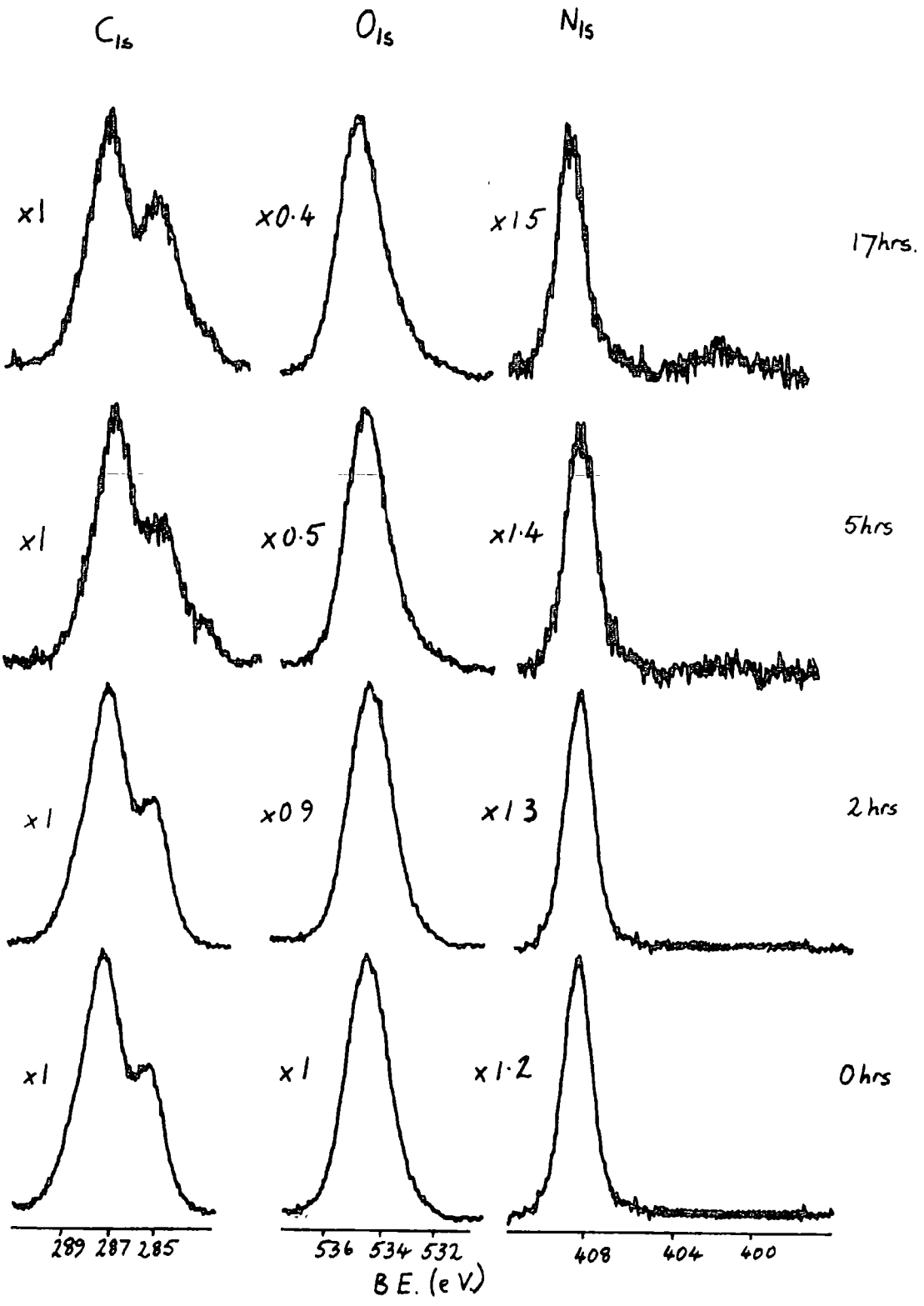

Figure 5.13 $Mg_{k\alpha}$ core level spectra after 0, 2, 5 and 17 hours at 130°C in air

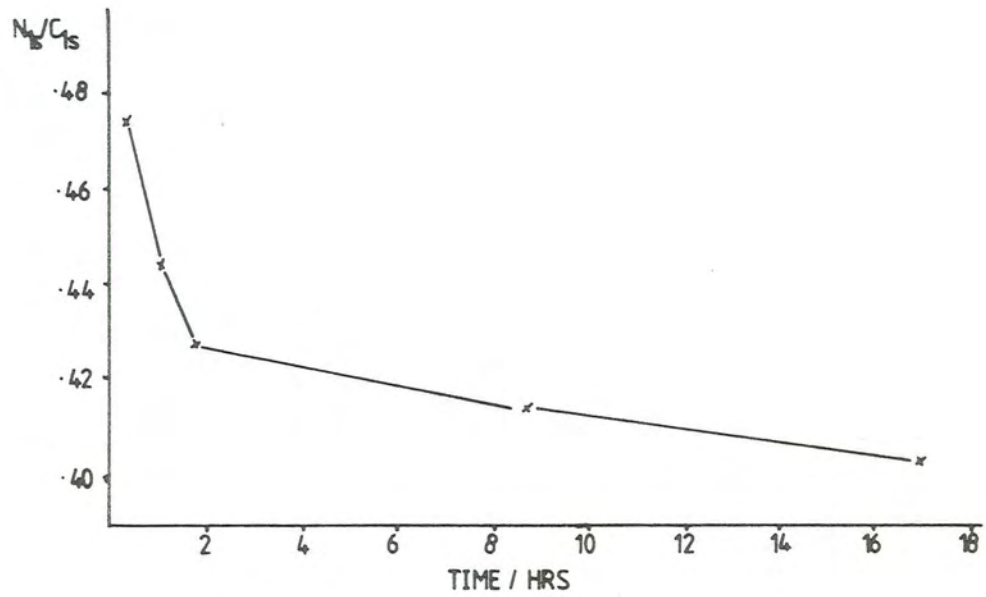

Figure 5.14 N_{1s}/C_{1s} area ratios *versus* time.

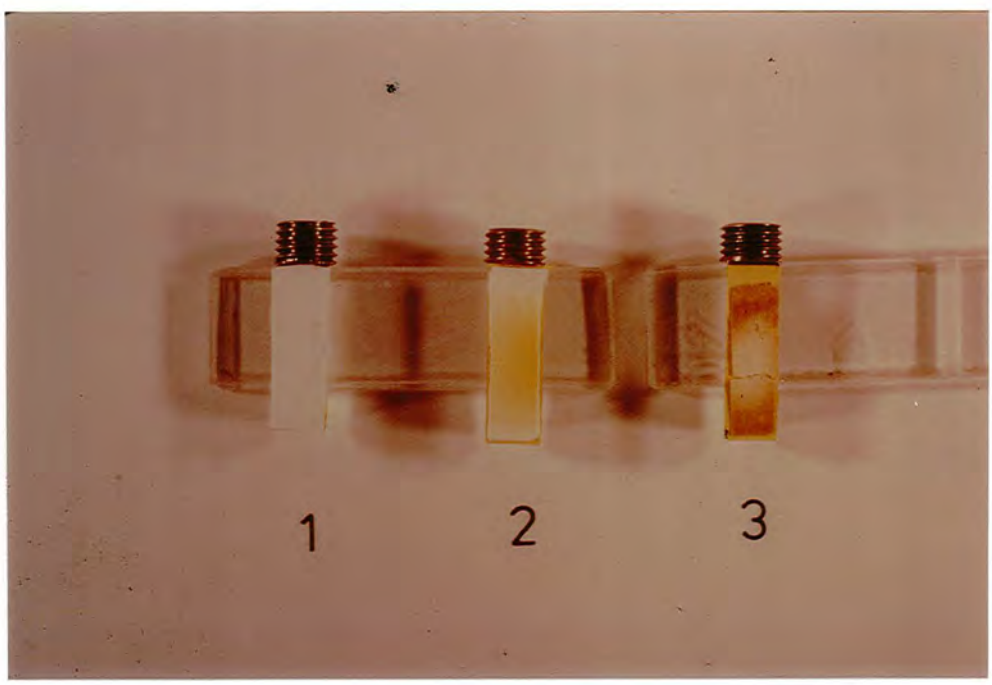

Plate 5.1 Photograph showing samples (1) pristine material, (2) X-ray induced degraded material and (3) thermally degraded material

reveals some startling contrasts (see Plate 5.1).

The starting cellulose nitrate in all cases is white and fibrous in nature (Sample 1). That of the X-ray degraded sample shows slight yellowing and there is no longer any fibrous character. The sample is powdery (Sample 2). The thermally degraded sample* is dark brown in colour. Fibrous character is still evident, although the sample is brittle and its dimensions had shrunk.

5.5.2 Thermal Degradation of a 2.6 DOS cellulose nitrate

The sample was prepared by standard procedures as outlined in this thesis. Again there is no evidence from the C_{1s} and N_{1s} core level spectra for any change in the surface except the N_{1s}/C_{1s} area ratios decrease slightly with time. The data are shown in Figure 5.15.

These results would tentatively suggest that either the thermal degradation of cellulose nitrates is more bulk orientated than surface, or the presence of an oxygen monolayer at the surface inhibits the formation of a low binding energy nitrogen component as was discussed in Section 5.4.

To determine the role of the latter is the substance of the next section.

Footnote: * Sample 3 has been scraped prior to photographing.

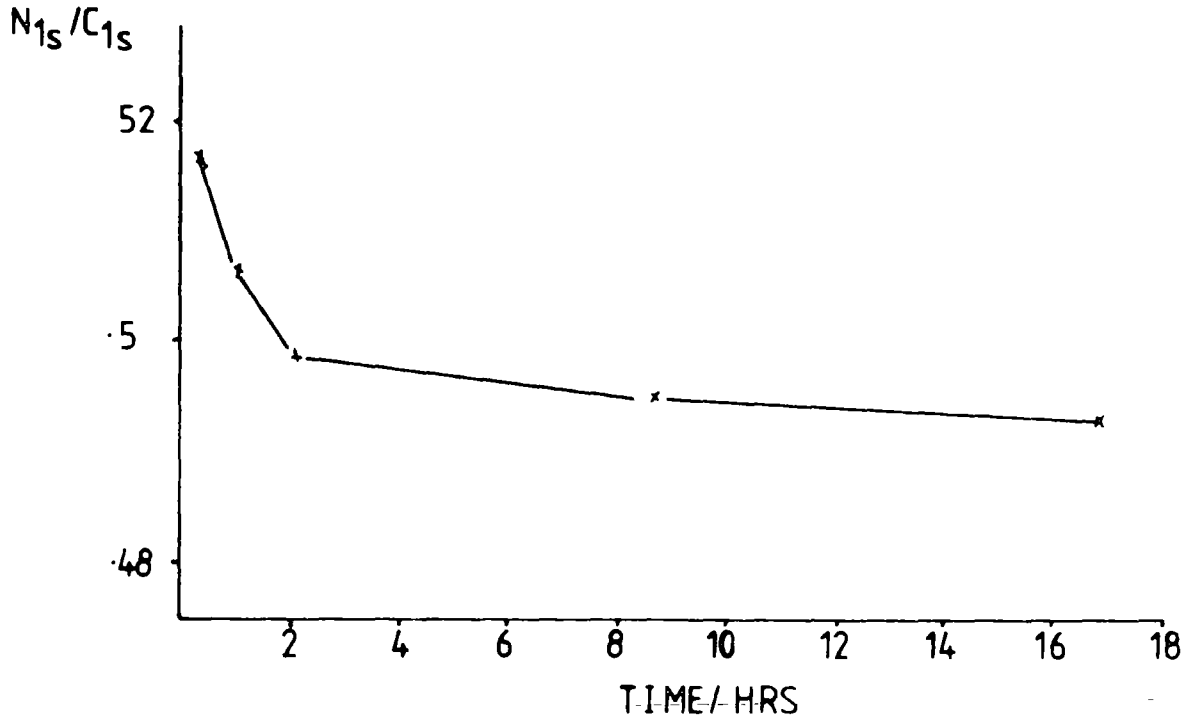

Figure 5.15 N_{1s}/C_{1s} area ratios *versus* time

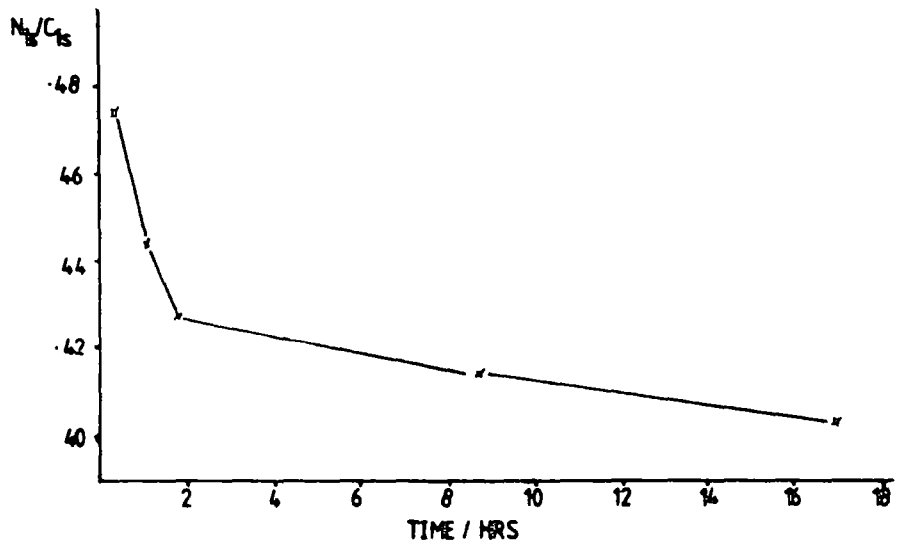

Figure 5.16 N_{1s}/C_{1s} area ratios *versus* time

5.5.3 The Thermal Degradation of 2.2 DOS cellulose nitrate in a flow of dry, oxygen free, nitrogen

An identical sample to that used in Section 5.5.1 was used. The oven (130°C) was flushed for four hours with dry, oxygen free, nitrogen gas prior to insertion of the sample. Figure 5.16 shows the slight decrease in N_{1s}/C_{1s} area ratios against time. Comparison with Figure 5.14 shows these curves to be similar within the experimental error. Again there is no evidence for a low binding energy nitrogen component or oxidised carbon environments within the top 50Å of the surface of the material. Therefore, the conclusion to be drawn is that the thermal degradation of cellulose nitrates is indeed a bulk phenomena as opposed to the electromagnetic degradation which we have shown to be surface oriented.

Similar contrasts between bulk and surface data for the thermal degradation of low density polyethylene[146] and Bisphenol-A-Polycarbonate[147] have been observed in this laboratory.

In the case of Bisphenol-A-polycarbonate[147] after 15 hours at 175°C (25° above the T_g) the sample is opaque and slightly brittle in nature. After ∿1000 hours, the sample is totally opaque and extremely brittle. However, in both cases the C_{1s} and O_{1s} envelopes appear identical as is the C_{1s}/O_{1s} area ratios. It is known from photo-oxidation work on the system[148] that after 1000 hrs. irradiation with a uv black lamp (λ>300nm, flux=0.25 watts.m^{-2}) there is extensive oxidation of the surface in air.

5.6 Comments

The use of ESCA has led to important advances in the understanding of the surface degradation of cellulose nitrates. The formation of the low binding energy nitrogen component has led to the postulation of a possible degradation pathway in these systems. However, one of the most interesting features of this work has been the difference in the degradation dependent on the mode used to degrade these materials. Thermal and electromagnetic modes of degradation appear to be two distinct mechanisms - one being surface oriented and the other bulk. Clearly a great deal of research has yet to be done on this interesting aspect; not only on cellulose nitrate systems but also on synthetic high polymers. Obviously the use of ESCA or other surface techniques and bulk techniques such as solid state and solution nuclear magnetic resonance spectroscopies must play an increasing rôle in the analysis.

CHAPTER SIX

A PRELIMINARY INVESTIGATION OF THE THERMAL AND X-RAY INDUCED DEGRADATION OF CELLULOSE NITRATES BY FAB/SIMS AND ^{13}C N.M.R.

6.1 Introduction

In Chapter Five of this thesis, the use of ESCA was reported in the study of the X-ray and thermally induced degradation occurring in the outermost top 40Å of the surface of cellulose nitrates. X-ray induced degradation produces pronounced changes in the ESCA spectra; the most notable being the loss of nitrate functionality and the possible formation of an oxime structure which were evident from the N_{1s} core level spectra. In contrast, only a slight decrease in nitrate concentration was observed for thermal degradation.

Visual examination of the samples revealed a slight surface yellowing for the X-ray degraded sample and an extensive dark brown discolouration plus shrinkage for thermal degradation. This data led to the suggestion that degradation arising from electromagnetic radiation is surface oriented, whereas thermal degradation is predominantly a bulk effect.

To complement these ESCA studies, this chapter outlines further investigations of these materials using FAB/SIMS (Fast Atom Bombardment Secondary Ion Mass Spectrometry) and ^{13}C NMR.

The application of SIMS to polymeric surfaces is still in its infancy[174-180] and more fundamental studies are required to enable the full potential of this technique to be realised. However, it will become apparent from the following results and discussion that this surface technique is complementary to ESCA, and highlights the differences in the nature of the surface chemistry of degraded cellulose nitrates.

It has already been alluded to in an earlier chapter of this thesis how solution state, proton noise decoupled ^{13}C n.m.r. has led to a better understanding of the bulk microstructure of these materials.[45,47,181] The use of this technique has been employed to monitor changes in the bulk chemistry of cellulose nitrates during degradation.

6.2 Experimental

The cellulose nitrate used was prepared by the standard method outlined previously, from Whatman-1 filter papers.[45,47] This gave a cellulose nitrate of degree of substitution of 2.2 from ESCA and bulk techniques (*i.e.* ^{13}C n.m.r. and micro-Kjeldahl).

Samples were degraded in a manner outlined in the previous chapter.

FAB/SIMS spectra were recorded on a Kratos SIMS 800 system, and analysed using the Kratos SIMSCAN software package employing a DEC PDP-11 minicomputer. Samples were introduced into the SIMS spectrometer *via* fast insertion locks. The base pressure of the system was $\sim 5 \times 10^{-10}$ torr. Argon gas was introduced into the ion gun to a pressure of 1×10^{-6} torr, and there subsequently to the neutralisation chamber of the FAB gun to a pressure of 3×10^{-6} torr. The 500V accelerating voltage used gave a secondary electron emission current of $\sim 5 \times 10^{-9}$ A. The 3kV beam gave a secondary electron emission current of $\sim 5 \times 10^{-6}$ A.

^{13}C n.m.r. (90.56 MHz), proton noise decoupled spectra were run on a Bruker WH-360 spectrometer at the University of Edinburgh. 10% by weight solutions were made up in DMSO-d_6.

Spectra were taken at a temperature of $\sim 80^{\circ}C$.

6.3 Results and Discussion

6.3.1 FAB/SIMS

The FAB/SIMS spectra displayed in Figure 6.1 (a,b,c) were obtained from a sample of cellulose nitrate (a) of DOS 2.2, and then (b) thermally degraded, (17 hrs. @ $130^{\circ}C$ in air) and (c) X-ray induced degradation [12 hrs, $Ti_{k\alpha}$ (13.5kV, 18mA)] using a 500V accelerating voltage and a 3 minute acquisition time. In all the spectra, peaks are evident at 23, 27 and 39 amu and arise from Na^+, Al^+ and K^+ contaminants.[182,183] These are invariably present in SIMS spectra. Fragments of mass greater than 60 amu only appear at low intensity.

Apart from the addition to the complexity of the spectra arising from the presence of a patched hydrocarbon overlayer, known to be present at the surface from ESCA studies,[11] the fragments sputtered from the surface may undergo reactions before reaching the detector. It is therefore not the intention in this chapter to undertake a comprehensive analysis of the spectra, but rather to highlight certain features which are obviously different on comparing the three sets of spectra.

The peaks at 29, 30, 31, 41, 43 and 46 amu, whose possible assignments are given in Table 6.1, are taken in the present case as a monitor for the differences in the three samples.

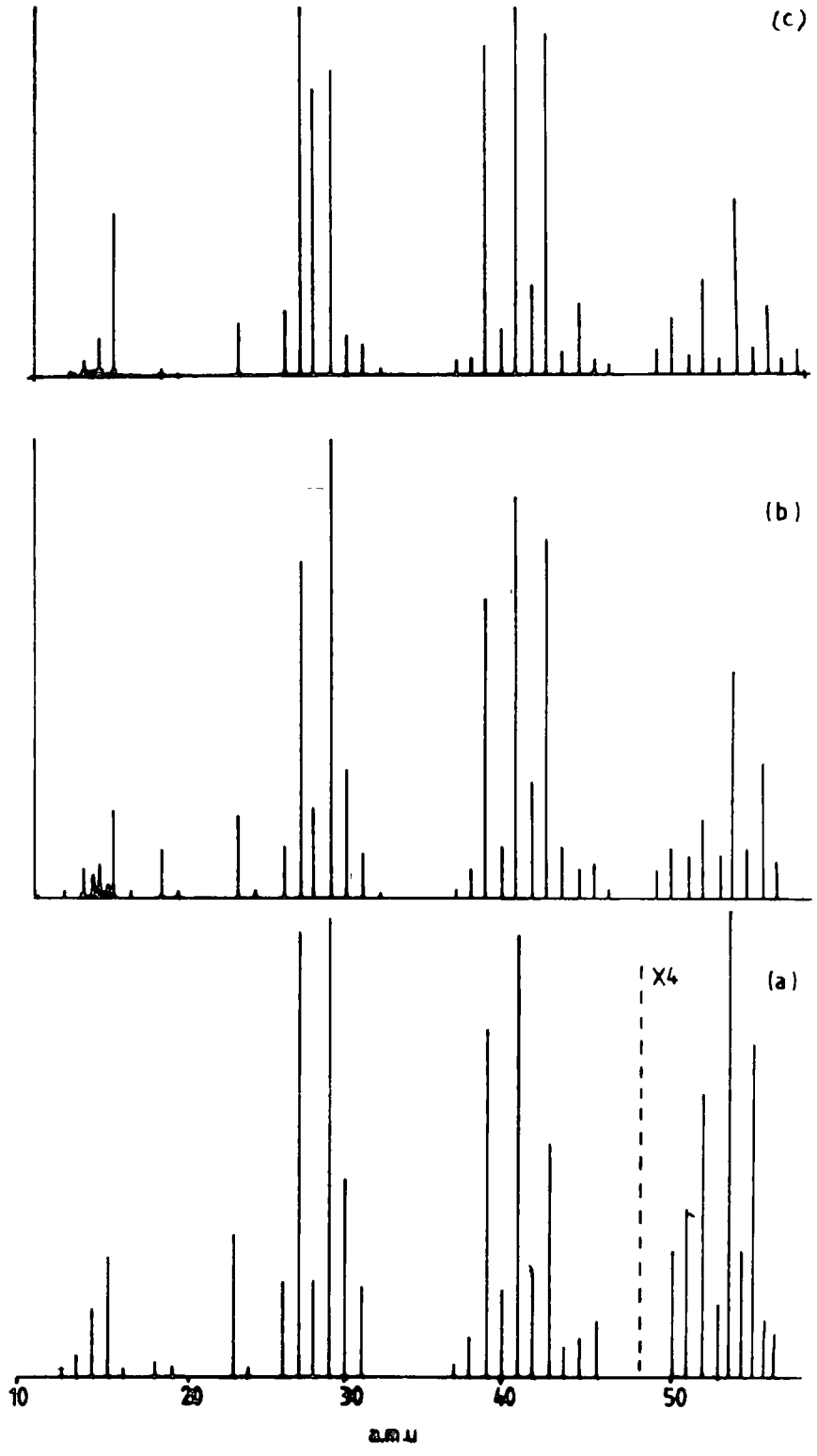

Figure 6.1 FAB/SIMS spectra of cellulose nitrate and degraded materials

TABLE 6.1

PEAK/amu	Possible Assignment
29	$C_2H_5^+$, CHO^+
30	NO^+, CH_2O^+
31	CH_2OH^+
41	$C_3H_5^+$, $CH_2C{=}N^+$
43	$C_3H_7^+$, $CH_3C{=}O^+$
46	NO_2^+

It is evident for the pristine material that the peak at 46 amu (NO_2^+) is not very intense, which is in contrast to that obtained in simple aliphatic nitrates utilising electron impact (EI) ionisation.[184] However, the peak at 30 amu is intense. By comparison with Figure 6.1 (b,c) and from the known nitrate ester group concentrations at the surface from ESCA studies (*c.f.* Chapter Five),[185] a major contribution to this peak would appear to arise from NO^+. This suggests that either NO^+ is preferentially sputtered from the surface or that NO_2^+ undergoes dissociation on passing through the high energy region at the surface/vacuum interface.[176]

It is evident from Figure 6.1 that the main difference occurring in the peaks listed in Table 6.1 for thermal degradation are decreases in intensity at 30 and 46 amu relative to the other peaks at *e.g.* 29, 41 and 43 amu. These observed differences in the FAB/SIMS spectra are indicative of only a small loss of NO_2 from the nitrate ester groups,

and are as such complementary to the ESCA studies where a slight decrease in the number of nitrate groups in the outermost top 40Å of the sample was observed.[185]

The FAB/SIMS spectra for the X-ray degraded sample, which from the ESCA studies is known to have a major depletion in the nitrate ester concentration,[185] reveals very low intensity peaks at 30 and 46 amu, in comparison with the pristine and thermally degraded materials.

It is clear from these results that a major loss of nitrate ester functionality in the surface of cellulose nitrate is only observed for X-ray induced degradation. In addition, for this latter sample, a major change in the relative intensities of the 28 and 29 amu peaks is observed. From a ∿0.22:1 ratio in the undegraded cellulose nitrate and thermally degraded sample; on X-ray induced degradation this ratio changes to ∿1:1, and is strongly indicative for the presence of other degradative residues apart from those left by the loss of NO_2 in the surface regions.

In a SIMS study of cellulose acetate by Briggs,[179] prominent peaks appear at 81, 97, 111, 127 and 169 amu and were assigned to aromatic heterocyclic ions derived from the β-D-glucopyranose ring system. The FAB/SIMS spectra of cellulose nitrates does not give rise to such peaks and highlights the significant differences in the fragmentation patterns of the two esters.

Investigation of polymer surfaces by SIMS[174-180] and ion beam bombardment of polymers[186] as studied by ESCA have revealed that extensive degradation of the pristine

material occurs. Extreme care must therefore be taken to prevent significant sample damage occurring before a SIMS spectrum representative of the true surface can be recorded.

Figure 6.2 reveals the peak intensities as a function of scan number for the original cellulose nitrate (500V, 3 mins. per scan). As is evident from Figure 6.2 the peak intensities remain essentially constant over the first seven scans (∿21 minutes) and then rapidly decrease indicative of significant sample damage. Similar trends are observed for signal intensities as a function of scan number for the degraded materials.

For comparison, positive ion spectra were also recorded at a 3kV accelerating voltage. As can be seen from Figure 6.3, the signal intensities decrease exponentially. For example, after the third scan (here 1 scan = 60 seconds) the 46 amu peak has decreased in intensity by ∿75%. These data therefore indicate that low accelerating voltages should be preferentially used when investigating materials by FAB/SIMS to prolong the lifetime and integrity of the sample surface.

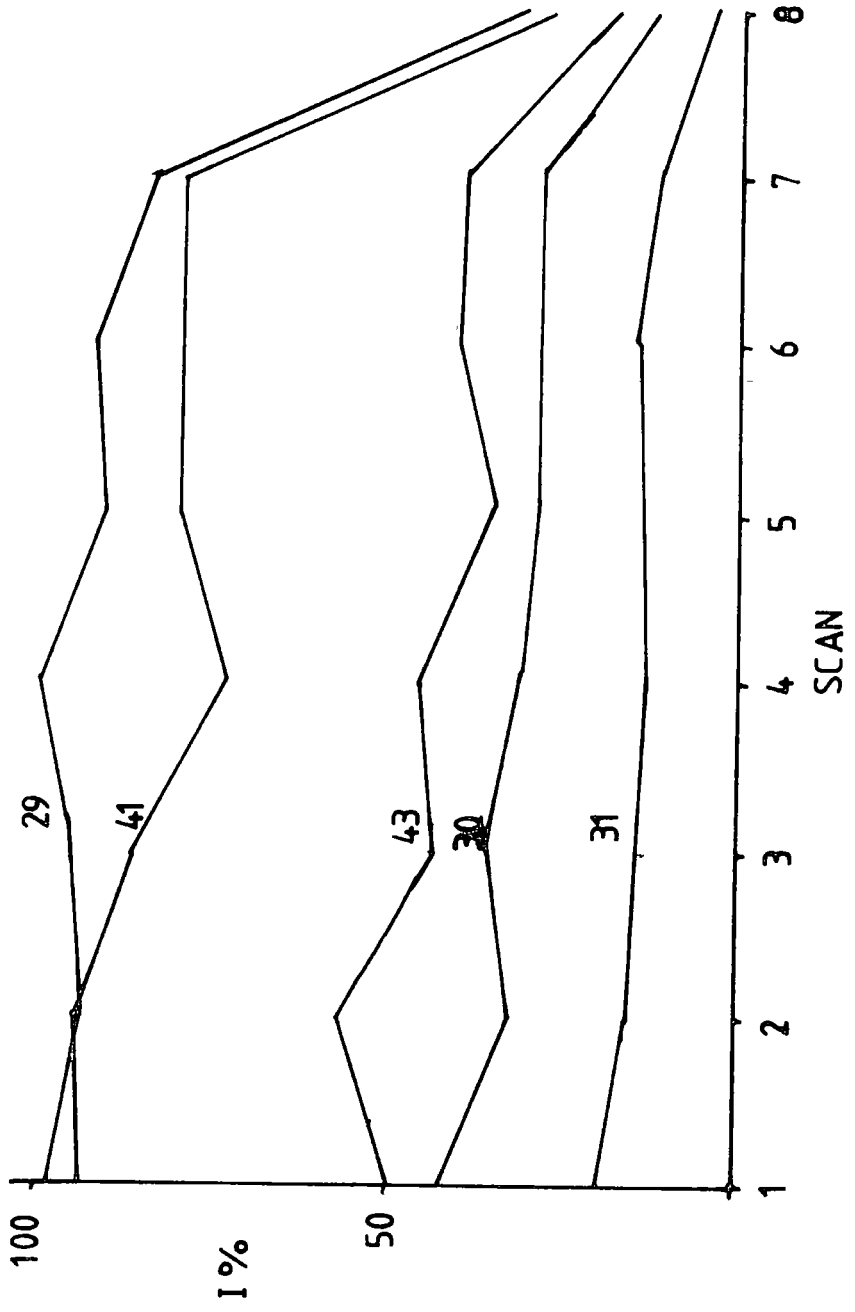

Figure 6.2 Peak intensities as a function of scan number for pristine cellulose nitrate

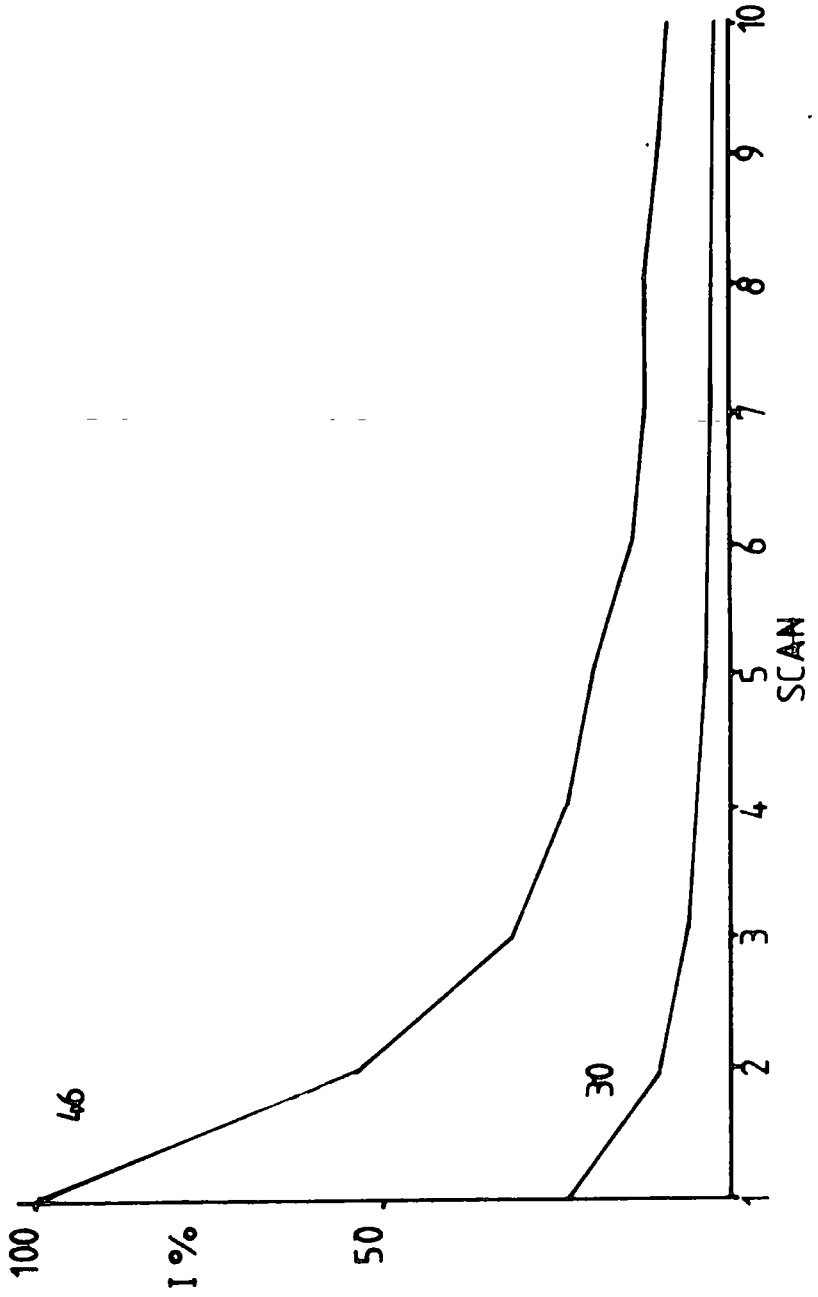

Figure 6.3 Peak intensities as a function of scan number

6.3.2 ^{13}C n.m.r.

The above discussion on the SIMS data and the previously discussed (Chapter Five) ESCA studies[185] imply that in cellulose nitrates, thermal degradation is a bulk-orientated phenomenon. Solution state, proton noise decoupled, ^{13}C n.m.r. has led to a better understanding of the bulk microstructure of cellulose nitrates,[45,47,181] and as such should give a good indication of the changes in the bulk chemistry during thermal degradation. Unfortunately, the sample size of the X-ray induced degraded sample is too small to allow analysis by ^{13}C n.m.r. Figures 6.4 and 6.5 show the relevant ^{13}C solution n.m.r. spectra for the undegraded pristine material and the thermally degraded samples respectively. The assignment of the peaks in Figure 6.4 are shown in Chapter Two of this thesis.

From a comparison of these spectra, it is clear that the thermally degraded sample shows a relative loss of the 2,6-di, 3,6-di and 6-monosubstituted residues. The 2,3,6-trisubstituted residues appear to remain constant although this is not conclusive. A striking feature of the spectrum shown in Figure 6.5 is the raised background in the regions 55-90 ppm. and 90-110 ppm. This feature is indicative of a numerous variety of atomic environments which merge into a manifold of nuclear states arising from the degradation of the material.

It was also noted that the thermally degraded material dissolved easily in DMSO-d_6 and this solution was not viscous. This is in contrast to a normal cellulose

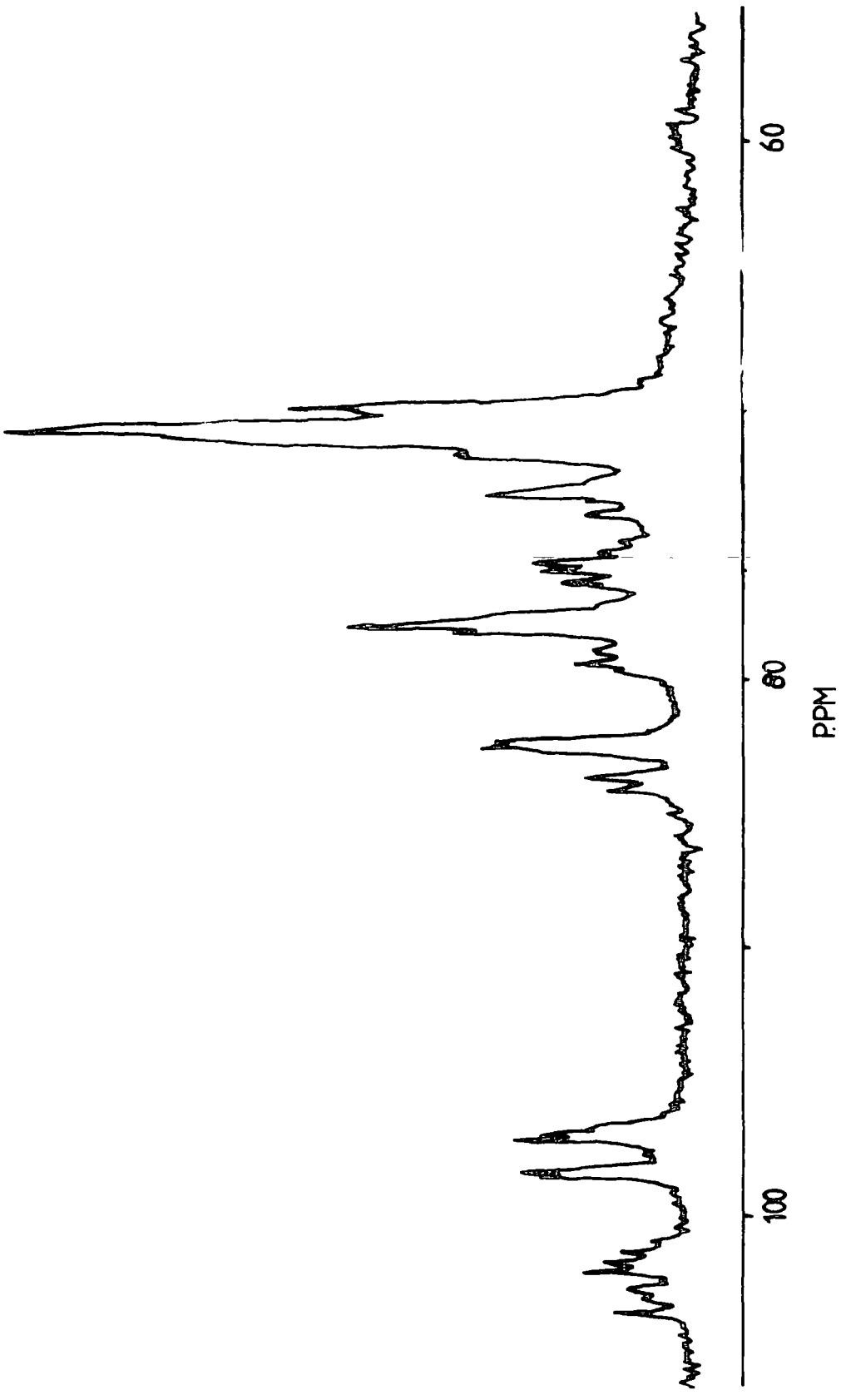

Figure 6.4 ^{13}C n.m.r. (90.56 MHz) solution spectrum of an undegraded cellulose nitrate

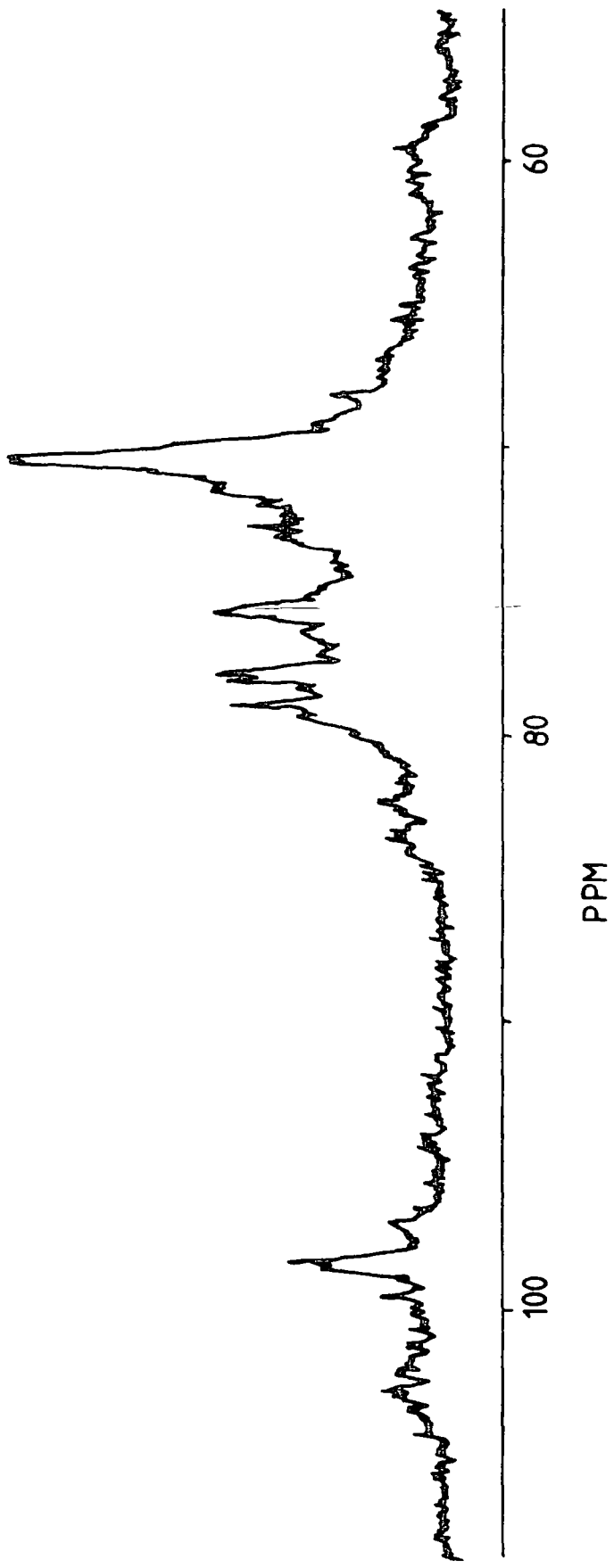

Figure 6.5 ^{13}C n.m.r. (90.56 MHz) solution spectrum of a thermally degraded cellulose nitrate.

nitrate where dissolution is slow (requires heat to $\sim 80^{\circ}C$) and the resultant solution is viscous at room temperature.

The data presented in this chapter suggests further evidence for the bulk-orientated effect of the thermal degradation of cellulose nitrate.

CHAPTER SEVEN

THE SURFACE TREATMENT OF CELLULOSIC MATERIALS WITH TRIFLUOROACETIC ANHYDRIDE

7.1 Introduction

The rôle of polymeric materials can be greatly enhanced by modifying the surface properties. It is the surface which interfaces with the surroundings, and hence many uses of polymeric materials are due to their surface properties. It has been shown that a wide variety of surface treatments, both wet chemical[187-189] and those occurring at solid-gas interfaces[190-197] may be used to modify the wettability, printing and laminating characteristics of a polymer without affecting the desirable bulk properties of the material. Grafting processes are of prime importance in the textile manufacture and finishing industries,[198] thereby reducing static charge build-up,[199] shrinkage and biological attack.[200]

ESCA has an important part to play in the evaluation of functional group analyses for correlation with surface properties of interest. Hence it is hoped that surfaces can be tailor-made for specific needs.[201,202]

Quantitative ESCA analysis of specific surface functionalities is often hindered by the coincidence in binding energy arising from atoms of the same element in differing chemical environments. Many organic nitrogen containing species are overlapping, for example, amide, amine, oxime and nitrogen in many heterocyclic structures. Carbon-carbon unsaturation and phenyl groups are difficult to distinguish from saturated carbons, although shake-up structure may be used as a distinguishing feature. Recently,[186] this laboratory is researching into short and long range unsaturation *via* the asymmetry of peaks and the so-called 'step-function'.

In surface oxidation, ambiguities often arise.[79,80,103] For example, signals arising from carbon singly bonded to oxygen can originate from peroxides, esters, carbonates, *etc.* as well as simple ethers and alcohols. Although the O_{1s} core level is potentially useful concerning the oxidised surface species, the limited resolution and small range of binding energies (typically ~2 eV) makes peak-fitting of most O_{1s} envelopes ambiguous.[79]

Therefore, derivatisation techniques have been developed which are not only specific, but also enable a degree of signal enhancement to be achieved. These methods utilise reagents which label or tag a specific chemical functionality. The label or tag should be more readily detectable under ESCA analysis, hence simplifying the complex situation.

Chemical tagging or labelling procedures,[203-205] however, are fraught with difficulties, but a perusal of the recent literature allows one to draw up a table of available labelling reagents (see Table 7.1). It must be stressed that this table is anything but complete.

Many of the techniques employ wet chemical conditions (where solvent effects may be pronounced), or vapour phase techniques. A good chemical tagging agent must be highly specific and ideally react 100% with the substrate. Also the stability and mobility of the tag must be evaluated.

A reaction of considerable current interest is the trifluoroacetylation of hydroxyl groups as proposed by Hammond *et al.*[206] Everhart and Reilly[204] have applied the use of TFAA (trifluoroacetic anhydride) to labelling the hydroxyl groups formed on the surface of low density polyethylene film after

TABLE 7.1 ESCA Studies Using Polymer Surface Derivatisation

Substrate	Reaction	
Na treated PTFE	$>C=C< \xrightarrow{Br_2} -\overset{Br}{\underset{|}{C}}-\overset{Br}{\underset{|}{C}}-$	Riggs and Dwight[189,211]
Bovine Albumin	$\textcircled{P}-NH_2 \xrightarrow{Et\text{-}S\text{-}C(O)\text{-}CF_3} \textcircled{P}\text{-}\overset{H}{\underset{|}{N}}-\overset{O}{\underset{\|}{C}}-CF_3$	Millard and Masri[212]
Plasma initiated PAS grafts on PP	$-CO_2H \xrightarrow[H_2O]{BaCl_2} (-CO_2^-)\ Ba^{2+}$	Bradley and Czuka[213,214]
MMA + hydroxypropyl MA copolymer	$\overset{OH}{\underset{|}{-CH_2}} \xrightarrow{(CF_3CO)_2O} \overset{O-C(=O)CF_3}{\underset{|}{-CH_2}}$	Hammond *et al*[206]
Epoxy/ester primer	$-CO_2^-Na^+ \xrightarrow{AgNO_3} -CO_2^-Ag^+$	Hammond *et al*[206]
Corona treated PE	$>C=C< \xrightarrow{Br_2} -\overset{Br}{\underset{|}{C}}-\overset{Br}{\underset{|}{C}}-$	Spell and Christenson[215]
	$-CO_2H \xrightarrow{NaOH} -CO_2^-Na^+$	Briggs and Kendal[216]
	$-CH_2-\overset{O}{\underset{\|}{C}}- \xrightarrow{Br_2} -\overset{Br}{\underset{|}{C}}-\overset{O}{\underset{\|}{C}}-$ (Br)	Briggs and Kendal[216]
	$>C=O \xrightarrow{C_6F_5\text{-}NH\text{-}NH_2} >-C=N-NH-C_6F_5$	Briggs and Kendal[216]
	$\textcircled{P}\ -CO_2H \xrightarrow{TlOEt} \textcircled{P}\ -CO_2Tl$	Batich and Wendt[203]
Photooxidised Bisphenol-A-Polycarbonate	$-CH_2\text{-}O\text{-}OH \xrightarrow{SO_2} -CH_2\text{-}O\text{-}SO_3H$	Munro[217]

exposure to Ar and N_2 r.f. plasmas. Their method of derivatisation involved a solution phase reaction in benzene followed by Soxhlet extraction from diethyl ether. This is perhaps an unsatisfactory method as the effect of the solvent may not be apparent. Munro used a vapour phase reaction of Bisphenol-A-polycarbonate[207] and TFAA to label hydroxyl groups prior to and after uv irradiation. Also, Wilson [208] has used this vapour phase treatment on polyvinylalcohol and a variety of coals and bitumens.

Trifluoroacetylation has also found use in labelling amines, epoxides and carboxylates. A recent study by Dickie *et al*[209] involved using TFAA to derivatise a series of hydroxyl functional acrylic copolymers. Angle dependant ESCA studies of these samples, which had undergone complete reaction with TFAA, were analysed using single and multiple overlayer models[209] (see Chapter Two).

The advantages of TFAA as a surface tag are four-fold:

(1) The introduction of fluorine may easily be detected by monitoring the F_{1s} core level.

(2) The F_{1s} photoionisation peak has a high cross section, and hence a small amount of fluorine in the sample gives rise to a high intensity of the photoionisation peak.

(3) Three fluorine atoms are introduced per functionality labelled.

(4) The signal arising from $\underline{C}F_3$ is shifted ∿8 eV to the high binding energy side of the hydrocarbon peak at 285.0 eV, and therefore in the systems encountered in this thesis, is easy to distinguish.

The ability to monitor the extent of reaction using data from one core level (*e.g.* C_{1s}), and using relative intensity ratios of two core levels (*e.g.* C_{1s}/F_{1s}) aids analysis appreciably, since then possible effects of differing depths for the core levels concerned may be proved (see later).

The aim of this work is to have a 'back-titration' effect on the DOS of cellulose nitrates. Obviously, before this can be attempted, it is preferable to obtain data on the effect of the vapour phase treatment of TFAA on other cellulosic, and cellulosic-type molecules.

In this chapter, the use of TFAA as a chemical tag for cellulosic materials is discussed. Systems used include cellobiose, cellulose and cellulose nitrate.

7.2 Experimental

The cellobiose was obtained from Aldrich Chemical Company and was not further purified. Both samples were dried for several days in a P_2O_5 vacuum dessicator.

The cellulose used was Whatman-1 filter papers which were prepared to use as described in Chapter Three of this thesis. The cellulose nitrates were prepared by standard methods already outlined.

The trifluoroacetic anhydride was prepared in the laboratory from the reaction of phosphorus pentoxide on trifluoroacetic acid. The sample was checked for purity by gas-liquid chromatography, to ensure that no acid was present. This sample was degassed to constant pressure on a vacuum line prior to reaction with the substrate.

The experimental set-up for the vapour phase treatment is shown schematically in Figure 7.1. It is noted that grease-free vacuum lines are used to eliminate contamination of the surface from grease, silicon, *etc.*

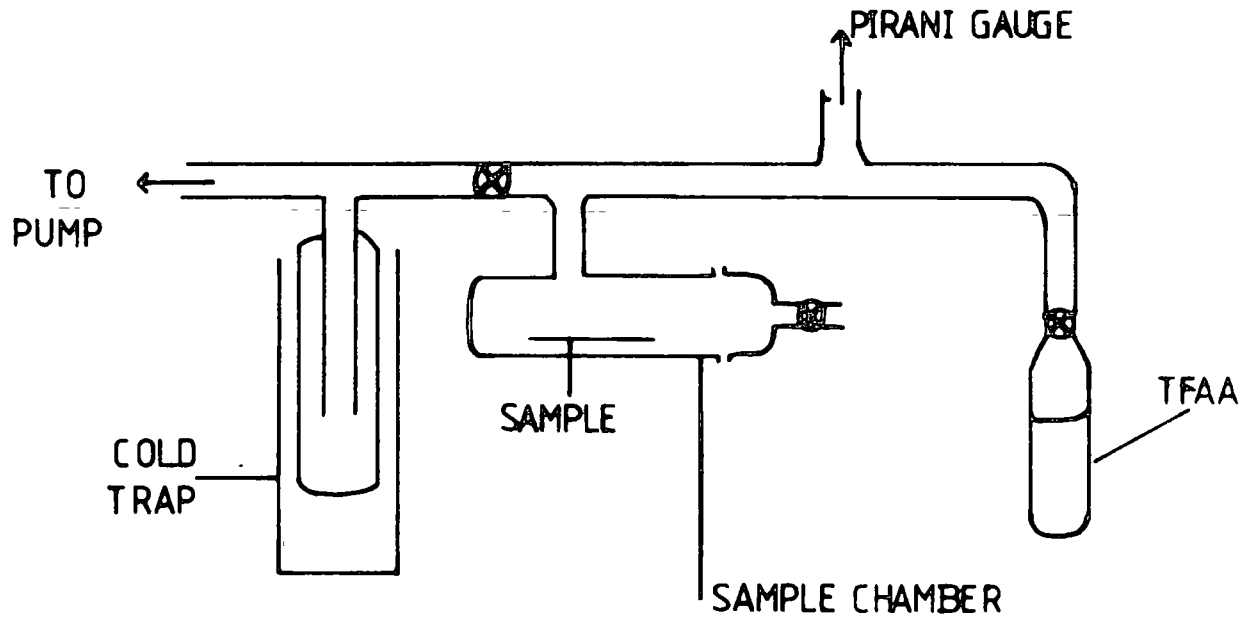

Figure 7.1 Experimental set-up for the vapour phase treatment of cellulosic materials with TFAA

ESCA spectra were run on a Kratos ES300 electron spectrometer employing a Mg and Ti dual anode. Spectra were analysed using the Kratos DS300 data station.

The area ratio and stoichiometry data presented in the following sections of this chapter are treated in the manner outlined below. N_{1s}/C_{1s} and N/C ratios are quoted after

subtraction of the area due to the $\underline{C}F_3$ and O-$\underline{C}$=O groups. This approach therefore eliminates the two extra carbons added per trifluoroacetate group, and enables a direct comparison to be drawn with the N_{1s}/C_{1s} area ratios quoted elsewhere in the thesis. This has not been done for the F_{1s}/C_{1s} area ratio in the figures, because it will become apparent in the script, the reaction of TFAA is not vertically homogeneous.

7.3 Results and Discussion

7.3.1 Reaction of TFAA with cellobiose as a function of time

The C_{1s}, O_{1s} and F_{1s} core level spectra of cellobiose obtained using the ES300 $Mg_{k\alpha_{1,2}}$ source (12kV, 8mA) for the untreated material and after TFAA treatment are displayed in Figure 7.2.

The C_{1s} core level spectrum of the starting material may be peak-fitted to reveal three component peaks. The central component at ∿286.7eV binding energy arises from the carbon atoms singly bonded to one oxygen atom in the molecule. The carbon atom uniquely attached to two oxygen atoms in the cyclic hemiacetal formulation of the β-D-glucopyranose ring system is responsible for the component peak situated at high binding energy. The peak at 285.0eV binding energy, as discussed earlier, is due to extraneous hydrocarbon at the surface. Consideration of the O_{1s}/C_{1s} area ratio, allowing for the hydrocarbon contaminant peak, indicates that the cellobiose contains very little residual water.

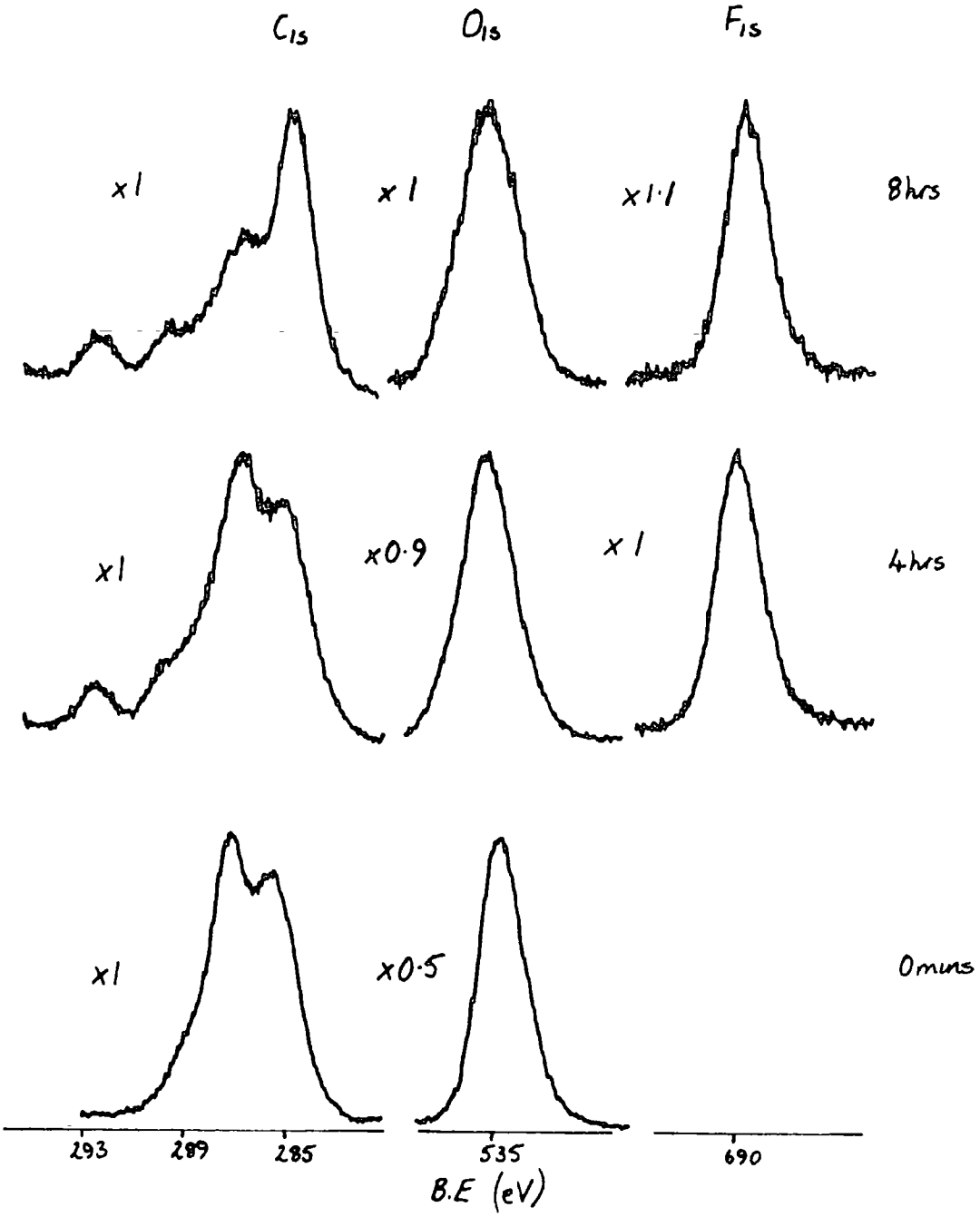

Figure 7.2 $Mg_{k\alpha}$ C_{1s}, O_{1s} and F_{1s} core level spectra as a function of treatment time.

On exposure to TFAA vapour for 15 minutes, there is clear evidence for trifluoroacetylation as shown by the appearance of a single F_{1s} photoionisation signal, accompanied by the development of $\underline{C}F_3$ and $CF_3\underline{C}(=O)(-O^-)$ ester in the C_{1s} envelope at 293.6eV and 290.1eV respectively.

A graph of F:C stoichiometry *versus* time of exposure is shown in Figure 7.3.

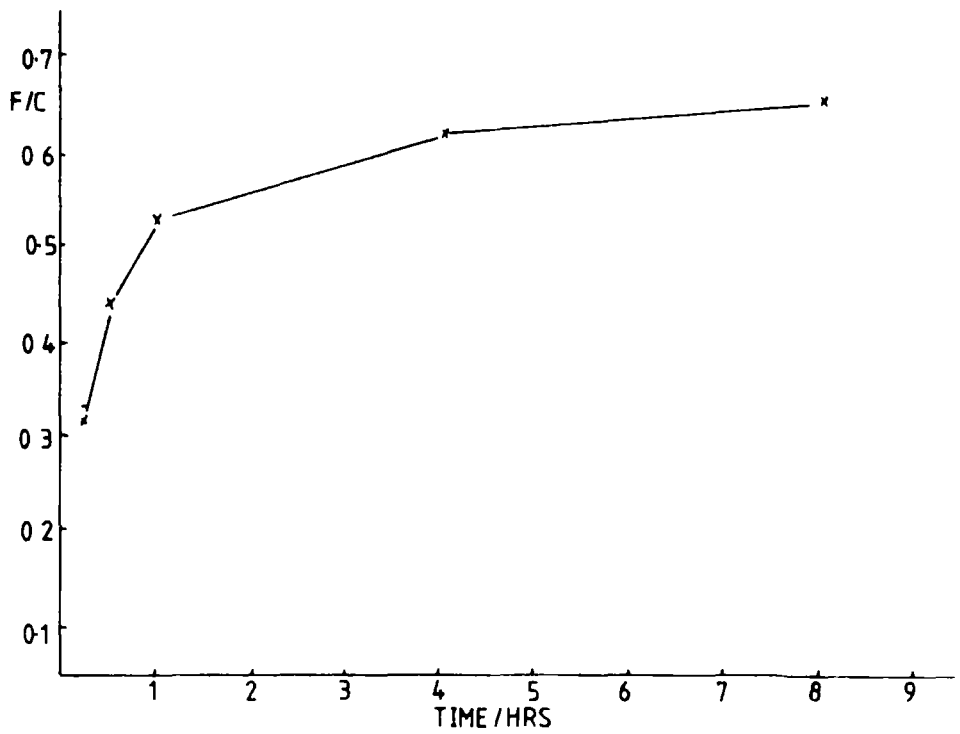

Figure 7.3 F/C stoichiometric ratios *versus* treatment time

Assessment of the extent of reaction, in terms of the number of hydroxyl groups reacted, and the corresponding

tensive studies by Clark and co-workers have investigated the magnitude of electron mean free paths as a function of kinetic energy for a variety of polymeric systems. For linear polymer systems, under $Mg_{k\alpha_{1,2}}$ radiation, typical mean free paths corresponding to photoemission from F_{1s}, O_{1s} and C_{1s} core levels with kinetic energies of ∿560eV, ∿720eV and ∿969eV are ∿9Å, ∿10Å and ∿15Å, giving effective sampling depths of ∿27Å, ∿30Å and ∿45Å respectively.

Hence, the percentage component of the C_{1s} envelope due to the $\underline{C}F_3$ groups, is that at which ∿95% of that signal is from a depth of ∿45Å. However, the F/C stoichiometries of the systems predicts a higher percentage of CF_3 groups since here the F_{1s} signal arises from a sampling depth of only ∿27Å. Therefore the data suggest a concentration profile into the bulk. This suggestion can be checked by employing the depth profiling facility of the ES300 electron spectrometer using the $Ti_{k\alpha}$ anode (see Section 7.3.2).

7.3.2 A Depth Profiling Investigation employing $Ti_{k\alpha}$ X-ray radiation

The C_{1s}, O_{1s} and F_{1s} core level spectra as a function of exposure time are shown depicted in Figure 7.4 using the $Ti_{k\alpha}$ (13.5kV, 18mA) X-ray source.

The C/O stoichiometry for the untreated cellobiose spectrum shows no evidence for hydrocarbon contamination, supporting the fact that the hydrocarbon is only situated at the very surface and is extraneous.

After exposure to TFAA for 15 minutes, pronounced

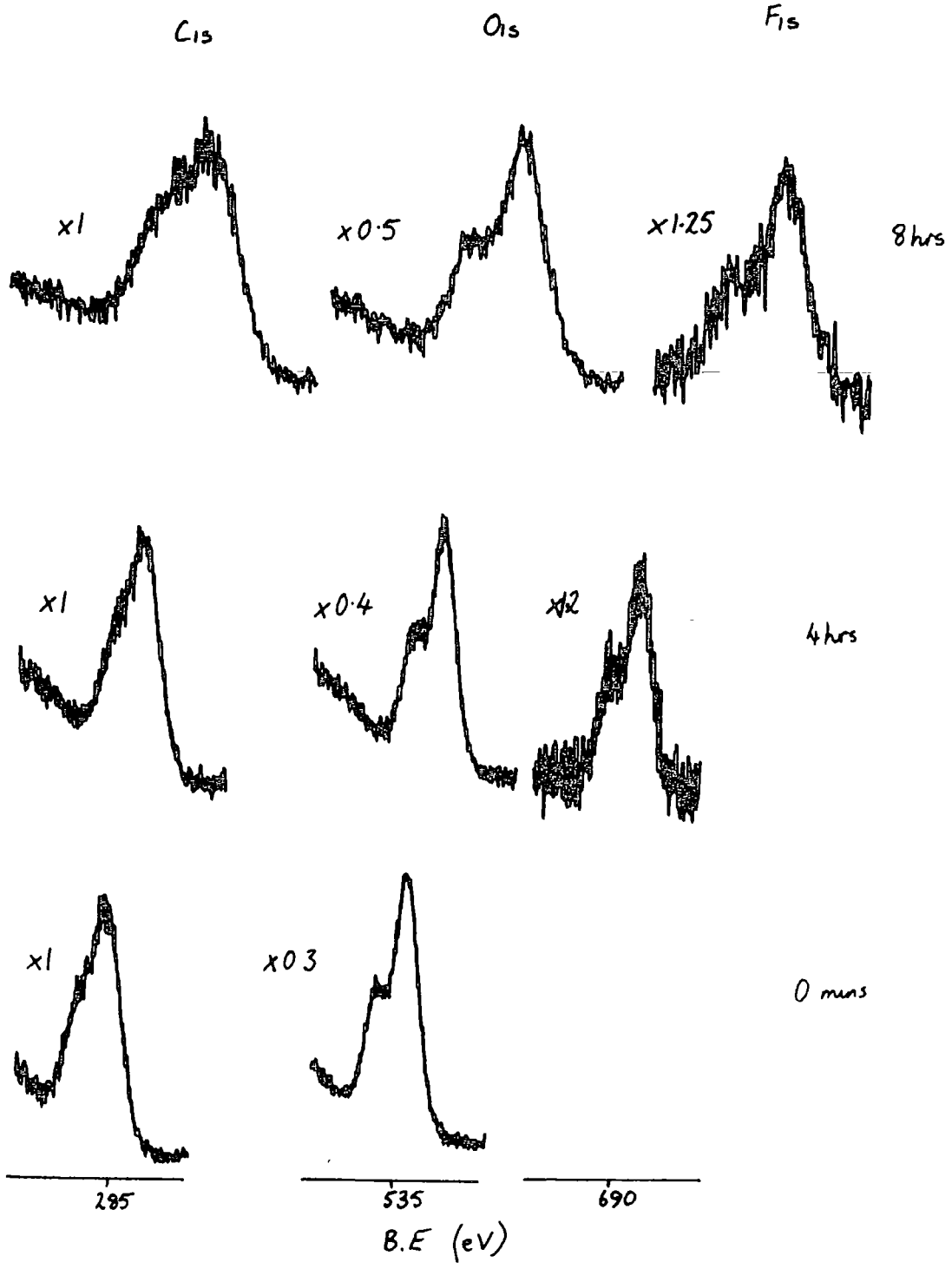

Figure 7.4 $Ti_{k\alpha}$ C_{1s}, O_{1s} and F_{1s} core level spectra as a function of treatment time

changes are seen to occur. The introduction of fluorine into the sample is evident from the sharp F_{1s} core level signal. Figure 7.5 depicts graphically the F/C stoichiometry as a function of time. By comparison with Figure 7.3 it is clearly evident that the rate of reaction at ∿130Å follows similar trends as that at ∿40Å. However, the level of reaction is considerably less, which adds evidence to the concentration profile mentioned in Section 7.3.1.

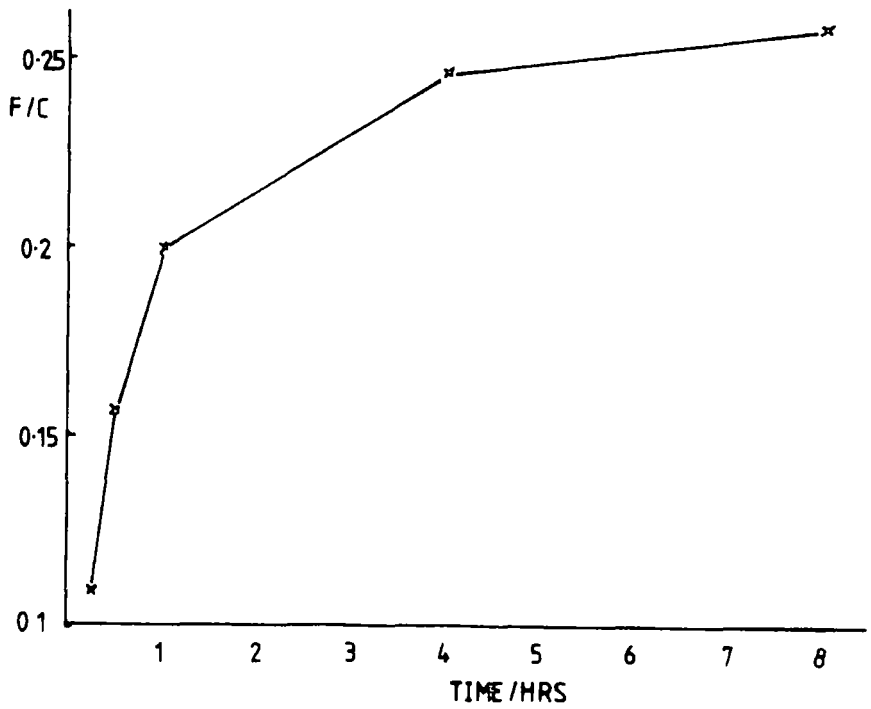

Figure 7.5 F/C stoichiometric ratios *versus* treatment time

It must be stressed, however, that the trace level of reaction at ∿130Å is less than that depicted in Figure 6.5 because of contributions to the signal intensities from ∿40Å (see Chapter Two, Section 2.7).

In conclusion, the reaction of TFAA with cellobiose does not appear to go to completion, however, interesting trends suggest that some hydroxyls of the cellobiose are more reactive than others. Unfortunately, ESCA is incapable of adding any further evidence to this effect.

7.3.3 Reaction of Cellulose with TFAA as a Function of Time

The reaction of trifluoroacetic anhydride with the free hydroxyl groups in cellulose is expected to be similar as that shown with cellobiose. Cellobiose is taken as the repeat unit in the cellulose structure. Therefore any apparent differences must be due either to morphological effects or the absence in cellulose of the end group hydroxyls.

The experiment is identical to that used for cellobiose; the cellulose being dried thoroughly before use. Figure 7.6 depicts the C_{1s}, O_{1s} and F_{1s} core level spectra as a function of exposure time. Figure 7.7 depicts graphically the F/C stoichiometry at the surface as a function of time. Clearly the initial reaction is fairly rapid, but as in the cellobiose case,the reaction appears to plateau out after about 1 hour exposure time. Comparison with Figure 7.3 clearly shows the similarity between the reaction of TFAA with cellulose and cellobiose. For example, after 15 minutes exposure time the F/C stoichiometry for cellulose and cellobiose are 0.39 and 0.32 respectively. At 1 hour exposure time the stoichiometries are 0.53 and 0.53 and again after two hours, 0.61 and 0.59.

relative intensity for the trifluoromethyl carbon, reveals that a complete esterification of the available hydroxyl groups is not accomplished even after prolonged exposure time.

However, it is evident from Figure 7.3 that the reaction has not reached an equilibrium value. If one considers the cellobiose molecule, it is clear that if only one hydroxyl is replaced by a trifluoroacetate group then the F/C stoichiometry shown equals 0.214. Clearly, after ten hours exposure time the F/C stoichiometry is approaching that expected if five of the eight hydroxyls had been replaced.

It is also of note that within 15 minutes, the F/C stoichiometry has reached a value whereby two of the hydroxyl groups have reacted fairly rapidly.

From the component analysis of the C_{1s} envelope it is evident that the number of CF_3 groups (see Table 7.2) is not as large as the F/C stoichiometry would suggest.

TABLE 7.2

TIME	F/C	% CF_3 (expr.)	% CF_3 (expected)
15 mins.	0.32	5.3	10.6
30 mins.	0.44	10.75	14.6
1 hr.	0.53	15.0	17.6
4 hr.	0.61	18.3	20.3
10 hr.	0.65	20.1	21.6

The data must be explained by the differing sampling depths of the C_{1s} and F_{1s} core electrons. This thesis has already alluded to the concepts of electron mean free paths and sampling depths within the ESCA experiment. Ex-

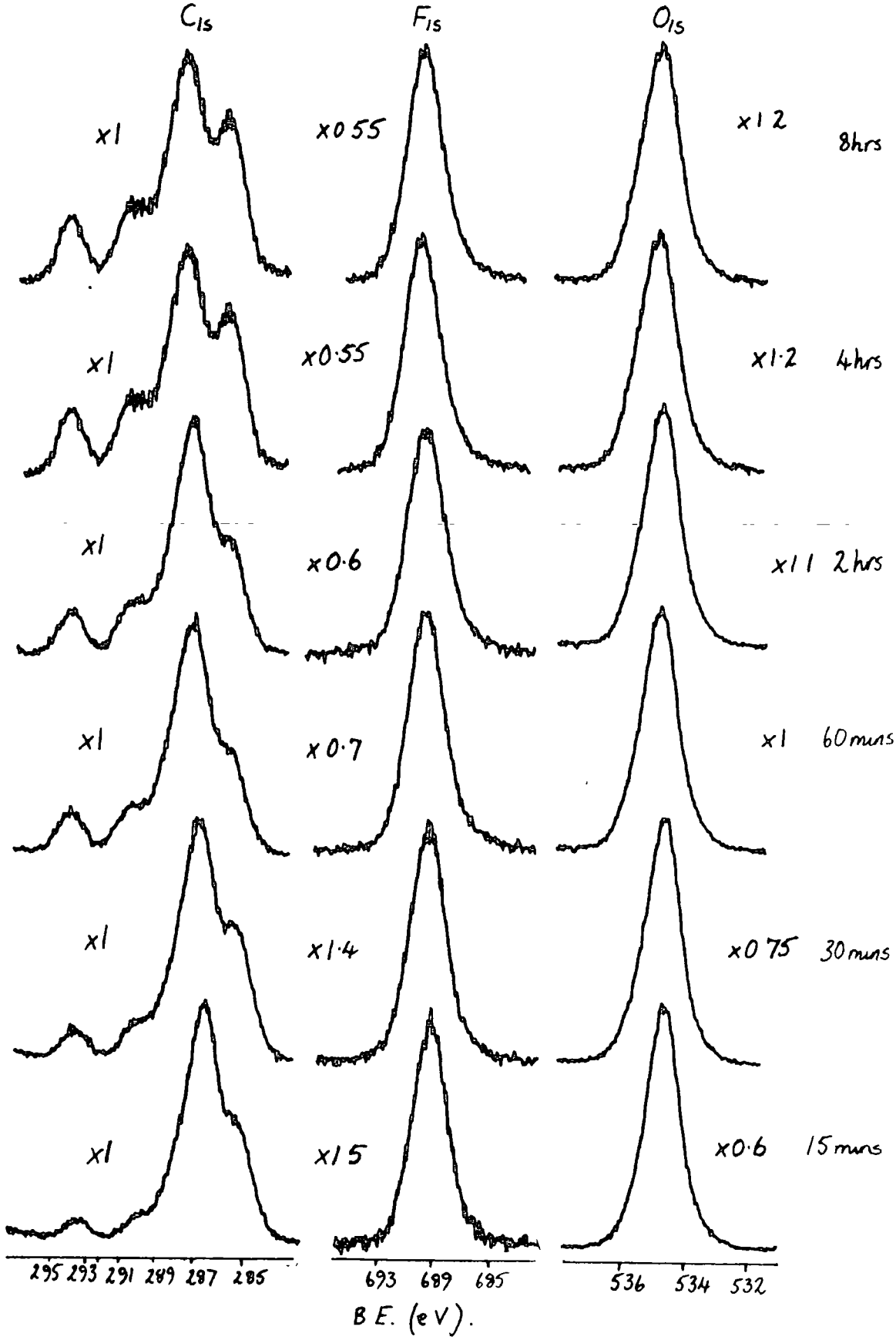

Figure 7.6 $Mg_{k\alpha}$ C_{1s}, O_{1s}, F_{1s} for cellulose

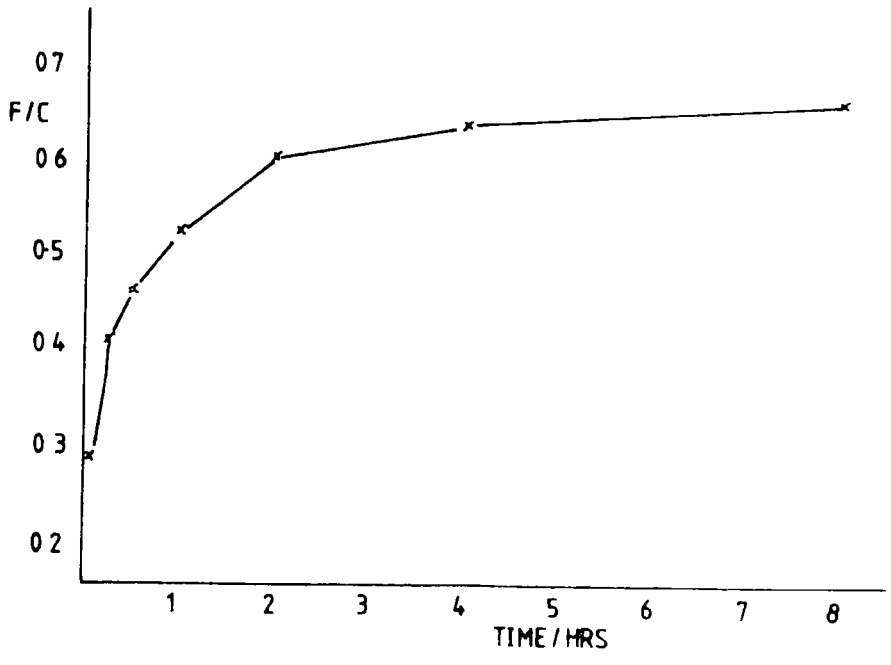

Figure 7.7 F/C stoichiometric ratios *versus* treatment time

Therefore, it may be concluded from a comparison of the data for cellulose and cellobiose that surface morphology plays little part in the vapour phase reaction of TFAA with these materials. Clearly, it is the reactivities of the hydroxyl groups within these molecules which determine the extent and rate of reaction.

The reaction of TFAA with β-D-glucose was attempted but it was clear from the core level spectra that the reaction was clearly not just an esterification process. It is believed that epimerisation and other side reactions took place. However, it did prove that glucose is a 'bad' monomer unit for cellulosic materials.

In the case of cellobiose and cellulose there is an increase in the magnitude of the sample charging on progressive fluorination of the cellulosic materials. Figure 7.8 depicts this sample charging, relative to the untreated materials, as a function of exposure time.

The results presented so far in this chapter have shown that, under the conditions employed, trifluoroacetylation of all the available hydroxyl groups in cellulose or cellulose-type 'monomers' is not accomplished, even after prolonged treatment with TFAA.[210] This is in contrast to the work of Wilson[108] on polyvinyl alcohol where complete chemical tagging using TFAA is accomplished within 15 minutes. The use of TFAA as a label for hydroxyls on cellulose has previously been attempted by Wilson[108] and similar trends have been shown to occur.

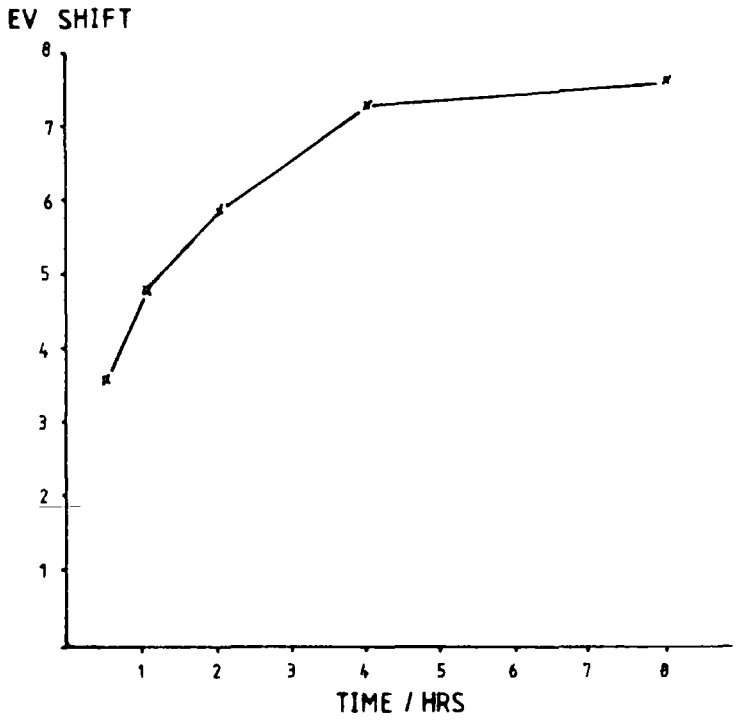

Figure 7.8 Sample charging as a function of treatment time

The next section of this thesis explores the possible use of TFAA as a blocking agent to study the rôle of the remaining hydroxyl groups in the chemistry of cellulose nitrates.

7.3.4 The Reaction of TFAA with a 2.2 DOS Cellulose Nitrate

If in the case of cellulose nitrates the remaining hydroxyls can be esterified by the use of trifluoroacetic anhydride then a "back-titration" effect will be accomplished. Then the use of ^{19}F nmr could be employed to determine primary and secondary hydroxyls, and their sequence distribution. Although this can also be established *via* ^{13}C n.m.r., the use of ^{19}F nmr has many advantages, *e.g.* 100% abundant spin

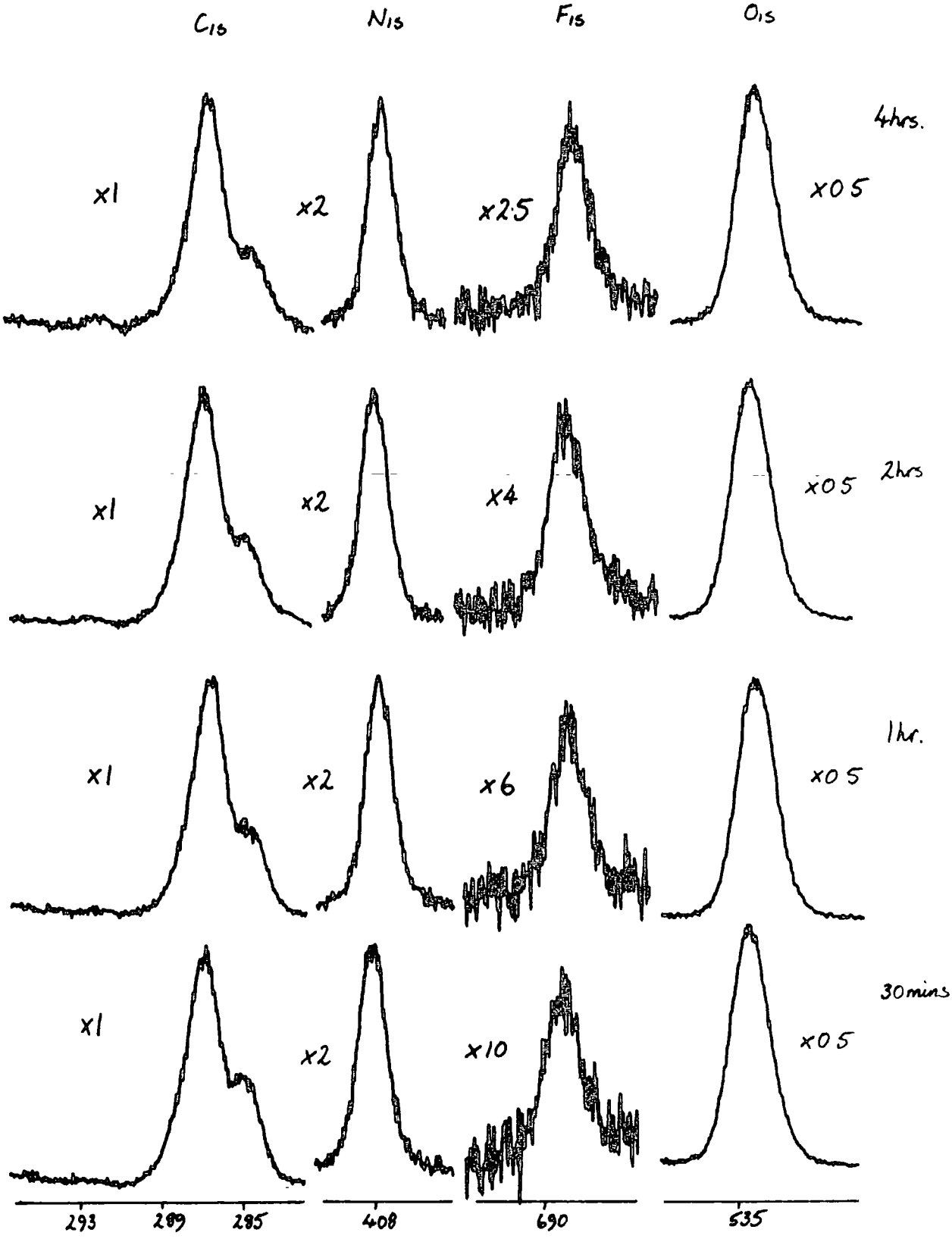

Figure 7.9 C_{1s}, O_{1s}, N_{1s} and F_{1s} core level spectra as a function of exposure time.

nuclei, large chemical shifts, *etc*. However, before this can be employed one needs to determine whether all the free hydroxyls at the surface can be esterified, *i.e*. is TFAA on cellulose nitrate a good chemical tag.

Figure 7.9 depicts C_{1s}, O_{1s}, N_{1s} and F_{1s} core level spectra as a function of exposure time to TFAA at ambient temperature. Figure 7.10 shows a graph of F/C and N/C stoichiometric ratios as a function of exposure time. As is clear from Figure 7.10 complete esterification of the hydroxyls does not occur, and in comparison with the reaction of TFAA with cellulose (see Figure 7.7) the reaction with cellulose nitrate is slightly more rapid although the extent of reaction is less.

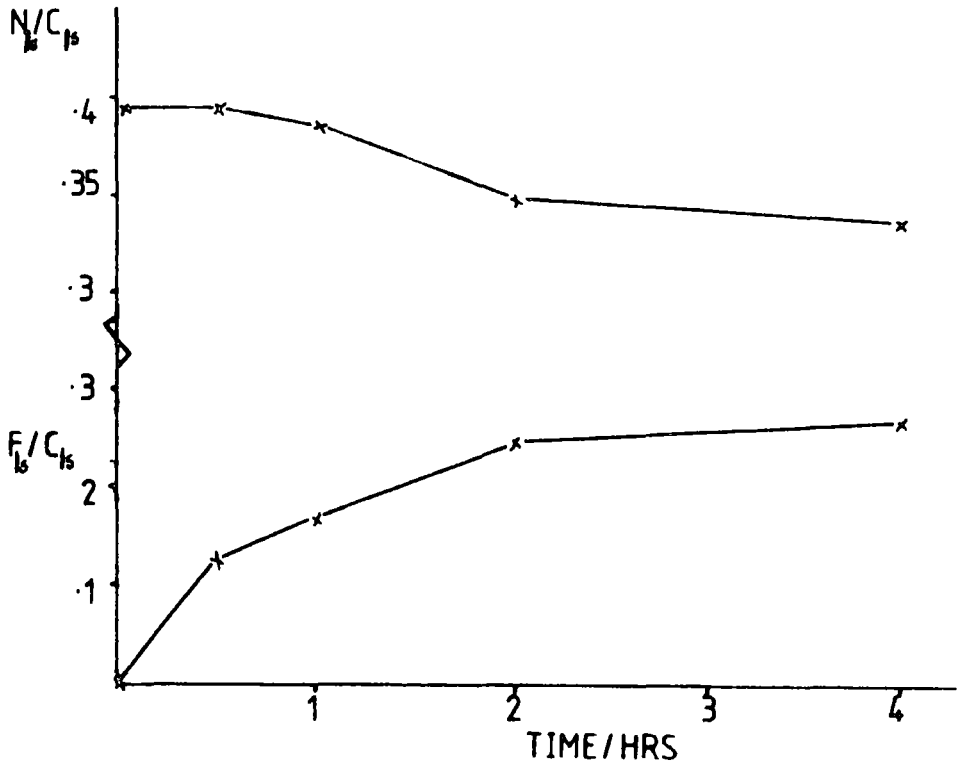

Figure 7.10 F/C and N/C stoichionetric ratios as a function of exposure time

In Section 7.3.1 of this chapter, the differing sampling depths of F_{1s} and C_{1s} core level photoelectrons were discussed. Table 7.3 shows the experimental and expected percentages of $\underline{C}F_3$ groups from the C_{1s} envelopes. It is clearly seen that at two hours treatment time the expected $\underline{C}F_3$ and experimental $\underline{C}F_3$ percentages are identical. This is evidence for a concentration profile being set up. Therefore it is obvious that although the very surface has reached an equilibrium (*i.e.* a percentage of the free hydroxyls have been esterified), and then diffusion of the TFAA enters the bulk, *i.e.* a concentration profile is established.

It can also be clearly seen from Figure 7.10 that a slight decrease occurs in the N/C stoichiometric ratio indicative of an ester exchange reaction.

It is also apparent from Figure 7.10 that an induction period exists before the ester exchange reaction. Ester exchange reactions are normally acid-catalysed, suggesting that it is not until an amount of acid is present at the surface (*i.e.* free hydroxyls have been esterified by the anhydride) that the ester exchange reaction with the nitrate esters becomes important.

7.4 Conclusions

The series of experiments presented in this chapter have tried to establish whether trifluoroacetic anhydride would be a good chemical "tagging agent" for the surface of cellulosic materials. In general, TFAA is no use in this context as 100% reaction has not been achieved. However, model studies

have shown that, as far as the surface is concerned, cellulose and cellobiose react to approximately the same extent and the same rate, indicative of the rate determining step being the attack of the anhydride on the hydroxyl group.

TABLE 7.3

TIME	% CF_3 (expr.)	% CF_3 (expected)
30 mins.	1.75	2.2
1 hr.	2.4	2.9
2 hr.	4.05	4.1
4 hr.	4.5	4.5

APPENDIX ONE

A.1 The ESCA Instrumentation

An ESCA spectrometer comprises four essential components which are shown schematically in Figure A.1.1.

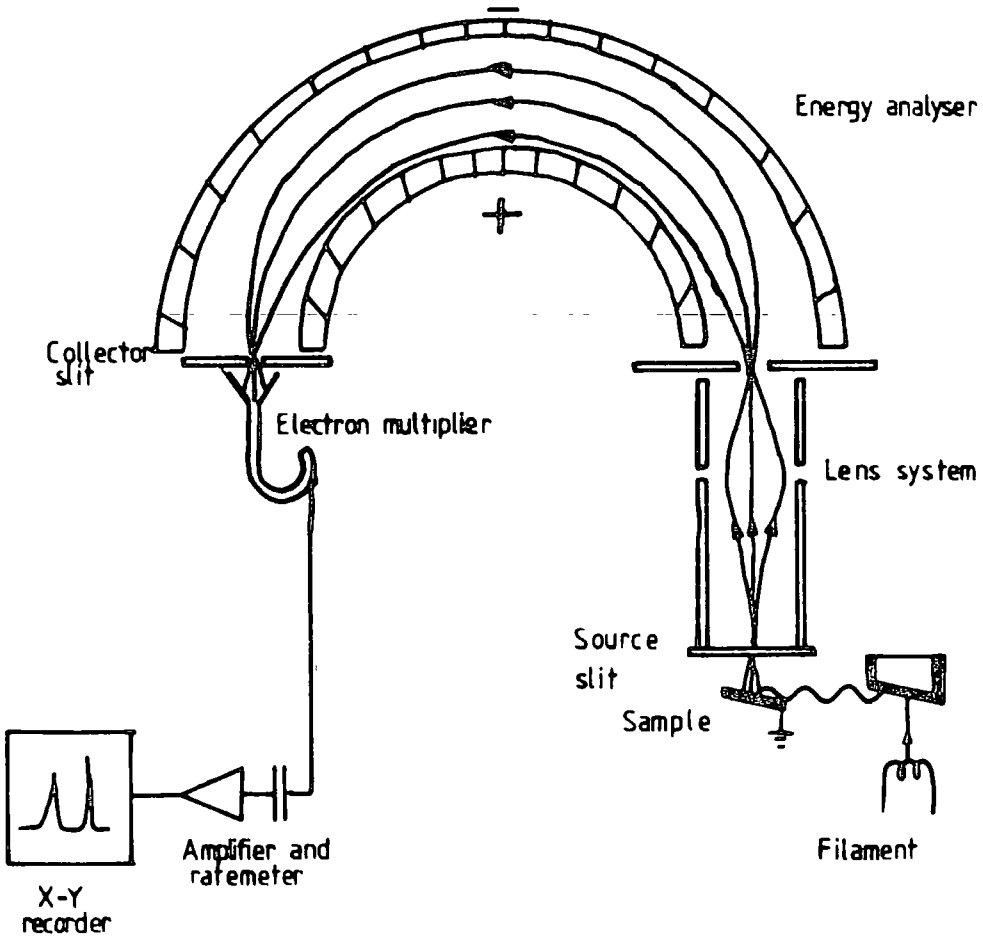

Figure A.1.1 Schematic of ESCA Instrumentation

(1) X-ray source

(2) Sample Chamber

(3) Electron Energy Analyser

(4) Electron Detection and Data Handling.

A.1.1 X-ray source

Both spectrometers have an X-ray gun of the Henke or hidden filament type. The ES200AA/B spectrometer is equipped with a single $Mg_{k\alpha}$ ($h\nu$ = 1253.6eV) source driven by a Marconi Elliott GX5 high voltage supply with integrally variable voltage in the region of 0-60KV and 0.80mA emission current. Under normal working conditions the X-ray flux is of the order of 0.1 rads s^{-1}.

The ES300 spectrometer is equipped with a dual-anode X-ray gun, with magnesium and titanium targets and a monochromatised $Al_{k\alpha_{1,2}}$ source.

The characteristic emission of Mg anodes are derived from K-series transitions. In addition to the $K\alpha_{1,2}$ line, a series of satellites are also present. The position and intensity of these satellites relative to the major peak is given below in Table A.1.

TABLE A.1 X-ray Satellite Energies and Intensities

	$K\alpha$.	$\alpha_{1,2}$	α_3	α_4	α_5	α_6	β
Mg	Displacement (eV)	0	8.4	10.2	17.5	20.0	48.5
	Relative intensity	100	8.0	4.1	0.55	0.45	0.5.

A.1.2 Sample Analysis Chamber

The sample analysis chambers for the ES200AA/B and ES300 are shown schematically in Figures A.1.2 and A.1.3. The sample chambers are, in each case, equipped with a variety of access ports and viewports. In each case, fast entry insertion locks permit rapid sample introduction.

A. Analyser. B. $Mg_{K\alpha}$ X-ray Source.

C. $Al_{K\alpha}$ X-ray Source. M. Monochromator.

S. Sample Analysis Position. V. Viewport.

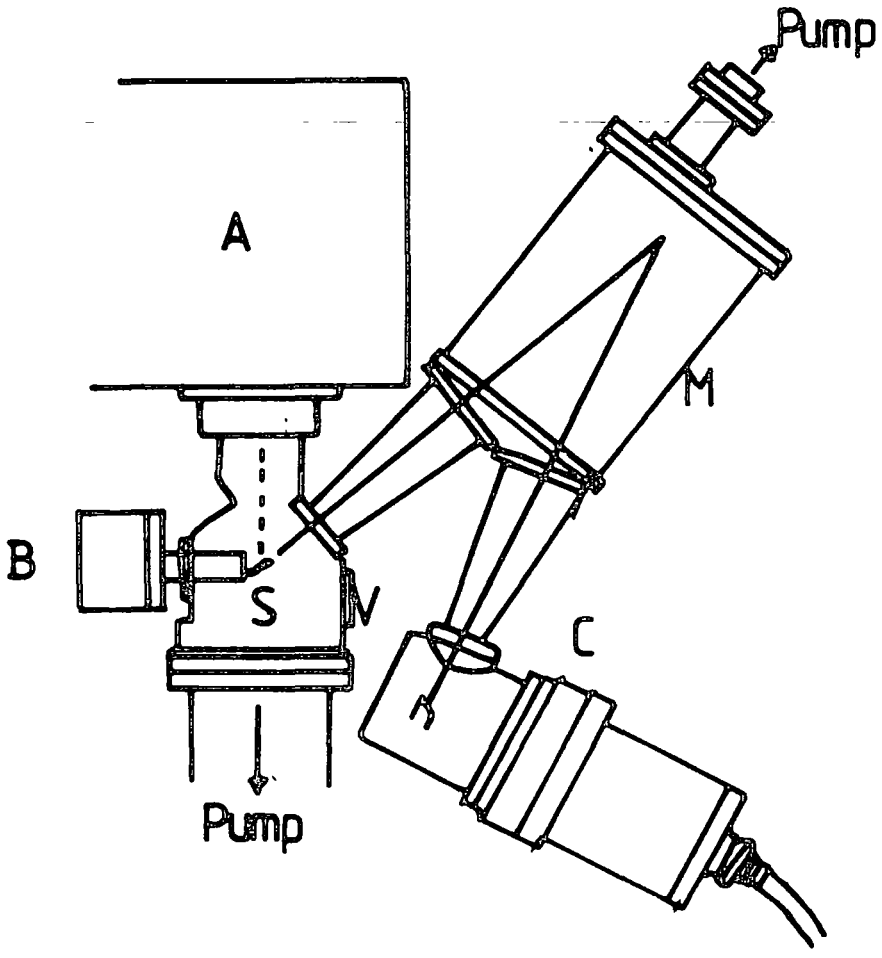

Figure A.1.2 Schematic of ES200 Sample Analysis Chamber

A. Analyser. B. To Pumping. C. Catcher Tray.

D. Penning Gauge. F. AG5 Ion Gun and Wien Filter.

H. Viewport. I. Sample Insertion Lock. J. Insertion Lock for Reservoir Shaft. K. Unused. L. Viewport.

M. To Monochromated $Al_{K\alpha_{1,2}}$ Source. P. Insertion Probe.

S. Sample in Analysis position in front of X-ray source.

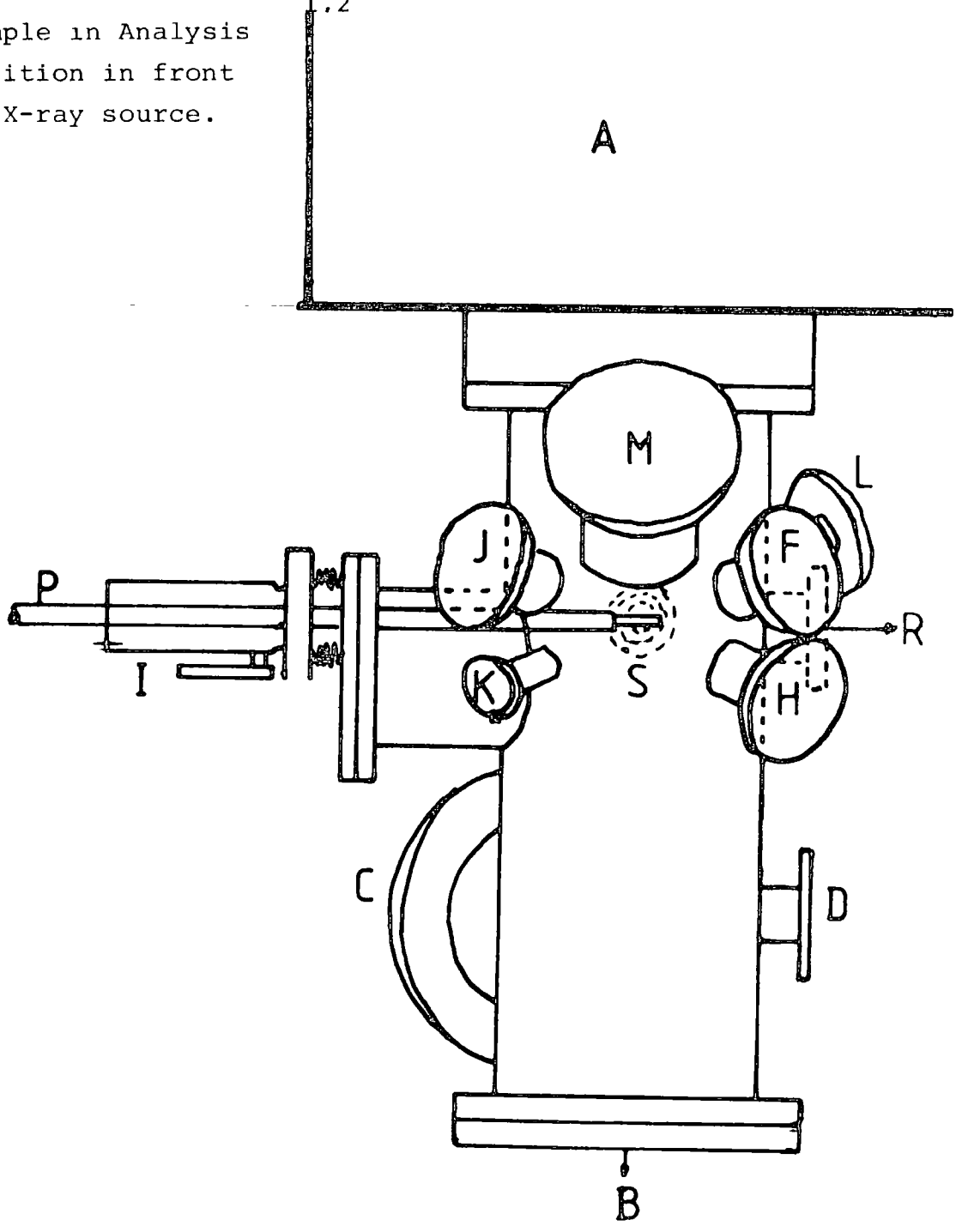

Figure A.1.3 Schematic of ES300 Sample Analysis Chamber

The ES200AA/B sample chamber and analyser are pumped independently by liquid nitrogen cooled diffusion pumps, as is the X-ray source, giving a typical base pressure of $\sim 2 \times 10^{-8}$ torr.

The ES300 spectrometer employs electrically driven turbomolecular pumps for pumping of the sample and analyser regions, using Alcatel 370 ls^{-1} and 120 ls^{-1} pumps respectively. The dual anode X-ray gun and monochromator are pumped by small ion pumps. The typical base pressure of this system is $\sim 2 \times 10^{-9}$ torr.

The ES300 also possesses a preparation chamber pumped by an Edwards E04 diffusion pump with a long-life cold trap backed by an Edwards EDM6 rotary pump. This preparation chamber also houses an electron gun (VG LEG 31).

A.1.3 Electron Energy Analyser

Both the ES200AA/B and ES300 spectrometers employ hemispherical double focussing analysers, mu-metal shielded, based upon the principle described by Purcell.[106] For ESCA, an analyser must be capable of a resolution better than 1 in 10^4. The analyser resolution is related to R, the mean radius of the hemispheres, and the combined width of the source and collector slits, W, by $\frac{\Delta E}{E} = \frac{W}{R}$.

A focussing and retarding lens arrangement is used to reduce the velocity of the electrons prior to entry, thus reducing the resolution requirements of the analyser.

The analyser may be operated in two modes:

(1) The retarding potential[107] applied to the lens is scanned and the pass energy as dictated by the potential applied across the hemispheres, is kept constant; or

(2) Scanning the retarding potential and the potential between the analyser hemispheres in unison, keeping a constant ratio between the two potentials.

The first method is Fixed Analyser Transmission (FAT), has greater sensitivity at lower kinetic energies ($S \propto {}^{1}/_{E}$), resolution being fixed throughout the scan range. The second, Fixed Retardation Ratio (FRR), has greater sensitivity at higher kinetic energies ($S \propto E$), resolution is not here constant over the scan range.

A.1.4 Electron Detection and Data Acquisition

Electrons emerging from the exit slits of the analyser pass into the inlet aperture of a channeltron electron multiplier. These output pulses are amplified and fed to a data handling system. The ESCA spectra can be generated in one of two ways:

(1) The continuous scan - the pass energy of the analyser is linearly ramped with time from a start KE; a rate-meter monitors the signals from the multiplier. Hence, a plot of counts per second *versus* KE of the electrons may be plotted on a X-Y recorder.

(2) The step scan - the pass energy is increased in preset increments. At each step, the counts are (a) measured for a fixed time, or (b) a fixed number of counts are timed. The data from such scans is stored in a multi-channel analyser or transferred directly to mini or micro-computer.

The spectrometers used in this study can both produce spectra in analogue for (X-Y plotter) or digitally (MCA-ES200, DS300 data system - ES300).

The DS300 data system is based on an LSI-11 mini-computer running under RT11. Data acquired is stored on floppy disc. In addition to controlling the acquisition of data, it also provides for the simultaneous analysis of data.

The data analysis package provides for, *inter alia*, the addition, subtraction, comparison, differentiation and integration of spectra, the subtraction of satellites from spectra and a peak fitting/synthesis package.

APPENDIX TWO

A.1 Kjeldahl Analysis for Nitrogen

The Kjeldahl nitrogen determinations reported in this thesis were performed according to a procedure developed at P.E.R.M.E., Waltham Abbey. As in all distillation methods the sample is first digested in acid or alkaline conditions to yield inorganic nitrates. This is then, if necessary, made alkaline and Devardas Alloy is added to reduce the nitrate to nitrite and finally ammonia. The ammonia is distilled into boric acid solution for titration with standard 0.1N hydrochloric acid. The digestion stage is the most critical, especially in the analysis of cellulose nitrates since some samples (>12.7% N) may not be fully digested by standard alkaline methods. Hence two procedures, designated A and B are adopted, depending on the estimated nitrogen content of the cellulose nitrate. These two methods are described below.

A.2 Method A. Alkaline Digestion for Samples <12.7% N

50-120mg of NC were weighed into a glass ampoule and then deposited into the base of a semi-micro flask. The ampoule was broken and 2.0mls of H_2O, 0.1mls of 30% H_2O_2 and 8.0mls of 20% NaOH were then added. The flask was then heated by $\sim 100^{\circ}C$ and maintained at this temperature for ~20 mins. to dissolve the sample. 20mls of H_2O were then added and the solution was heated again to $\sim 100^{\circ}C$ to destroy the remaining H_2O_2. After the mixture had cooled to $\sim 30^{\circ}C$, 1.00±0.01 gms of Devardas Alloy (weighed into a glass ampoule) were deposited into the flask. The stream inlet tube was attached to the neck of the flask (as shown in the diagram), and the condenser

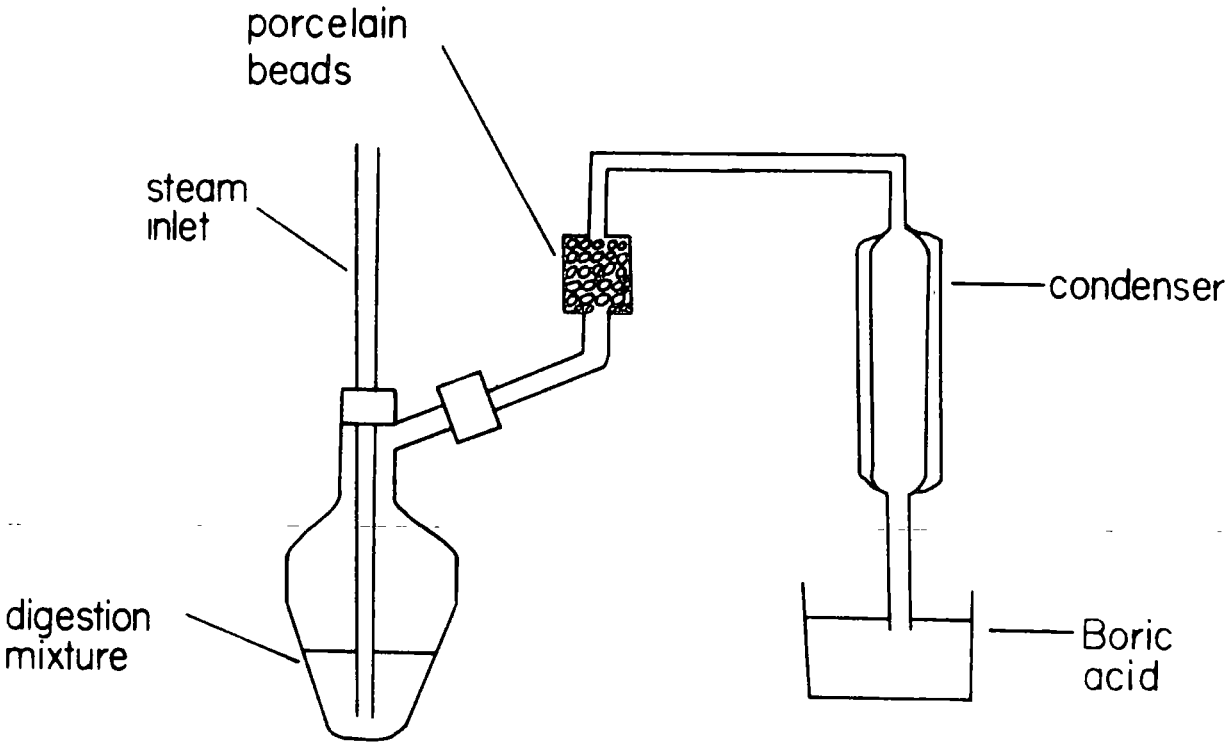

Fig. A.2.1 Schematic of apparatus for Kjeldahl analysis

outlet tube was allowed to dip ∿10mm below the surface of the boric acid in the receiver flask (25mls of 4% Boric acid). The heating of the flask was controlled to prevent excessive foaming. The ammonia liberated was steam distilled over with ∿50mls of H_2O and then titrated (using Bromocresol green as indicator) with 0.1N HCl. The volume of solution in the flask should remain constant during the distillation.

A.3 Method B. Samples 12.7% N Acid Digestion

50-120mg of NC weighed into the reaction flask and cooled in an ice-water bath. 2mls. of concentrated H_2SO_4 were added dropwise to the flask and left to dissolve the sample for 30-60 mins. The solution was then carefully diluted by adding 10gms. of crushed ice and 15-17 mls of 30% NaOH. Continued as in A.

Since Devardas Alloy has its own nitrogen content it is necessary to carry out a blank determination using all reagents except the NC for each distillation. The method is generally calibrated using Potassium Nitrate. The nitrogen content is quoted to two decimal places although the choice of the wrong digestion method can give inaccurate results.

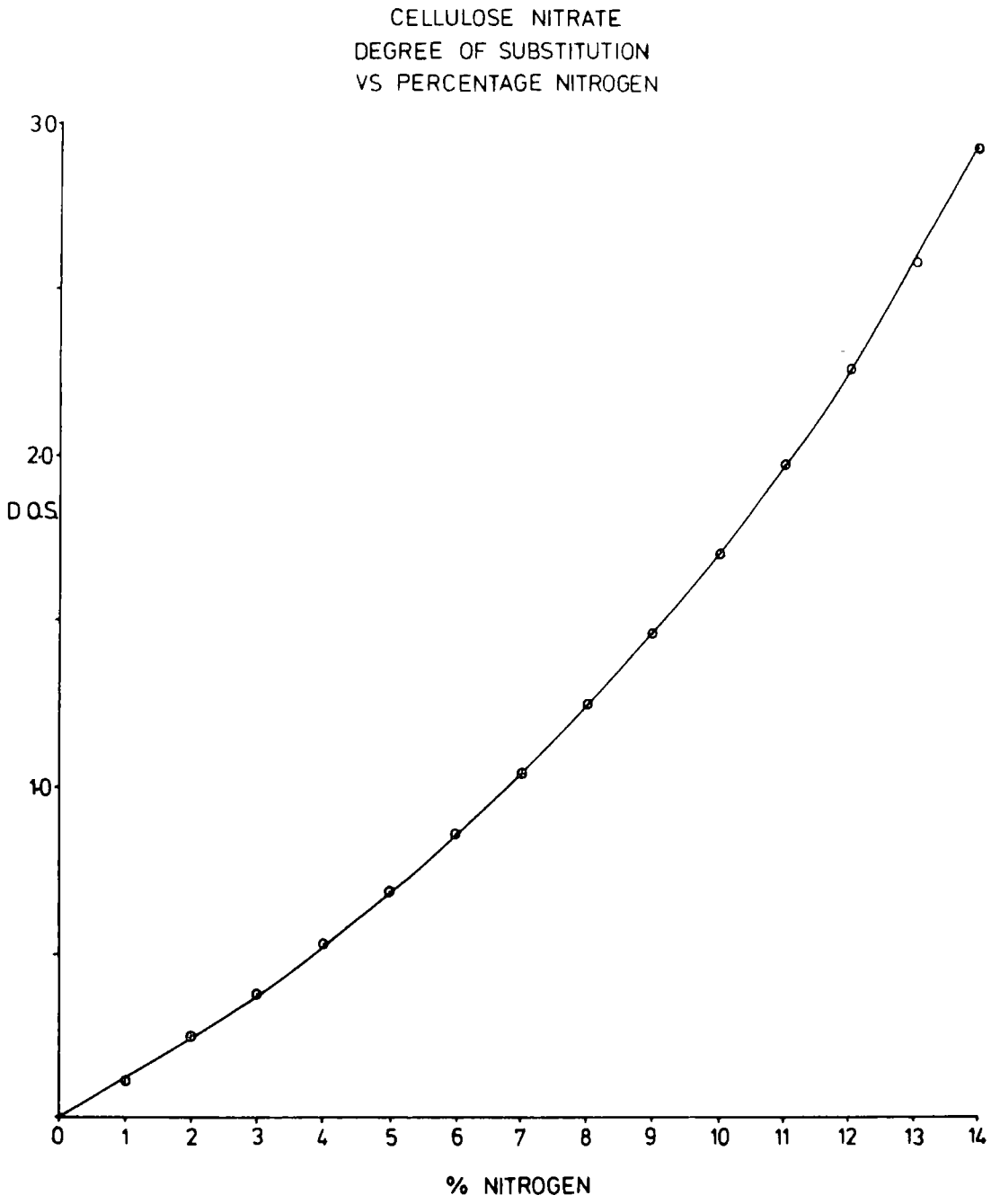

Fig. A.2.2 Graph of DOS *versus* % Nitrogen.

COLLOQUIA AND CONFERENCES

The Board of Studies in Chemistry requires that each research thesis contains an appendix listing:

(A) all research colloquia, research seminars and lectures arranged by the Department of Chemistry and the Durham University Chemical Society during the period of the writer's residence.

RESEARCH COLLOQUIA, SEMINARS AND LECTURES

Durham University Chemistry Department Colloquia

1981

14 October — Prof. E. Kluk (University of Katowice), "Some aspects of the study of molecular dynamics"

6 November — Dr. W. Moddernan (Monsanto Ltd.) "High Energy Materials"

1982

20 January — Dr. M.R. Bryce (University of Durham), "Organic metals".

27 January — Dr. D.L.H. Williams (University od Durham), "Nitrosation and nitrosoamines".

3 February — Dr. D. Parker (University of Durham), "Modern methods of determining enantiomeric purity".

10 February — Dr. D. Pethrick (University of Strathclyde), "Conformation of small and large molecules".

17 February — Prof. D.T. Clark (University of Durham), "Plasma Polymerization".

24 February — Prof. R.D. Chambers (University of Durham), "Recent reactions of fluorinated internal olefins".

2 March — Dr. L. Field (University of Oxford), "Applications of N.M.R. to biosynthetic studies on pencilllin".

3 March — Dr. P. Bamfield (I.C.I. Organics Division), "Computer aided design in synthetic organic chemistry".

17 March — Prof. R.J. Haines (University of Natal), "Clustering around Ruthenium, Iron and Rhodium".

7 April — Dr. A. Pensak (DuPont, U.S.A.), "Computer aided synthesis".

5 May — Dr. G. Tennant (University of Edinburgh), "Exploitation of the aromatic nitro-group in the design of new heterocyclisation reactions".

7 May — Dr. C.D. Garner (University of Manchester), "The structure and function of Molybdenum centres in enzymes".

26 May — Dr. A. Welch, (University of Edinburgh), "Conformation patterns and distortion in carbometalloboranes".

14 June — Prof. C.M.J. Stirling (University College of Wales, Bangor), "How much does strain affect reactivity?"

28 June — Prof. D.J. Burton (University of Iowa, U.S.A.), "Some aspects of the chemistry of fluorinated phosphonium salts and their phosphonates".

2 July — Prof. H.F. Koch (Ithaca College, University of Cornell, U.S.A.), "Proton transfer to and elimination reactions from localized and delocalized carbanions".

13 September — Prof. R. Neidlein (University of Heidelberg, FRG), "New aspects and results of bridged annulene chemistry".

27 September Dr. W.K. Ford (Xerox Research Center, Webster, N.Y.), "The dependence of the electron structure of polymers on their molecular architecture".

13 October Dr. W.J. Feast (University of Durham), "Approaches to the synthesis of conjugated polymers".

14 October Prof. H. Suhr (University of Tubingen, FRG), "Preparative Chemistry in Non-equilibrium plasmas".

27 October Dr. C.E. Housecroft (Oxford High School/Notre Dame University) "Bonding capabilities of butterfly-shaped Fe_4 units implications for C-H bond activation in hydrocarbon complexes".

28 October Prof. M.F. Lappert, F.R.S. (University of Sussex), "Approaches to asymmetric syntheses and catalyses using electron-rich olefins and some of their metal complexes".

15 November Dr. G. Bertrand (University of Toulouse, France), Crutius rearrangement in organometallic series. A route for hybridised species".

24 November Prof. G.G. Roberts (Applied Phhysics, University of Durham), "Langmiur-Blodgett films: Solid state polymerisation of diacetylenes".

2 December Dr. G.M. Brook (University of Durham), "The fate of the ortho-fluorine in 3,3-sigmatropic reactions involving polyfluoroaryl and -heteroaryl systems".

8 December Dr. G. Wooley (Trent Polytechnic), "Bonds in transition metal-cluster compounds).

1983

12 January Dr. D.C. Sherrington (University of Strathclude), "Polymer-supported phase transfer catalysts".

9 February — Dr. P. Moore (University of Warwick), "Mechanistic studies in solution by stopped flow F.T.-N.M.R. and high pressure N,R line broadening".

21 February — Dr. R. Lynder-Bell (University of Cambridge), Molecular motion in the cubic phase of NaCN".

2 March — Dr. D. Bloor (Queen Mary College, University of London), "The solid-state chemistry of diacetylene monomers and polymers".

8 March — Prof. D.C. Bradley, F.R.S. (Queen Mary College, University of London), "Recent developments in organo-imido-transition metal chemistry".

9 March — Dr. D.M.J. Lilley (University of Dundee), "DNA, Sequence, Symmetry, Structure and supercooling".

11 March — Prof. H.G. Viehe (University of Louvain, Belgium), "Oxidations on Sulphur", "Fluorine substitutions in radicals".
[The W.K.R. Musgrave Lecture]

16 March — Dr. I. Gosney (University of Edinburgh), "New extrusion reactions: Organic synthesis in a hot-tube".

25 March — Prof. F. G. Baglin (University of Nevada, U.S.A.), "Interaction induced Raman spectroscopy in supra-critical ethane".

21 April — Prof. J. Passmore (University of New Brunswick, U.S.A.) "Novel selenium-iodine cations".

4 May — Prof. P.H. Plesh (University of Keele), "Binary ionisation equilibria between two ions and two molecules. What Ostwald never thought of".

10 May — Prof. K. Burger (Technical University of Munich, FRG), "New reaction pathways from trifluoromethyl-substituted heterodienes to partially fluorinated heterocyclic compounds".

11 May — Dr. N. Isaacs (University of Reading), "The Application of high pressures to the theory and practice of organic chemistry".

13 May — Dr. R. de Koch (Caloin College, Grand Rapids, Michigan/Free University Amsterdam), "Electronic structural calculations in organometallic cobalt cluster molecules. Implications for metal surfaces".

16 May — Prof. R.J. Lagow (University of Texas, U.S.A.), "The chemistry of polylithium organic compounds. An unusual class of matter".

18 May — Dr. D.M. Adams (University of Leicester), "Spectroscopy at very high pressures".

25 May — Dr. J.M. Vernon (University of York), "New heterocyclic chemistry involving lead tetraacetate".

15 June — Dr. A. Pietrzykowski (Technical University of Warsaw/ University of Strathclyde), "synthesis, structure and properties of Aluminoxanes".

22 June — Dr. D.W.H. Rankin (University of Edinburgh), "Floppy molecules - the influence of phase on structure".

5 July — Prof. J. Miller (University of Camfinas, Brazil), "Reactivity in nucleophilic substitution reactions".

5 October — Prof. J.P. Maier (University of Basel, Switzerland), "Recent approaches to spectroscopic characterization of cations".

12 October — Dr. C.W. McLeland (University of Port Elizabeth, Australia), Cyclization of aryl alcohols through the intermediacy of alkoxy radicals and aryl radical cations".

19 October — Dr. N.W. Alcock (University of Warwick), "Aryl tellurium (IV) compounds, patterns of primary and secondary bonding".

26 October — Dr. R.H. Friend (Cavendish Laboratory, University of Cambridge), Electronic properties of conjugated polymers".

30 November — Prof. I. Cowie (University of Stirling), "Molecular interpretation of non-relaxation processes in polymer glasses".

14 December — Prof. R.J. Donovan (University of Edinburgh), "Chemical and physical processes involving the ion-pair states of the halogen molecules".

1984

10 January — Prof. R. Hester (University of York), "Nanosecond laser spectroscopy of reaction intermediates".

18 January — Prof. R.K. Harris (University of East Anglia), Multi-nuclear solid state magnetic resonance".

8 February — Dr. B.T. Heaton (University of Kent), "Multi-nuclear n.m.r. studies".

15 February — Dr. R.M. Paton (University of Edinburgh), "Heterocyclic syntheses using nitrile sulphides".

7 March — Dr. R.T. Walker (University of Birmingham), "Synthesis and biological properties of some 5-substituted uracil derivatives; yet another example of selendipity in antiviral chemotherapy".

21 March — Dr. P. Sherwood (University of Newcastle), "X-ray photoelectron spectroscopic studies of electrode and other surfaces".

DURHAM UNIVERSITY CHEMICAL SOCIETY LECTURES

1981

22 October — Dr. P.J. Cornish (Dunlop Ltd.), "What would life be like without Rubber?"

12 November — Prof. A.I. Scott (Edinburgh University), "An organic chemist's view of life in the NMR tube".

26 November — Dr. W.O. Ord (Northumbrian Water Authority), "The role of the Scientist in a Regional Water Authority".

3 December — Dr. R.E. Hester (York University), "Spectroscopy with Lasers".

1982

28 January — Prof. I. Fells (University of Newcastle upon Tyne), "Balancing the Energy Equations".

11 February — Dr. D.W. Turner (University of Oxford), "Photo-electrons in a Strong Magnetic Field".

18 February — Prof. R.K. Harris (University of East Anglia), "N.m.r. in the 1980s".

25 February — Prof. R.O.C. Norman, F.R.S. (University of York), "Turning Points and Challenges for the Organic Chemist".

4 March — Dr. R. Whyman (I.C.I. Ltd., Runcorn), "Making Metal Clusters Work".

14 October — Mr. F. Shenton (County Analyst, Durham), "There is death in the pot".

28 October — Prof. M.F. Lappert, F.R.S. (University of Sussex), "The Chemistry of Some Unusual Subvalent Compounds of the Main Group IV and V Elements".

4 November — Dr. D.H. Williams (University of Cambridge), "Studies on the Structures and Modes of Action of Antibiotics".

11 November Dr. J. Cramp (I.C.I. Ltd.), "Lasers in Industry".

25 November Dr. D.H. Richards, P.E.R.M.E. (Ministry of Defence), "Terminally Functional Polymers, their Synthesis and Uses".

1983

27 January Prof. D.W.A. Sharp (University of Glasgow), "Some Redox Reactions in Fluorine Chemistry".

3 February Dr. R. Manning (Department of Zoology, University of Durham), "Molecular Mechanisms of Hormone Action".

10 February Sir Geoffrey Allen, F.R.S. (Unilever Ltd.), "U.K. Research Ltd.".

17 February [R.S.C. Centenary Lecture], Prof. A.G. MacDiarmid, (University of Pennsylvania), Metallic Covalent Polymers: $(SN)_x$ and $(CH)_x$ and their Derivatives".

3 March Prof. A.C.T. North (University of Leeds), "The Use of a Computer Display System in Studying Molecular Structures and Interactions".

20 October Prof. R.B. Cundall (University of Salford), "Explosives".

3 November Dr. G. Richards (University of Oxford), "Quantum pharmacology".

10 November Dr. J. Harrison (Sterling Organic), "Applied Chemistry and the Pharmaceutical Industry".

24 November Prof. D.A. King (University of Liverpool), "Chemistry in two dimensions".

1 December Dr. J.D. Coyle (The Open University), "The problem with sunshine".

1984

26 January — Prof. T.L. Blundell (Birkbeck College, London), "Biological recognition: Interactions of macro-molecular surfaces".

2 February — Prof. N.B.H. Jonathan (University of Southampton), "Photoelectron spectroscopy - a radical approach".

16 February — Prof. D. Phillips (The Royal Institution), "Lumin-escence and photochemistry - a light entertainment".

23 February — Prof. F.G.A. Stone, F.R.S. (University of Bristol), "The use of carbene and carbyne groups to synthesise metal clusters".
[The Waddington Memorial Lecture].

1 March — Prof. A.J. Leadbetter (Rutherford Appleton Labs.), "Liquid Crystals"

8 March — Prof. D. Chapman (Royal Free Hospital School of Medicine, University of Lobdon), Phospholipids and biomembranes: basic structure and future techniques".

28 March — [R.S.C. Centenary Lecture].
Prof. H. Schmidbaur (Technical University of Munich, FRG), "Ylides in coordination sphere of metals: synthetic, structural and theoretical aspects".

2 April — Prof. K. O'Driscoll (University of Waterloo, France), "Chain Ending Reactions in Free Radical Polym'ns".

Conferences Attended 1981-1984

April 1982	Graduate Symposium, University of Durham
21 April 1983	Graduate Symposium, University of Durham
28 April 1983	Royal Society of Chemistry - Faraday and Perkins Divisions, London.
11 April 1984	Graduate Symposium, University of Durham*
16-20 July 1984	Cellucon '84*, Wrexham

* papers presented by the author.

REFERENCES

1. Hon, H.S., J.Polym.Sci. (Polym.Chem.Ed.), 1976, 14, 2497

2. Allen, T.C., J.Polym.Sci. (Macro Rev), 1973, 7, 184-262.

3. Bracconot, H., Annl.Chim.Phys., 1819, 12, 185.

4. Miles, F.D., "Cellulose Nitrate", Interscience, London,1953.

5. *c.f.* MacDonald, Historical Papers on Modern Explosives, 2nd Edn., London, 1917.

6. Schönbein, C.F., History of Explosives, 2nd Ed., London,1917.

7. Parkes, *c.f.* Miles, F.D. in "Cellulose Nitrate" (ref.4).

8. Schlatter, M., Chem.Met.Eng., 1921, 25, 281-86.

9. Lewis, T.J., J.Appl.Polym.Sci., 1979, 23, 2661-671.

10. Trommel, J., Commun.N.V. Konninkl.Ned.Springstoffen-fabrieken, Amsterdam, No.13.

11. Clark, D.T. and Stephenson, P.J., Polymer, 1982, 23, 1034.

12. Bouchonnet, Trombe and Petitpas., Mem.Des.Poudres, 1938, 28, 277.

13. Berl, E. and Smith, Ber.Der. Deutsch.Chem.Ges., 1908, 41, 1837.

14,15, 16,17 Bouchonnet, Mem.Des.Poudres et Saltpetre, 1838, 28, 295.

18. Chedin., Mem.Des.Services.Chem.de L'Etat., 1944, 31, 113.

19. *c.f.* Worden, E.C., "Technology of Cellulose Esters", Eschenbach Printing Co., Easton Pennsylvania, 1928, 1(3), 2325.

20. *c.f.* ref. 19, p.2354.

21. Blay, N.J., in "Chemical Problems connected with the Stability of Explosives", Ed.Hanson, J., Proceedings 1973 at Sektionen F. Detonik Forbranning, Sundyberg, Sweden.

22. Gagnon, P., Can.J.Chem., 1958, 36, 212.

23. Smith, A.C., Ardeer, 1947.

24. Gagnon, P., Can.J.Chem., 1958, 36, 212, 673, 695 and 1041.

25. Kullgren, T., Svensk Kem.Tidskr., 1944, 56, 221.

26. Berl, E. and Klaye, R., Z.des Gesamte Scheiss-und Springstoffenwessen, 1907.

27. Fabel, K., Nitrocellulose, 1934, 10, 3-5 and 24-26.

28. Demougin, P., Mem.Des.Poudres, 1930, 24, 147.

29. Bonnet, J., Mem.Des.Poudres, 1930, 24, 157.

30. Bikales, N.S. and Segal, L. "Cellulose and Cellulose Derivatives, High Polymers Part IV", Publ. Interscience,1972.

31. Connor, R.T., "Cellulose and Cellulose Derivatives High Polymers", Part V, 1971, 51-87.

32. Rowan, J.W., *et al*, J.Natl.Bur.Std., 1947, 39, 133.

33. Mitchell, J.A., Annal.Chem., 1957, 29, 499.

34. Marrian, H. and Mann, J., J.Appl.Chem., 1954, 4, 204.

35. Barker, S. *et al*, J.Chem.Soc., 1954, 3468.

36. Higgins, H.G., J.Aust.Chem.Soc., 1957, 10, 496.

37. Kuhn, L., Annal.Chem., 1950, 22, 276.

38. Higgins, H.G., J.Polym.Sci., 1961, 51, 59.

39. *c.f.* Jones, D., in ref. 30.

40. Jeffries, R. and Warwicker, J., Shirley Pamphlet No.93 of the Shirley Inst., Didsbury, Manchester, England.

41. Fyfe, C.A., Stephenson, P.J., Deslandes, Y., and Marchessault, R.H., J.Macro.Sci., Macro Rev., 1984, in press.

42. *c.f.* Matthieu, M., 1936, l.c. p.41, *c.f.* F.D. Miles, J.Phys.Chem., 1930, 34, 2607.

43. Clark, D.T. and Stephenson, P.J., Polymer, 1982,23, 1295.

44. Atkins, E.D.T., Polymer, 1978, 19, 1371.

45. Clark, D.T., Stephenson, P.J. and Heatley, F., Polymer, 1981, 22, 1112.

46. Wu, T.K., Macromolecules, 1980, 13, 74.

47. Clark, D.T. and Stephenson, P.J., Polymer, 1982, 23, 1295.

48. Wasylishen, R.E. and Fyfe, C.A., Annu.Rev.N.m.r.,

49. Lyerla, J.R., Contemporary Topics in Polymer Science, Vol.3, Plenum.

50. Fleming, W., Fyfe, C.A., Kendrick, J., Lyerla, J.R. and Yannoni, C.S., ACS Symposium Series No.142, Washington, D.C., 1980.

51. Schaeffer, J. and Stejstal, E.O., J.A.C.S., 1976, 98, 1031.

52. Fyfe, C.A., Dudley, R.L., Stephenson, P.J., Deslandes, Y., Hamer, G.K. and Marchessault, R.H., J.Macromol.Sci.-Rev.Macromol.Chem.Phys., C23, 1983, 187.

53. Fyfe, C.A., Stephenson, P.J., Deslandes, Y. and Marchessault, R.H., J.A.C.S., 1983, 105, 2469.

54. Clark, D.T., Fowler, A.H.K. and Stephenson, P.J., J.Macromol.Sci.-Rev.Macromol.Chem.Phys., C23, 1983, 217-246.

55. Kohlbeck, J.A., J.Appl.Polym.Sci., 1976, 20, 153.

56. Lewis, T.J., Polymer, 1982, 23, 710.

57. Bradshect, R.B., Kjeldahl Method for Organic Nitrogen, Academic, N.Y., 1965.

58. Clark, D.T. and Stephenson, P.J., 1982, 23, 1024.

59. Clark, D.T. and Stephenson, P.J., Polym.Degn. and Stab., 1982, 4(3), 185.

60. Clark, D.T. and Munro, H.S., Polym.Degn. and Stab., 1982, 4(6), 441.

61. Wallace, I.G. and Powell, R.J., 5th Symposium on Chemical Problems Related to the Stability of Explosives, Bastad, Sweden, 1979.

62. Stuart, R.D., Ahad, E. and Derrault, G., "Conference on Standardisation of Safety and Performance Tests for Energetic Materials", U.S. Arradcom Dover, N.J., 21-23 June 1977.

63. Siegbahn, K. *et al*, Nucl.Phys., 1956, 1, 137.

64. Nordling, C., *et al*, Phys.Rev., 1957, 105, 1676.

65. Steinhardt, R.J. Jr., Granados, F.A.D. and Post, G.I., Anal.Chem., 1955, 27, 1046.

66. Siegbahn, K., Nordling, C., Fahlman, A. *et al*, 'E.S.C.A. Atomic, Molecular and Solid State Structure Studied by Means of Electron Spectroscopy', Almquist and Wiksells, Uppsala, 1967.

67. Siegbahn, K., Nordling, C., Johansson, G., *et al*, "ESCA Applied to Free Molecules", North-Holland Publ.Co., Amsterdam, 1969.

68. Cederbaum, L.S. and Domcke, W., J.Elect.Spec.Rel.Phenom, 1978, 13, 161.

69. Clark, D.T., 'Structure and Bonding in Polymers as Revealed by ESCA' in 'Electronic Structure *c.f.* Polymers and Molecular Crystals', Eds.J.Ladik and J.M. Andre, Plenum Press, N.Y. (1975).

70. Dilks, A., Ph.D. Thesis, University of Durham 1977 in 'The Application of E.S.C.A. to Structure, Bonding and Reactivity of some Polymer Systems'.

71. Rosen, A. and Lindgren, I., Phys.Rev., 1968, 176, 114.

72. Bagus, P.S., Phys.Rev., 1965, 139A, 619.

73. Shirley, D.A. in 'Advances in Chemical Physics', 23, 85, Ed.I.Prigogine and S.A.Rice, Wiley, N.Y., 1973.

74. Gelius, U. and Siegbahn, K., Farad.Disc.Chem.Soc., 1972, 54, 257.

75. Snyder, L.C., J.Chem.Phys., 1971, 55, 95.

76. Adams, D.B. and Clark, D.T., Theoret.Chim.Acta.,1973, 31, 171.

77. Clark, D.T., 'Chemical Aspects of E.S.C.A.' in Electron Emission Spectroscopy', Ed. W. Dekeyser and D. Reidel. D. Reidel Publ. Co., Dordrecht, Holland, 373, 1973.

78. Koopmans, T.A., Physika, 1933, 1, 104.

79. Clark, D.T. and Harrison, A., J.Polym.Sci.Chem.Ed., 1981, 19, 1945.

80. Clark, D.T. Cromarty, B.J. and Dilks, A., J.Polym.Sci., Polym.Chem.Ed., 1978, 16, 3173.

81. Jolly, W.L. and Hendrickson, D.N., J.A.C.S., 1970, 92, 1863.

82. Murrel, J.N. and Ralston, B.J., J.Chem.Soc., Faraday Trans.II, 1972, 68, 1393.

83. Schwartz, M.E., Chem.Phys.Lett., 1970, 6, 631.

84. Shirley, D.A., Chem.Phys.Lett., 1972, 15, 325.

85. Fadley, C.S., in 'Electron Spectroscopy', Ed. D.A. Shirley, North Holland Publ.Co. (1972).

86. Davis, D.W. and Shirley, D.A., J.Chem.Phys., 1972, 56, 669.

87. Watson, R.E. and Freeman, A.J., in 'Hyperfine Interactions' Eds.A.J.Freeman and R.B. Frankel, Academic Press, N.Y. (1967).

88. *c.f.* Atkins, P.W., 'Molecular Quantum Mechanics', Oxford Univ. Press, London (1970).

89. *c.f.* Cotton, F.A. and Wilkinson, G., 'Advanced Inorganic Chemistry', John Wiley, N.Y. (1972).

90. Novakov, T. and Hollander, J.M., Phys.Rev.Lett., 1968,21,1133.

91. Norakov, T. and Hollander, J.M., Bull.Amer,Phys.Soc., 1969, 14, 524.

92. Bancroft, G.M., Adams, I., Lampe, H. and Sham, T.K., Chem.Phys.Lett., 1975, 32, 173.

93. Gupta, R.P. and Sen.S.K., Phys.Rev.Lett., 1972, 28, 1311.

94. Huchital, D.A. and McKeon, R.T., Appl.Phys.Lett., 1972, 20, 158.

95. Thomas, H.R., Ph.D.Thesis, Univ. of Durham (1977).

96. Clark, D.T., Dilks, A., Shuttleworth, D. and Thomas, H.R., J.Polym.Sci., Polym.Chem.Ed., 1979, 17, 627.

97. Clark, D.T., Physica Scripta (Sweden), 1977, 16, 307.

98. Hutton, D.R., Ph.D.Thesis, Univ. of Durham, 1983.

99. Carlson, T.A. and McGuire, G.E., J.Elect.Spec.1972, 1, 161.

100. Fadley, C.S., Baird, R.J. and Siekhaus, W., J.Elect.Spec., 1974, 4, 93.

101. Schofield, J.H., Laurence Livermore Lab. Report, U.C.R.L.-51326, Jan. 1973.

102. Huang, J.J., Rabelais, J.W. and Ellison, F.O., J.Elect. Spec., 1975, 6, 85.

103. Clark, D.T. and Thomas, H.R., J.Polym.Sci.Polym.Chem. Ed., 1977, 16, 2843.

104. Penn, D.R., J.Elect.Spec. and Rel.Phen. 1976, 9, 29.

105. *c.f.* Shuttleworth, D., Ph.D. Thesis, Univ. of Durham, 1978.

106. Purcell, E.M., Phys.Rev., 1938, 54, 818.

107. Helmer, J.C. and Weichert, N.H., Appl.Phys.Lett., 1968, 13, 268.

108. Murray, G.E. and Purves, C.B., J.A.C.S., 1940, 62, 3197.

109. Stephenson, P.J., Ph.D. Thesis, Univ.of Durham, 1981.

110. Shafizadeh, F. and McGinnis, G.D., Adv.Carbohyr,Chem. Biochem., 1971, 26, 297.

111. Blackwell, J. and Kolpack, F.J., Macro.1975, 8.

112. Gritsan, V.N., Zhbankov, R.G. and Kachur, V.G., Acta. Polym., 1982, 33(1), 20.

113. Woodcock, C. and Sarko, A., Macro., 1980, 13, 1183.

114. Whistler, R.L. and Martin, A.N., J.Res.Nat.Bur.Stand., 1940, 24, 555.

115. Ramesh, R. *et al*, Makromol.Chem., 1977, 178(1), 227.

116. Chanzy, H.D., Colston Pap., 1975, 26, 417.

117. Chanzy, H,D. and Roche, E.J., J.Polym.Sci. (Polym.Phys. Ed), 1975, 13, 1859.

118. Kolpack, F.J., Weih, M. and Blackwell, J., Polymer, 1978, 19, 123.

119. Marrinan, H.J. and Mann, J., J.Polym.Sci., 1956, 21, 301.

120. Marchessault, R.H. and Sarko, A., Adv.Carbohydr.Chem., 1967, 22, 421.

121. Blackwell, J. and Marchessault, R.H., in 'Cellulose and Cellulose Derivs.', Eds., N. Bikales and L.E. Segal. Wiley, N.Y., 1971.

122. Wellard, H.J., J.Polym.Sco., 1954, 13, 471.

123. Segal *et al*, J.Polym.Sci., 1954, 13, 193.

124. Ellefsen, O. and Norman, N., J.Polym.Sci., 1962, 58, 769.

125. Mathieu, M.C.R., Acad.Sci.(Paris), 1935, 200, 401.

126. Happey, F., J.Text.Inst., 1950, 41, 381.

127. Sathyanarayana, B.K., and Rao, V.S.R., Biopolymers, 1971, 10, 1605.

128. Crofton, D.J. and Pethrick, R.A., Polymer, 1981, 22, 1048.

129. Crofton, D.J., Moncrieff, D. and Pethrick, R.A., Polymer, 1982, 23, 1605.

130. Crofton, D.J. and Pethrick, R.A., Polymer, 1982, 23, 1609.

131. Crofton, D.J. and Pethrick, R.A., Polymer, 1982, 23, 1615.

132. Doyle, S., Malhotra, B.D., Peacock, N. and Pethrick, R.A., Brit.Polym.Jour., 1984, 16, 15.

133. Malhotra, B.D. and Pethrick, R.A., J.Chem.Soc., Faraday Trans. II, 1982, 78, 297.

134. Pethrick, R.A., Jacobson, F.M., Mogensen, O.E. and Eldrup, M.J., J.Chem.Soc. Faraday Trans.II, 1980, 76, 225.

135. Malhotra, B.D. and Pethrick, R.A., Polym.Commun., 1983, 19, 457.

136. *c.f.* Bragg, W.H. and Bragg, W.L. in 'X-rays and Crystal Structure', G. Bell and Sons, London, 1924.

137. Ranby, B. and Rabek, J.F., 'Photodegradation, photo-oxidation and photo-stabilisation of Polymers', Wiley Interscience, London (1973).

138. Phillips, L., Nature, 1950, 165, 564.

139. Lewis, T.J., private communcation.

140. Gestetner, G., *et al*, J.Phys.Chem., 1956, 60, 1260.

141. Barton, D.H.R., J.Chem.Soc., 1953, n23, 1027.

142. Barton, D.H.R., Helv.chim.Acta., 1959, 42, 2604.

143. Barton, D.H.R., Beaton, J.M., Geller, L.E. and Pechet, M.M., J.A.C.S., 1961, 83, 4076.

144. Golding, B., private communcation.

145. *c.f.* Carruthers, W. (Ed.) in 'Some Modern Methods of Organic Synthesis', 2nd Edition, Cambridge University Press, 1978.

146. Munro, H.S. and Allaker, R.S., Polym.Degn. and Mtab., to be submitted.

147. Munro, H.S. in preparation.

148. Munro, H.S. and Clark, D.T., Polym.Deg. and Stab., 1982, 4, 441.

149. *c.f.* Atkins, P.W. in 'Physical Chemistry', Oxford University Press, 1978.

150. Sendo, K., J.Cellulose Inst., Chem.Abs., 1933, 33, 2802.

151. Kagawa, C., J.Soc.Chem.Ind.Japan, 1937, 40, 151B.

152. Vandoni, Mem.des. Services Chim. de l'État, 1944, 31, 87.

153. *c.f.* ref. 151.

154. Wilson, G.L. and Miles, F.D., Ardeer, 1937.

155. Taylor and Hall, J.Phys.Chem., 1947, 51, 580 and 593.

156. Jessup and Prosen, J.Res.Nat.Bureaux of Standards, 1950, 44, 387.

157. Klein, R. and Mentser, M., J.A.C.S., 1951, 73, 5888.

158. Bayliss, N.S. and Watts, D.W., Aust.J.Chem., 1963, 16, 943.

159. Chédin, J., C.r. hebd.Séanc.Acad.Sci., Paris, 1935, 200, 1397.

160. Chédin, J., Mém.des Services.Chem.de l'État., 1944, 31, 113.

161. Gillespie, R.J., Hughes, E.D. and Ingold, C.K., J.Chem. Soc., 1950, 2552.

162. Goddard, D.R., Hughes, E.D. and Ingold, C.K., J.Chem. Soc., 1950, 2559.

163. Ingold, C.K. and Millen, D.J., J.Chem.Soc., 1950, 2612.

164. Hughes, E.D., Ingold, C.K. and Reed, R.I., J.Chem.Soc., 1950, 2400.

165. Halberstadt, E.S., Hughes, E.D. and Ingold, C.K., J.Chem. Soc., 1950, 2441.

166. Ingold, C.K., 'Substitution at Elements other than Carbon', Jerusalem, The Wiezmann Science Press of Israel, 1959.

167. Ingold, C.K., Millen, D.J. and Poole, H.G., J.Chem.Soc., 1950, 2576.

168. Gillespie, R.J. and Millen, D.J., Q.Rev.Chem.Soc., 1948, 2, 277.

169. Grison, E., Ericks, K. and de Vries, J.L., Acta Crystallogr., 1950, 3, 290.

170. Hantzsch, A. (a) Ber.dt.chem.Ges., 1925, 58, 941; (b) Z.Phys.Chem., 1930, 149, 161; (c) Z.Phys.Chem. 1908, 61, 257; 1909, 62, 178 and 626; 1910, 65, 41; 1910, 68, 204.

171. Gillespie, R.J., Graham, J., Hughes, E.D., Ingold, C.K. and Peeling, E.R.A., J.Chem.Soc., 1950, 2504.

172. Ingold, C.K. 'Structure and Mechanism in Organic Chemistry', 2nd Edn., London: Bell, p.334 (1969).

173. Saporschnikow, A., Z.Phys.Chem., 1904, 49, 697.

174. Gardella, J.A. and Hercules, D.M., Anal.Chem., 1980, 52, 226.

175. Gardella, J.A. and Hercules, D.M., Anal.Chem., 1981, 53, 1879.

176. Rabalais, J.W. in 'Photon, Electron, and Ion Probes of Polymer Structure and Properties', ACS Symposium Series 162, Eds. Dwight, D.W., Fabish, T.J. and Thomas, H.R., 1981, 237-246.

177. Briggs, D. and Wootton, A.B., Surf.Interface Anal., 1982, 4, 109.

178. Briggs, D., Surf. Interface Anal., 1982, 4, 151.

179. Briggs, D. in 'Ion Formation of Organic Solids', Springer series in Chem.Phys., 25, Springer-Verlag, N.Y., Ed. Benninghoven, A., 1982, 156-161.

180. Briggs, D., Brown, A., Van Den Berg., J.A. and Vickermann, *ibid*, 1982, p.162-166.

181. Clark, D.T., Fowler, A.H.K. and Peeling, J., Polym. Comms., 1983, 24, 119.

182. *c.f.* ref. 177.

183. *c.f.* ref. 178.

184. Silverstein, R.M., Bassler, G.C. and Morrill, T.C. in 'Spectrometric Identification of Organic Compounds', John Wiley and Sons, N.Y., 4th Edn., 1981.

185. Fowler, A.H.K., Munro, H.S. and Clark, D.T., Polym.Degn. and Stab., in press (1984).

186. Hutton, D.R., Ph.D. Thesis, University of Durham, 1983.

187. Briggs, D., Brewis, D.M. and Konieczko, M., J.Mater.Sci., 1976, 11, 1270.

188. Briggs, D., and Brewis, D.M., Polymer, 1981, 22, 7 and references therein.

189. Riggs, W.M. and Dwight, D.W., J.Elec.Spectro.Rel.Phenom., 1974, 5, 447.

190. Clark, D.T. and Dilks, A., J.Polym.Sci. (Polym.Chem.Ed.), 1978, 16, 791.

191. Clark, D.T. in 'Polymer Surfaces', Eds. D.T. Clark and W.J. Feast, Wiley, Chichester, Chapter 16 (1978).

192. Clark, D.T., Dilks, A. and Shuttleworth, D., in 'Polymer Surfaces', *Ibid*, Chapter 9.

193. Clark, D.T. and Dilks, A., J.Polym.Sci. (Polym.Chem.Ed.), 1977, 15, 2321.

194. *Ibid*, 1979, 17, 957.

195. Clark, D.T. and Wilson, R., J.Polym.Sci. (Polym.Chem.Ed.), 1983, 21, 837.

196. Clark, D.T. and Shuttleworth, D., J.Elec.Spectro.Rel. Phenom., 1979, 17, 15.

197. Clark, D.T., Dilks, A., Shuttleworth, D. and Thomas, H.R., J.Elec.Spectro.Rel.Phenom., 1978, 14, 247.

198. Gawne, E.J. and Derke, B.V., 'Dress: The Clothing Textbook', 3rd Edn, C.A. Bennet, Illinois (1969).

199. Wilson, N., 'Static Charges on Textile Surfaces' in 'Polymer Surfaces', Eds. D.T. Clark and W.J. Feast, Chapter 7, Wiley (1978).

200. Carraher, C.E., Burt, W.R., Giron, D.J., Schroeder, J.A. Taylor, M.L., Molloy, H.M. and Tierman, T.O., J.Appl. Polym.Sci., 1983, 28, 1919.

201. Rasmassen, J.R., Stedronsky, E.R. and Whitesides, G.M., J.A.C.S., 1977, 99, 4736.

202. Rasmassen, J.R., Bergbrieter, D.E. and Whitesides, G.M. JACS, 1977, 99, 4746.

203. Batick, C.D. and Wendt, R.C. in 'Photon, Electron and Ion Probes of Polymer Structure and Properties', Eds. Dwight, D.W., Fabish, T.J. and Thomas, H.R., ACS Symposium Series No.162, Washington, Chapter 15 (1981).

204. Everhart, D.S. and Reilly, C.N., Anal.Chem. 1981, 52, 655.

205. Everhart, D.S. and Reilly, C.N., Surf.Interface.Anal., 1981, 3, 126.

206. Hammond, J.S., Holubka, J.W., Dursin, A. and Dickie, R.A., 'Abstract from Colloid and Interfacial Science Section, ACS Meeting, Miami, September 1978.

207. Munro, H.S., Personal Communication, (1983).

208. Wilson, R., Ph.D. Thesis, University of Durham, 1983.

209. Dickie, R.A., Hammond, J.S., and Holubka, J.W., Anal. Chem., 1982, 54, 2045.

210. Geddes, A.L., J.Polym.Sci., 1956, 22, 31.

211. Riggs, W.M. and Dwight, D.W., J.Colloid and Interface Sci., 1974, 650.

212. Millard, M. and Marsi, M., Anal.Chem., 1984, 46, 1820.

213. Bradley, A. and Czuha, Jr.,M., Anal.Chem. 1975, 47, 1838.

214. Czuha,Jr., M. and Riggs, W.M., Anal.Chem., 1975, 47, 1836.

215. Spell, H.L. and Christensen, C.P., Tappi, 1979, 62, 77.

216. Briggs, D. and Kendal, C., Polym.Comms. 1979, 20, 1053.

217. Munro, H.S., unpublished data.